ELECTROCHEMICAL AND ELECTRON PARAMAGNETIC RESONANCE (EPR) STUDIES OF SOME OXIDISED METALLOPORPHYRINS

SYNOPSIS

BY

A. TOMBA SINGH

DEPARTMENT OF CHEMISTRY

SCHOOL OF PHYSICAL SCIENCES

SUBMITTED

IN PARTIAL FULFILMENT OF THE REQUIREMENT

OF THE DEGREE OF

DOCTOR OF PHILOSOPHY

IN

CHEMISTRY

TO

NORTH EASTERN HILL UNIVERSITY

SHILLONG - 793022

INDIA

FEBRUARY 2002

SYNOPSIS

SYNOPSIS

This thesis entitled " ELECTROCHEMICAL AND EPR STUDIES OF SOME OXIDISED METALLOPORPHYRINS" embodies the information, results of investigations on the oxidation products of some metalloporphyrins. It consists of five (5) chapters and an appendix. We restrict our investigations mainly to cyclic voltammetry and EPR studies of some transition metals like VO, Co and Ni porphyrins.

In the introduction occurrence of the metalloporphyrins π - cation in nature is briefly mentioned. Besides, the importance of the EPR and cyclic voltammetric studies of metalloporphyrins are also mentioned very briefly.

In chapter 1 a brief review of VO, Co and Ni meso-tetraphenylporphyrins are presented. Emphasis is given to the EPR and cyclic voltammetric studies. This review provides us the background information to pursue our research investigation in the right direction.

Chapter 2 describes the detail experimental procedures such as the synthesis, purification and characterization of samples as well as the purification of reagents and solvents used during the course of investigations. Besides, instrumental parameters and the procedure of measurements are also described.

Chapter 3 discusses the cyclic voltammetry, EPR and UV-vis spectra of substituted meso-tetraphenyl vanadyl porphyrins. In general the voltammograms of

vanadyl porphyrins exhibit two reversible oxidation waves. Thus, the voltammogram of VO(T(*m*-NO_2)PP) consists of two reversible one-electron oxidation – reduction waves. The oxidation potentials are shifted more positively and show higher potentials even compared to that of VOTPP(Xn) where X=Br systems.

The room temperature EPR spectra of the oxidations of VOTPP which are not available in the literature are also presented in this chapter. It also gives a good comparative study for the substituted VOTPP systems. The pre-oxidised species of VOTPP show line width inversion and reduction in the coupling constant.

The triplet state of these vanadyl porphyrins do not vanishes at room temperature but broadens out which are visible at higher modulation. Since all the substituted VOTPP systems show similar type of EPR spectra. We discuss the spectra of VO(T(*m*-NO_2)PP). The EPR of $[VO(T(m\text{-}NO_2)PP)]^+$ at 77K gives a triplet state spectrum which resembles that of the radical cation of VO meso-porphyrin. The data from the low temperature EPR spectrum are presented in the table 3.2.

A value of 3.575 ± 0.05Å is obtained as an inter-electron distance between the two unpaired electrons. Similarly, we obtain inter-electron distance for the rest of the vanadyl porphyrins. Shorter distance between the unpaired electrons indicates that the unpaired spin density is more in a_{1u}. But the room temperature spectra of the triplet state do not vanish. This also points that the unpaired spin density in a_{2u} is not negligible.

Chapter 4 deals with the EPR and cyclic voltammetric studies of Nickel porphyrins. Normally, Ni(II)P do not give any EPR spectrum because Ni(II) is d^8

system and the ligand field is square planer. However, in the presence of strong axial ligand, it assumes a distorted octahedral configuration leading to paramagnetism.

Ni(py)TPP(Br_2) which we have synthesised gives some interesting paramagnetic signal both at room temperature as well as at the liquid nitrogen temperature. Four lines spectrum along with some superhyperfine lines are observed at room temperature. This observation is quite unusual and so far no reports of such signals are available in the literature. The four lines corresponds to I=3/2 Nickel system with coupling constant $a \approx 89G$ and $g = 2.128$.

At liquid nitrogen temperature similar pattern is observed with well resolved superhyperfine structure. The g values are found to be, $g_{\parallel} = 2.247$, $g_{\perp} = 2.078$. The superhyperfine coupling constant$\approx$ 16G

A single line EPR spectrum is obtained on oxidation of Ni(py)TPP(Br_2) with $SbCl_5$ having g=2.019 (at room temperature). At 77K it gives the EPR spectrum corresponds to π-cation.

The molecular orbital coefficients calculation shows that the in-palne σ - bonding between the metal and the ligand is quite strong.

The cyclic voltammetric measurements exhibit two broad redox waves. Their ΔE values are quite large for one – electron transfer processes. Their i_{pa}/i_{pc} are also larger than 1. Therefore, the first redox wave appears to be an overlap of two waves. Since the metal oxidation and the first ligand oxidations are in the same range, this step may involve Ni(I)$\rightarrow$ Ni(II) and the other is π -cation.

UV-vis spectra of Nickel porphyrins exhibit hypso type of spectrum although the shifts are not much. Thus, it is likely that metal – ligand back bonding does exist. On oxidation with $SbCl_5$ the Ni(py)P exhibit a split in the soret band. Besides, the intensity of the visible band decreases and a new broad band emerges in the region 600nm – 900nm.

Chapter 5 discusses the cyclic voltammetry and UV-vis spectra of the Cobalt porphyrins. As Co in also an electron active, oxidations will occur in both the metal center as well as the ligand. If there is a strong metal-ligand interaction, then on oxidation there may be some changes in the metal center oxidation potentials. However, we could not observe any accountable changes in the oxidation potential of the cobalt.

UV – vis spectra of Cobalt porphyrins do not show much difference on substitutions at different positions. Only some red shifts are observed for tetra bromo systems.

In the appendix, necessary theories such as voltammetry of metalloporphyrins, spin Hamiltonian for axially symmetric systems and other molecular orbital coefficients calculations are incorporated.

ELECTROCHEMICAL AND ELECTRON PARAMAGNETIC RESONANCE (EPR) STUDIES OF SOME OXIDISED METALLOPORPHYRINS

SYNOPSIS

BY

A. TOMBA SINGH

DEPARTMENT OF CHEMISTRY

SCHOOL OF PHYSICAL SCIENCES

SUBMITTED

IN PARTIAL FULFILMENT OF THE REQUIREMENT

OF THE DEGREE OF

DOCTOR OF PHILOSOPHY

IN

CHEMISTRY

TO

NORTH EASTERN HILL UNIVERSITY

SHILLONG - 793022

INDIA

FEBRUARY 2002

DECLARATION

NORTH-EASTERN HILL UNIVERSITY

DECEMBER 2001

I Shri ***A. Tomba Singh,*** *hereby declare that the subject matter of this thesis is the record of work done by me, that the contents of this thesis did not form basis of the award of any previous degree to me or to the best of my knowledge to anybody else, and that the thesis has not been submitted by me for research degree in any other University/ Institute.*

This is being submitted to the North - Eastern Hill University for the ***Ph.D.*** *degree in* ***Chemistry.***

A. Tomba Singh
(CANDIDATE)

Prof. K. Ismail
(HEAD)
DEPARTMENT OF CHEMISTRY
NEHU

Dr. A. Lemtur
(SUPERVISOR)

ACKNOWLEDGEMENTS

It is a great pleasure for me to express my sincere and heartiest gratitude to Dr. A. Lemtur for his guidance, inspiration and encouragement throughout the course of this investigation.

I express my sincere gratitude to Head of Chemistry Department Prof. K. Ismail and the faculty members of the Department for encouraging me throughout the Course.

I take this opportunity to thank Prof. J. Subramanian, Head, Department of Chemistry, Pondicherry University, Pondicherry for his advice, suggestions and valuable discussions for the simulation programme and allowing me to use the programme.

I would like to express my sincere thanks to Dr. S.N. Rai, Director, Computer Center, NEHU, Shillong, Dr. Sinha, P.P.Dey, S. Ghosh, B. Rynjah and Nirmala for their help in computational work.

I further would like to thank all the staff, RSIC, NEHU, Shillong for providing the spectral and analytical data of the compounds described in this thesis.

My special thanks go to Miss Cornelia Mary Lyngdoh for her moral support and invaluable assistance in every possible way and for being with me to lend a helping hand.

I also thank my lab mate Wandondor, Cheerful, Berna and S.K. Prashad for their help and moral support.

I sincerely thank all the research colleagues, non-teaching staff and especially the Librarian for their support, cooperation and help rendered throughout the course of my work.

I wish to express my gratitude to Prof. Rage and Mrs. Rage for their constant encouragement.

I also thank Nireeja, Deepa and R. Kannapan research scholar, Department of Chemistry, Pondicherry University, Pondicherry for recording EPR spectrum.

I also acknowledge my sincere thanks to Dr. Mukherjee, Dr. Deborah Buam, Dr. Okram Barum, Dr. Sanju, Dr. Sunil, Dr. Akhilesh Kumar Gupta, K. Sharma, O.P. Tripathi, Th. Somananda Singh (VSAT), Tiken, Dhiren, Munindro, Ulen, Tarun, Amarjeet, Jibon, AK. Jugendro, Somarendro, Nonibala Kh., Y. Premabati Devi and all my Shillong friends.

I also thank to the University Grant Commission (SAP and DRS), for providing me financial assistance.

It is not possible for me to express my deep sense of gratitude to my parents, brother and sisters in words. I thank them for their affection, patience and constant encouragement throughout my career.

Above all, I thank God for giving me the strength in pursuing my task and completing this thesis successfully.

CONTENTS

LIST OF TABLES

LIST OF FIGURES

Preface

Porphyrin Chemistry is an extensively researched field. This is because porphyrins are involved in many fundamental biological functions. Physico – chemical research on porphyrins and metalloporphyrins have provided more understanding of their roles in biological systems, applications in medicine and possible use as semiconductors. Inspite of the extensive research work done, more new information emerges out of the recent research works. This prompted us to carry out more physico-chemical research in porphyrins. Thus, this thesis embodies the new results and information, which are not reported so far in the literature.

This thesis consists of five chapters. The significance of the metalloporphyrins π – cation in the biological system is briefly highlighted in the introduction.

Chapter 1 briefly discusses the review on the electrochemical and EPR studies of the oxidation products of vanadyl, cobalt and nickel meso-tetra phenyl porphyrins and substituted meso-tetraphenyl porphyrins.

All the experimental details employed in the course of the investigation are described in chapter 2.

Chapter 3 deals with electrochemical and electron paramagnetic resonance studies of the oxidation products of VOTPP and substituted VOTPP.

Chapter 4 embodies the cyclic voltammetry and electron paramagnetic resonance investigations Ni(py)TPP and substituted Ni(py)TPP.

Chapter 5 discusses the oxidation behaviour of CoTPP and its derivatives by cyclic voltammetry and UV - visible spectrum.

Chapter 3, 4 and 5 are framed with introduction, results, discussion and conclusions.

All the theoretical background is given in the appendix.

INTRODUCTION

INTRODUCTION

This thesis embodies the information, results and discussions of investigations on the oxidation products of some metalloporphyrins. We restrict our investigations mainly to the cyclic voltammetry and electron paramagnetic resonance studies of MTPP systems. Our motivations in pursuing this research work is two – fold:

1. Metalloporphyrin π - cation radicals occur in nature
2. Electron paramagnetic resonance and cyclic voltammetric studies provide data for development of theoretical interpretations of such systems.

1. Metalloporphyrin π - cation radicals in nature :

The possible occurrence of metalloporphyrin π-cation in nature has been compared, studied and reported in the literature. Here we present the review very briefly.

(I) Photosynthesis : It has been suggested that the photochemical step in photosynthesis involves the photo oxidation of chlorophyll **a**[1-7]. Oxidation of chlorophyll **a** ($cha^{+\cdot}$) has been compared with the oxidised metalloporphyrins and chlorins. Electrochemical oxidation of metalloporphyrins unambigously demonstrated the similarity of the oxidation of the chlorophyll **a**. Similar comparison between the oxidation of Bchl and metalloporphyrins were done conclusively.

(II) Cytochromes and Heme Catabolism: The formation of π - cation radical of Fe(II) porphyrins on oxidation with peroxides suggests that the electron transfer

involving cytochrome takes place via ring oxidation followed by rapid internal conversion[8,9].

(III) Catalase and peroxidase: The similarity in the optical spectra $[Co(III)OEP]^{2+\cdot}$, ground states Cat I and HRP I strongly suggests that the Cat I is a π-cation radical in $^2A_{1u}$ ground state while that of HRP I is a π - cation radical in $^2A_{2u}$ ground state[7].

The oxidation of Fe(III)P is well established for enzymes like catalase and peroxidase. On the basis of the room temperature EPR and optical spectra of the oxidised Fe(III)P, the oxidised species has been identified as Fe(III)P radical cation. It is also worth mentioning that a compound of the type Fe(IV)O(TMP$^{\cdot}$)Cl is a good model for HRP I[10].

2. EPR and CV data for theoretical Calculation[11 - 14] : Molecular orbital coefficient can be obtained from the EPR data (see appendix B). The coefficients α and α′ give the information about the in plane σ - bonding between the metal - nitrogen (M - N) while β_1 and β described the in – plane π - bonding and out of plane π - bonding respectively. Similarly, α_1 etc. can be found out. From the superhyperfine coupling, one can obtain the value of γ, the hybridisation coefficient and the α′. One can also calculate the distance between the two unpaired electron in the metalloporphyrin π - cation radical using the EPR data (see appendix B).

Normally, a metalloporphyrin is D_{4h} or C_4 symmetry giving rise to a square planar complex. The two highest occupied MO's (HOMO) a_{2u} and a_{1u} are nearly degenerate.

The energy of separation between these two levels is around 0.5eV. Generally, OEP types have a_{1u} ground state and that TPP types have a_{2u} ground state. This difference can also be identified from the EPR spectra.

From the cyclic voltammetric measurements one can obtain the redox potentials. One can ascertain the difference between the metal oxidation and the ligand oxidation. Apart from the redox potential data one can also study the dimerisation, aggregation etc.

REFERENCES

1. D. H. Kohl, in " Biological applications of Electron Spin Resonance", H. M. Swartz, J. R. Bolton and D. C. Borg. Ed., Wiley – Interscience, New York, N.Y., 1972, p. 213.
2. J. D. McElroy, G. Feher, and D. Mauzerall, *Biochem. Biophys. Acta.* **267**, 363 (1972).
3. W. W. Passon, *Biochem. Biophys. Acta.* **153**, 248 (1968).
4. P. A. Loach and K. Walsh, *Biochemistry* **8**, 1908 (1969)
5. J. R. Bolton, R. K. Clayton and D. W. Reed, *Photo Chem. Photo biol.* **9**, 209 (1969).
6. J. T. Warden and J. R. Bolton, *J. Am. Chem. Soc.* **94**, 4351 (1972).
7. D. Dolphin and R.H. Felton, *Acc. Chem. Res.* **7**, 26 (1974).
8. C. E. Castro, *J. Theor. biol.* **33**, 475 (1972).
9. (a) N. Sutin, and A. Forman, *J. Am. Chem. Soc.* **93**, 5274 (1971).
   (b) N. Sutin, *Chem. Brit.* **8**, 148 (1972).
10. C. A. Reed, in "Electrochemical and Spectrochemical studies of Biological Redox components", Advances in chemistry series, Edited by K. M. Kadish (American Chemical Society, Washington D.C., 1982), 201, p333.
11. A. H. Maki and B. R. McGarvey, *J. Chem. Phys.* **29**, 31 (1958).
12. E. M. Roberts, W. S. Koski and W.S. Caughey, *J. Chem. Phys.* **34**, 591 (1961).
13. D. Kivelson and R. Neiman, *J. Chem. Phys.* **35**, 149 (1961).
14. J. Subramanian, in "Porphyrins and Metalloporphyrins", Edited by K.M. Smith (Elsevier, Amsterdam, 1975), p. 555.

CHAPTER 1

BRIEF REVIEW OF VO, Co AND Ni PORPHYRINS

CHAPTER – 1

1.1. INTRODUCTION

In this chapter a brief review of the VO, Co and Ni porphyrins with special reference to substituted TPP systems are presented. Emphasis is given to the studies of Electron Paramagnetic Resonance(EPR) and Cyclic voltammetry(CV).

1.2. VANADYL PORPHYRIN

Reports on EPR of VOTPP and its oxidised products are available in the literature[1-3]. Selyutin et al.[2] observed that VOTPP on oxidation with $Br_2/SbCl_5/SnCl_4/TiCl_4$ formed pre-oxidised complexes. The biradical/triplet state generated by $SbCl_5$ could not be observed even in the glass state. The pre-oxidised complexes could also be observed only at low temperature. The reason for not observing these complexes was attributed to thermodynamic instability of the complexes. The EPR data of the two pre-oxidised complexes at liquid nitrogen temperature were reported as $g_{\parallel}$ = 1.977, $g_{\perp}$ = 1.973, A=141x10^{-4} cm^{-1}, B = 39x10^{-4} cm^{-1} for $[V^{4+}OSbCl_4Cl^-(TPP)]$ while $g_{\parallel}$ = 1.977 A=140x10^{-4} cm^{-1} for $[V^{4+}OSbCl_4\ Cl^-\ (TPP)]\ SbCl_5$. The EPR data for the dication were $g_{\parallel}$ = 1.973, $g_{\perp}$ = 1.980, A=144x10^{-4} cm^{-1}, B = 44x10^{-4} cm^{-1} for $[VOTPP^{2+}]2Br_2$; $g_{\parallel}$ = 1.973, $g_{\perp}$ = 1.980, A=144x10^{-4} cm^{-1}, B = 44x10^{-4} cm^{-1} for $[V^{4+}\ OSbCl_4\ Cl^-\ (TPP^{2+})]2Cl^-$ and $g_{\parallel}$ = 1.973, $g_{\perp}$ = 1.962, A=147x10^{-4} cm^{-1}, B = 41x10^{-4} cm^{-1} for $[V^{4+}OTiCl_3\ Cl^-\ (TPP^{2+})]2Cl^-$. The smaller value of the hyperfine coupling constant

was attributed to the compression along N-V-N bonding due to the additional bonding of $[SbCl_4]^+$ or $[TiCl_3]^+$ with the oxygen of the vanadyl with Cl^-.

Hoshino et al[3]. irradiated the VOTPP in TCE (1, 1´, 2, 2´ - tetra chloroethane) with γ-radiation and generated the triplet state at 77K. EPR spectra corresponding to $\Delta m_s = \pm 1$ transitions could not be observed due to very intense background signal from VOTPP. Only the half – field signals with coupling constant of 90G were observed. On the basis of the visible spectrum i.e. broad band around 615nm and 850nm the species was assigned to $VOTPP^{+\cdot}$ The D value was estimated as $D \leq 0.024$ while the distance of the vanadium atom was estimated to be 0.5Å out of the porphyrin plane. It was also suggested that $VOTPP^{+\cdot}$ to be in $^2A_{2u}$ state.

Oxidation potentials of VOTPP are well documented in the literature[4-6]. Electro-reductions of substituted VOTPP systems are also available in the literature but very little information on the electro-oxidation are available.

Kadish et al.[6] reported the electrochemistry of $[VO(TpyP)]^{2-}$, VO[T(*p*-SO_3Na)PP] and VO[T(*p*-Et_2N)PP] in DMF.

VO(DMF)[T(pyP)] exhibited two reversible processes at $E_{½} = -0.82$ and –1.27V. Besides these potentials no other oxidation or reduction were observed in DMF between –2.0V and +1.4V.

VO(DMF)[T(*p*-SO_3Na)PP] showed oxidation at $E_{½} = 1.02$V and $E_p = 1.45$V. The two oxidation processes were observed to be overlapped. At room temperature the controlled-potential oxidation at 1.1V indicate 2.7 electrons transfer while controlled – potential electrolysis at positive of 1.1V yielded much more electrons transfer. At –

63°C higher oxidations were found to be irreversible but involved one electron transfer. Setting the oxidation at higher potential (1.7V) the visible spectrum exhibited the regeneration of the original form. This process was attributed to the catalytic oxidation of DMF. VO[T(*p*-Et_2N)PP] in DMF exhibited oxidations at $E_{½}$ = 0.68V and E_p = 1.04V at room temperature. In this case DMF solvent molecule did not show any co-ordination. The first oxidation was reversible but $Ep_a - Ep_c \approx 45 + 5mV$ which was large for a two electron transfer redox process. The second oxidation involved multi - electron transfer.

It was concluded that the electron – withdrawing substituents such as pyridyl in the meso position leads to easier reduction while making oxidations difficult. The situation was reversed in the case of electron – donating substituents.

1.3. NICKEL PORPHYRINS

Ni(II) is a d^8 system with square planar ligand field in Ni(II)P and is diamagnetic. Ligation with a strong axial ligand it assumes a distorted octahedral complex giving rise to paramagnetism[7].

Wolberg and Manassen[8] reported the controlled – potential electro-oxidation of Ni(II) tetraphenylporphyrin in benzonitrile at room temperature. Two overlapping voltammetric waves were observed for the oxidation of Ni(II)TPP in benzonitrile. These two peaks were successive one electron transfer steps. The first one was reversible while the second one was irreversible. No EPR signal from the oxidised product was observed at room temperature. On cooling down the oxidised product to liquid nitrogen temperature an axially symmetric EPR signal was observed. The EPR

data were $g_{\parallel}$ = 2.116 and $g_{\perp}$ = 2.295. Allowing the solution to attain the room temperature, a symmetric but very weak EPR signal was observed. This signal showed a slight assymmetry cooling again to liquid nitrogen. The EPR data are $g_{\parallel}$ = 2.031 and $g_{\perp}$ =2.024. Thus, two different spectra were observed at liquid nitrogen. The first spectrum was assigned to Ni(III)TPP^{+} cation with square – planar d^7 configuration. The second spectrum was assigned to Ni(II)$TPP^{+\cdot}$ (free – radical). It was proposed that the second oxidation of Ni(III)TPP^{+} produced Ni(III)TPP^{2+} which was rapidly returned to the Ni(III)TPP^{+} cation on acquiring an electron. Further, it was proposed that Ni(III)TPP^{+} decomposed to Ni(II)TPP via Ni(II)$TPP^{+\cdot}$ but could not proved it.

Dolphin and Felton et al.[9] reported the electro-oxidation of Ni(II)TPP in CH_2Cl_2 and simultaneous monitoring of the electronic absorption spectrum indicated that the product was $[Ni(II)TPP]^{+\cdot}$ and was stable. The electronic absorption spectrum, magnetic circular dichroism spectrum and the EPR spectrum at 300K with g=2.0041 and peak to peak width of 48.2G characterised the formation of a porphyrin π - cation radical. Further electrolysis of $[Ni(II)TPP]^{+\cdot}$ at 1.44V yielded π - dication i.e. $[Ni(II)TPP]^{2+}$ and was identified by optical spectrum.

At liquid nitrogen temperature $[Ni(II)TPP]^{2+\cdot}$ in CH_2Cl_2 solidified into an orange – red solid. The free radical signal was changed to an EPR spectrum corresponding to the low – spin d^7 Ni(III) complex with $g_{\parallel}$ = 2.086 and $g_{\perp}$ =2.286.

The voltammogram of Ni(II)TPP in CH_2Cl_2 (Ag/AgCl as reference) exhibited two overlapping voltammograms. The two oxidation potentials were 1.20V and 1.29V. Both the redox potentials corresponded to single electron transfer.

Oxidations of Ni(T(*p*-X)PP) where X = – CH_3, – $COOCH_3$, –NO_2 in CH_2Cl_2 were reported in the literature[10]. Ni(T(*p*-CH_3)PP) showed two oxidations at 1.00V and 1.20V while Ni(T((*p*-$COOCH_3$)PP) showed a single oxidation at 1.17V. The peak current of the later indicated two electron transfer. For Ni(T(*p*-NO_2)PP) all peaks were found to be shifted anodically. The shift in the first oxidation was found to be more than for the second oxidation. Ni(T(*p*-X)PP), X= electron - donating or weak electron - withdrawing group exhibited two separate oxidations while for compounds containing X= strong electron -withdrawing group exhibited only a single oxidation. The first oxidation of Ni(T((*p*-CH_3)TPP) in CH_2Cl_2 yielded a brown coloured solution which corresponds to Ni(II)TPP^+. Removal of the second electron yielded a green coloured solution. Thus, Kadish and Morrison[10] proposed the mechanism.

$$[\text{ Ni(II)}(p\text{-X})\text{TPP}]^{\circ} \rightleftharpoons [\text{ Ni(II)}(p\text{-X})\text{TPP}]^{+} + e^{-}$$

$$[\text{Ni(II)}(p\text{-X})\text{TPP}]^{+} \rightleftharpoons [\text{ Ni(III)}(p\text{-X})\text{TPP}]^{2+} + e^{-}$$

They also pointed out that the metal reaction occurred after the cation radical was formed when X= electron – donating group while the process could be reversed for X = electron - withdrawing group.

Kadish et al.[11] reported the electron reduction of Ni[(T(*p*-X)PP)] where X = – Et_2N and (–Me_2N)F_4. Both the Ni(II)P were reduced in two reversible one electron transfer processes. The reduction potentials were presented in a table 1.1 as given below

Table 1.1

Half-Wave Potentials (V vs. SCE) for Electro-reduction of Ni(P) in THF, DMF or Py containing 0.1 M TBAP

Porphyrin	Solvent	1st reduction	2nd reduction	$\Delta E_{1/2}$ V
[Ni(T(*p*-Et_2N)PP)]	THF	-1.30	-1.77	0.47
	DMF	-1.32		
	Py	-1.30	-1.81	0.51
[Ni(T(*p*-Me_2N)PP)]	THF	-0.90	-1.39	0.48
	DMF	-0.89	-1.46	0.57
	Py	-1.08	-1.43	0.35

$\Delta E_{1/2}$ = difference between first and second reduction potential.

The large difference between the two reduction processes in DMF and pyridine were attributed to axial ligation by solvent molecules.

At room temperature both [Ni(T(*p*-Et_2N)PP)]$^-$ and [Ni(T(*p*-Me_2N)PP)]$^-$ in THF under N_2 atmosphere exhibited isotropic EPR spectra at g = 2.01 and ΔHpp = 10G

corresponding to Ni(II) porphyrins π - anion radicals. At low temperature under the same conditions, both showed anisotropy. The g values were g_{II} = 1.99 or 1.98, $g_{\perp}$ =2.01 and ΔHpp = 8.0G – 11.0G. The spectra were compared with that of the Ni tetraazamacrocycle complex in propylene carbonate and assigned to Ni(I) and Ni(II) π - anion radical hybrid.

The low temperature EPR spectra changed drastically when N_2 atmosphere was changed to CO atmosphere. The spectra became more anisotropic and showed three different g values. g_1 = 2.10, g_2 = 2.01 and g_3 = 1.99 for $[Ni(T(p\text{-}Et_2N)PP)]^-$ while g_1 = 2.16, g_2 = 2.06 and g_3 = 2.01 for $[Ni(T(p\text{-}Me_2N)PP)]^-$. A fifth co-ordination by CO was identified which was represented as

$Ni(II)(P) + e^- + CO \leftrightarrow [Ni(I)(CO)P]^-$. Similar EPR spectra of five co-ordinated non - porphyrin Ni(I) derivatives were reported.

It was shown that some solvent molecules co-ordinated to Ni as the fifth/sixth ligand. THF molecules weakly co-ordinated to the NiP and hence shown very little Ni(I) character. In contrast, solvents like DMF and pyridine strongly co-ordinated to $[NiP]^-$ and exhibited EPR spectra corresponding to Ni(I) complex at low temperature in N_2 atmosphere. In DMF the g values were 2.10, 2.01 and 1.93 for $[Ni(T(p\text{-}Et_2N)PP)]$ and 2.10, 2.00 and 1.95 for $[Ni(T(p\text{-}Me_2N)F_4PP)]$. Similar trends were observed in pyridine. It was also pointed out that the visible absorption bands had to be red shifted for the pyridine or DMF co-ordinated metalloporphyrin and the shift had to be larger for the soret band than the Q band.

1.4. COBALT PORPHYRIN

A brief review on the electrochemistry of CoP (P = TPP and substituted TPP) is presented. More emphasis is given to the oxidation potentials study by cyclic voltammetry.

Half-wave potentials data (V vs. SCE) of Co(II)TPP were reported in the literature[12-14]. Three oxidation potentials 0.32V, 1.06V and 1.26V were observed. The first wave was assigned to Co(II) → Co(III) oxidation while the other two to π - cation and dication of the ligand. In benzonitrile, oxidation potentials of 0.52V, 1.19V and 1.42V were obtained[15]. Three one-electron reversible oxidation steps were proposed as

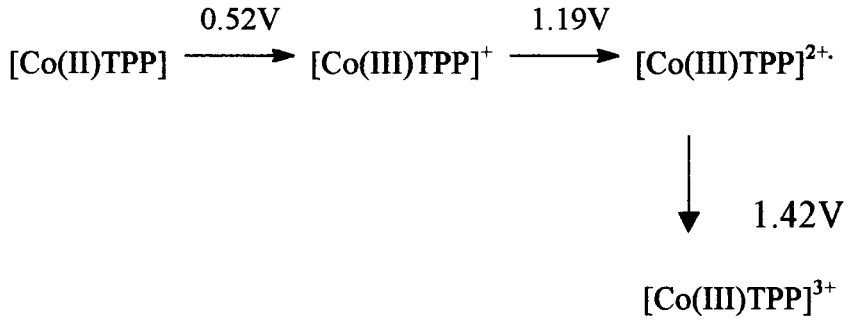

The first wave generated an EPR silent $[Co(III)TPP]^+$. This was due to the oxidation of $3d^7 \rightarrow 3d^6$. The second wave generated a paramagnetic species $[Co(III)TPP]^{2+\cdot}$, which exhibited a free radical signal. The third oxidation was also on the ligand and generated a diamagnetic dication.

Three reversible successive one-electron transfer oxidations were observed on oxidation of CoTPP in CH_2Br_2 / TBAP. The oxidation potentials were 0.78V, 0.97V

and 1.15V vs. SCE[16]. These values were almost identical with the values reported by Kadish et al[17,18].

One - electron oxidation of σ - bonded Cobalt porphyrins was characterised as Co(III) π - cation radicals and not Co(IV) porphyrins[20-23]. Migration of the σ - bonded of the organic ligand from the metal to nitrogen was also reported[19-24]. The possible electron transfer sites on the first oxidation of σ - bonded organo Co(III) porphyrins were also indicated[25]. The possible electron transfer sites were metal, π - electrons of the porphyrin ligand or σ-bonded axial organic ligand. The process depended on the solvent systems as well as the nature of the axial ligand. The rate of the R group migration was found to increase with the increased in the electron donor ability of R in the order Ph < Me <Et<Bu. The rate determining step was found to be the one in which the intra-molecular electron transfer was taken place from the R group to the Co(IV) metal of $[Co(R)(TPP)]^+$ It was observed that d^5 Co(IV) character was more if R was strong electron donor. Thus the following scheme was proposed as:

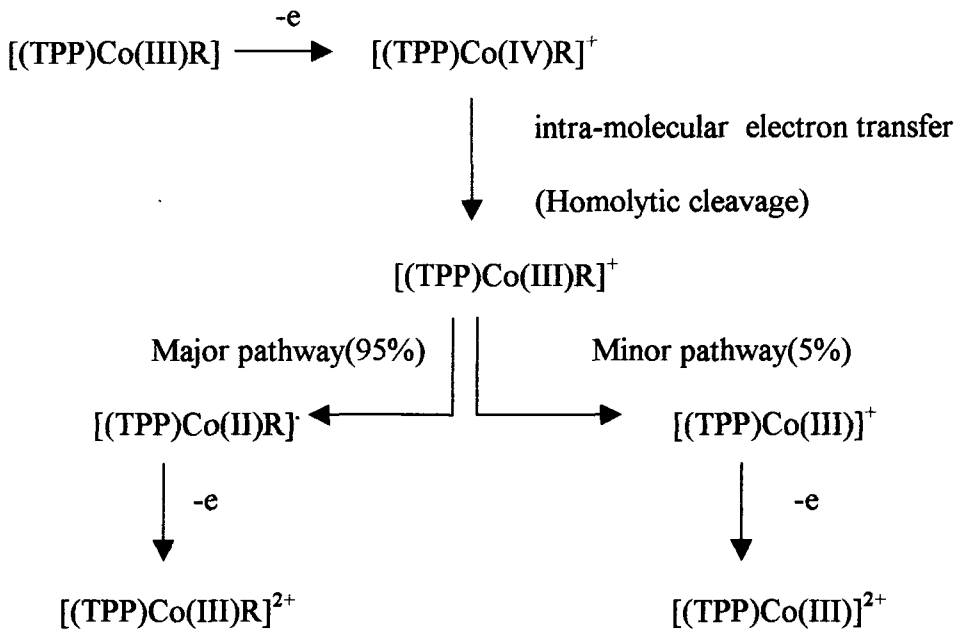

The cyclic voltammograms of [Co(R)(TPP)] where R = Ph / Me in acetonitrile/$CHCl_3$ (scan rate 100mV /s) at room temperature exhibited two reversible oxidations. The two reversible oxidation potentials were accounted for the slow migration of the σ- bonded axial ligands (i.e. formation of Co(IV) then electron transfer from the R group to the metal atom). On the contrary two anodic peaks without their corresponding cathodic peaks were observed for [(TPP)Co(Et)] and [(TPP)Co(Bu)] systems at room temperature. This was attributed due to very fast migration of the alkyl group. The voltammograms exhibited reversibility at 203K, which were attributed to the slow migration of the alkyl group. The oxidation potentials in neutral solvent such as CH_2Cl_2 were more positive than in solvent like MeCN/$CHCl_3$. This was due to $[(TPP)Co(R)(MeCN)]^+$.

The effect on the oxidation potentials were also observed due to the addition of base(L) such as pyridine. More significant effects were observed in UV-visible spectrum. The effect was also observed in the EPR spectra. The g values were increased as the pKa of the ligand increased. The higher the pKa value, more Co(IV) character was observed. Thus, $[(TPP)Co(R)(L)]^+$ showed d^5 Co(IV) character.

REFERENCES

1. C. M. Newton and D. G. Davis, *J. Magn. Resonance* **20**, 446 (1975).
2. G. E. Selyutin, A. A. Shklyaev and V. F. Anufrienko, *Dokl. Akad. Nauk. SSR*, **255**, 390 (1980).
3. M. Hoshino, S. Konishi, M. Imamura, S. Watanabe and Y. Hama, *Chem. Phys. Lett.* **102**, 259 (1983).
4. R. H. Felton, in " the porphyrins", Edited by Dolphin (Academic press, New York, 1979), Vol. V., p. 53.
5. D. G. Davis , in " the porphyrins", Edited by Dolphin (Academic press, New York, 1979), Vol. V., p. 127.
6. K. M. Kadish, D. Sazou, C. Araullo, Y. M. Liu, A. Saoiabi, M. Ferhat and R. Guilard, *Inorg. Chem.* **27**, 2313 (1988).
7. J. Subramanian, in "the porphyrins and metalloporphyrins", Edited by K.M. Smith (Elsevier, Amsterdam, 1975), p. 555.
8. A. Wolberg and J. Manassen, *Inorg. Chem.* **9, 10**, 2305 (1970).
9. D. Dolphin, T. Niem, R. H. Felton and I. Fujita, *J. Am. Chem. Soc.* **97**, 5288 (1975).
10. K.M. Kadish and M. M. Morrison, *Inorg. Chem.* **15**, 981 (1976).
11. K.M. Kadish and M. M. Franzen, B.C. Han, C. Araullo-McAdams and D. Sazou, *J. Am. Chem. Soc.* **113**, 512 (1991).
12. R. H. Felton and H. Linschitz, *J. Am. Chem. Soc.* **88**, 113 (1966).

13. A. Wolberg, *Isr. J. Chem.* **12**, 1031 (1974).

14. F. A. Walker, D. Beroiz and K. M. Kadish, *J. Am. Chem. Soc.* **98**, 3484 (1976).

15. A. Wolberg and J. Manassen, *J. Am. Chem. Soc.* **92**, 2982 (1970).

16. A. S. Hinman, B. J. Pavelich and K. Mc Garty, *Can. J. Chem.* **66**, 1589(1988).

17. X. Q. Lin and K.M. Kadish, *Anal. Chem.* **57**, 1498 (1985).

18. K.M. Kadish, in "progress in Inorganic Chemistry", Vol 34, Edited by S. J. Lippard (John Wiley, 1986), p. 435.

19. R. Guilard and K. M. Kadish, *Chem. Rev.* **88**, 1121 (1988).

20. D. Dolphin, D. J. Halko and E. Johnson, *Inorg. Chem.* **20**, 4348 (1981).

21. H. J. Callot, R. Cromer, R. A. Louati and M. Gross. Nouv. *J. Chem.* **8**, 765 (1984).

22. H. J. Callot and F. Metz, *J. Chem. Soc., Chem. Commun.* **947** (1982).

23 H. J. Callot and R. Cromer, *Tetrahedron Lett.* **26**, 3357 (1985).

24. K. M. Kadish, B.C. Han, and A. Endo, *Inorg. Chem.* **30**, 4502 (1981).

25. S.Fukuzumi, K. Miyamoto, T. Suenobu, E. V. Caemelbecke and K.M. Kadish, J. Am. Chem. Soc. **120**, 2880 (1998).

CHAPTER 2

EXPERIMENTAL SECTION

CHAPTER - 2

2.1. INTRODUCTION

This chapter describes the purification of solvents and reagents, preparation of supporting electrolytes, synthesis of porphyrins and metalloporphyrins. Brief descriptions of the EPR and CV instrumentation are also presented.

2.2. PURIFICATION SOLVENTS AND REAGENTS

2.2.1. Dichloromethane : Dichloromethane was refluxed with potassium carbonate (anhydrous) for 2hrs and allowed to stand overnight. It was distilled and stored over molecular sieves (Linde-4A).

2.2.2. Chloroform : Chloroform was purified by passing through a column of basic alumina and then the eluate was used directly.

2.2.3. Benzaldehyde : Benzaldehyde was washed thoroughly with NaOH solution to remove benzoic acid and then it was distilled.

2.2.4. Pyrrole : Pyrrole was purified by distillation under reduced pressure from KOH pellets and stored in a dark sealed vessel.

2.2.5. N-Bromosuccinimide : The commercial NBS was purified by recrystallisation from hot water and dried.

2.2.6. Methanol : Methanol was distilled and used.

2.2.7. The reagent grade, analytical grade such as $NiCl_2$(BDH) , vanadyl sulphate (CDH), Sodium acetate (S.Ds), pyridine (S.Ds) , acetic acid (MERCK) etc. were used as received.

2.3. PREPARATION OF SUPPORTING ELECTROLYTE

2.3.1. Preparation of tetrabutylammonium perchlorate (TBAP) :

TBAP was prepared according to the procedure as described[1] and thrice recrystallised from methanol.

2.3.2. Preparation of tetrabutylammonium hexafluorophosphate [TBA(PF_6)] :

It was purchased from Fluka and thrice recrystallised from ethanol.

2.4. SYNTHESIS OF PORPHYRINS AND METALLOPORPHYRINS

2.4.1. TPP : TPP was prepared by the method of Adler et al.[2] by the reaction of pyrrole and benzaldehyde in refluxing propionic acid. It was purified by the method of Badger et al.[3] and thrice recrystallised from benzene. The purity of the product was checked by TLC and UV-visible spectra.

λ_{max} (nm) (in chloroform): 449, 483, 514, 549, 590, 648.

2.4.2. Bromination of TPP : TPP was brominated by the method of Samuels et al.[4] or Callot[5] by refluxing the reaction mixture of meso-TPP and NBS in chloroform.

2.4.3. (T(*o*-Cl)PP) : It was prepared according to the Adler et al.[2] or Lindsey and Wagner[6]. It was also prepared by refluxing 2ml of freshly distilled pyrrole and 3.4ml of *o*-chloro benzaldehyde for 30minutes in 250ml of reagent grade propionic acid. The reaction mixture was cooled to room temperature and kept standing for 24hrs. The dark solid powder was collected by filtration on a buckner funnel and dried in a desiccator. The powdery solid was washed thoroughly with methanol till the greenish colour disappeared completely followed by hot water and air dried. The crude product was twice chromatographed on silica gel using chloroform as eluent. The product was

thrice recrystallised from chloroform - methanol (1:3) mixture and the purity was checked by TLC and UV-visible spectra.

λ_{max} (nm) (dichloromethane): 422, 480, 513, 545, 587, 644.

2.4.4. (T(*m*-Cl)PP) : The compound was prepared and purified according to the literature[7]. Also, we obtained a good product by the method of Adler et al.[2] as follows - the reaction mixture consisting of 1.1ml of freshly distilled pyrrole and 2.137g of *m*-chloro benzaldehyde was refluxed for 30 minutes in 150ml of propionic acid. The reaction mixture was cooled to room temperature, filtered in a buchner funnel and dried in the vacuum pump. The solid material was washed with methanol till the filtrate was colourless and followed by hot water and air dried.

The product was chromatographed using chloroform as eluent. The product was rechromatographed using benzene as eluent. The eluate was evaporated to dryness and thrice recrystallised from chloroform – methanol (1:3). The purity of the product was checked by TLC and UV-visible spectra.

λ_{max} (nm) (dichloromethane): 422, 483,513,547, 588, 646.

2.4.5. (T(*p*-Cl)PP) : The compound was prepared as described above for T(*m*-Cl)PP.

λ_{max} (nm) (dichloromethane): 423, 484, 514,549,591, 648.

2.4.6. (T(*o*-CH_3)PP) : The compound was prepared by the method of Lindsey and Wagner[6]. It was modified by refluxing the reaction mixture containing 3ml of freshly distilled pyrrole and 5.02ml of *o*-methyl benzaldehyde in 250ml of reagent grade

propionic acid for 30minutes. The reaction mixture was cooled to room temperature and kept standing for 6 days. The solid material was collected by filtration on a buchner funnel and dried in a vacuum pump. The powdery solid was washed thoroughly with methanol till the greenish colour disappeared followed by hot water and air dried. The crude product was twice chromatographed in dry silica gel eluting in benzene and then recrystallised from chloroform – methanol (1:3). The purity of the product was checked by TLC and UV - visible spectra.

λ_{max} (nm) (dichloromethane): 418, 484, 514, 549, 588, 645

2.4.7. (T(*m*-CH_3)PP) : The compound was prepared according to the procedure as described above for T(*o*-CH_3)PP.

λ_{max} (nm) (dichloromethane): 419, 486, 515, 551, 590, 647

2.4.8. (T(*p*-CH_3)PP) : The compound was prepared according to the procedure as described in the literature[7-9].

λ_{max} (nm) (dichloromethane): 420, 486, 516, 552, 591, 649

2.4.9. (T(*m*-NO_2)PP) : The compound was prepared according to the procedure of Bettelheim et al.[10] and also a good product was obtained by refluxing 1.7ml of freshly distilled pyrrole, 3.775g of *m*-nitro benzaldehyde (sigma chemical) and 300 ml of reagent grade propionic acid for 30minutes. The reaction mixture was cooled to room temperature and kept standing for 18hrs. The reaction mixture was filtered on a Buchner funnel and dried in the vacuum pump to remove the propionic acid. The solid material was dissolved in chloroform and kept in the dark for 36 days. The chloroform

was recovered, evaporated to dryness and washed with methanol followed by hot water till the filtrate was colourless. The product was purified by column chromatography using a mixture of benzene and chloroform. The purity of the product was checked by TLC and UV-visible spectra.

λ_{max} (nm) (dichloromethane): 423, 484, 515, 549, 590, 648.

2.4.10. (T(*m*-F)PP) : It was prepared according to the procedure described by Adler et al[2]. The reacting materials were 1.3ml of freshly distilled pyrrole, 2ml of *m*-fluoro benzaldehyde and 150ml of propionic acid. The compound was chromatographed by using benzene as eluent. The product was rechromatographed from chloroform. It was thrice recrystallised in chloroform-methanol (1:3). The purity of the product was checked by TLC and UV-visible spectra.

λ_{max} (nm) (dichloromethane): 419, 484, 515, 549, 589, 644

2.4.11. (T(*m*-OCH_3)PP) : It was prepared according to the standard procedure[7].

λ_{max} (nm) (dichloromethane): 423, 484, 515, 550, 589, 644

2.4.12. (T(*p*-OCH_3)PP) : It was prepared according to the literature[7].

λ_{max} (nm) (dichloromethane): 424, 488, 518, 556, 593, 651

2.4.13. (T(*o*-Br)PP) : It was prepared and purified as described above for T(*o*-Cl)PP.

λ_{max} (nm) (dichloromethane): 422, 482, 514, 544, 588, 655.

2.4.14. (T(*m*-Br)PP) : It was prepared and purified as described above for T(*o*-Cl)PP.

λ_{max} (nm) (dichloromethane): 422, 483, 514, 544, 589, 651.

2.4.15. (T(*p*-Br)PP) : The reaction mixture consisting of 0.51ml of freshly distilled pyrrole, 1.3852g of *p*-bromo benzaldehyde was added to 150ml of reagent grade propionic acid and refluxed for 30minutes. The reaction mixture was cooled to room temperature, filtered on a buchner funnel and dried in the vacuum pump. The solid material was washed thoroughly with methanol till the greenish colour disappeared followed by hot water and air dried.

Purification : The crude product was dissolved in chloroform and chromatographed on silica gel. The second fraction yielded bright purple colour crystal. Using a mixture of benzene and chloroform rechromatographed the first fraction. The purity of the product was checked by TLC and UV - visible spectra. The final product was twice recrystallised from chloroform - methanol(1:3).

λ_{max}(nm) (dichloromethane): 423, 484, 515, 550, 590, 646.

2.4.16. VOTPP(Br) : The complex was prepared as described in the literature[9,11] by refluxing 20ml of glacial acetic acid, 10ml of pyridine, 350ml of vanadyl sulphate and 200mg of TPP(Br) for 8hrs. The reaction mixture was extracted with chloroform and washed with water till the greenish colour disappeared. It was dried over anhydrous sodium sulphate, filtered and evaporated to dryness. The crude product was purified by column chromatography on silica gel with chloroform elution. The product was thrice recrystallised from chloroform – methanol (1:3) and the purity was checked by TLC and UV-visible spectra.

λ_{max} (nm) (dichloromethane): 423, 548.

Similarly VOTPP(Br)$_2$, VOTPP(Br)$_3$ and VOTPP(Br)$_4$ were prepared by the above procedure.

VOTPP(Br)$_2$: λ_{max} (nm) (in dichloromethane): 425, 549

VOTPP(Br)$_3$: λ_{max} (nm) (in dichloromethane): 427, 558

VOTPP(Br)$_4$: λ_{max} (nm) (in dichloromethane): 430, 591

2.4.17. The phenyl substituted vanadyl porphyrins were synthesised according to the procedure as described above VOTPP(Br)$_2$.

VO(T(*o*-Cl)PP) : λ_{max} (nm) (dichloromethane): 421, 546

VO(T(*m*-Cl)PP) : λ_{max} (nm) (dichloromethane): 422, 548

VO(T(*p*-Cl)PP) : λ_{max} (nm) (dichloromethane): 422, 546

VO(T(*o*-CH_3)PP) : λ_{max} (nm) (dichloromethane): 422, 546

VO(T(*m*-CH_3)PP) : λ_{max} (nm) (dichloromethane): 422, 547

VO(T(*p*-CH_3)PP) : λ_{max} (nm) (dichloromethane): 423, 548

VO(T(*m*-NO_2)PP) : λ_{max} (nm) (dichloromethane): 423, 546

VO(T(*m*-F)PP) : λ_{max} (nm) (dichloromethane): 421, 545

VO(T(*m*-OCH_3)PP) : λ_{max} (nm) (dichloromethane): 423, 547

VO(T(*p*-OCH_3)PP) : λ_{max} (nm) (dichloromethane): 428, 550

VO(T(*o*-Br)PP) : λ_{max} (nm) (dichloromethane): 423, 548

VO(T(*p*-Br)PP) : λ_{max} (nm) (dichloromethane): 423, 547

2.4.18. NiTPP(Br) : The complex was prepared by refluxing 250mg of TPP(Br) with 60ml of glacial acetic acid, 30ml of pyridine, 490mg of sodium acetate, 400mg of $NiCl_2$ till the reaction was completed. The reaction mixture was extracted with chloroform and washed with water till the greenish colour disappeared. The reaction mixture was dried over anhydrous sodium sulphate, filtered and evaporated to dryness. The crude product was purified by column chromatography on silica gel with chloroform elution. The product was thrice recrystallised from chloroform – methanol (1:3) and the purity was checked by TLC and UV-visible spectra. Similarly, $NiTPP(Br)_2$, $NiTPP(Br)_3$ and $NiTPP(Br)_4$ were prepared.

NiTPP(Br) : λ_{max} (nm) (dichloromethane): 416, 527

$NiTPP(Br)_2$: λ_{max} (nm) (dichloromethane): 419, 527

$NiTPP(Br)_3$: λ_{max} (nm) (dichloromethane): 420, 532

$NiTPP(Br)_4$: λ_{max} (nm) (dichloromethane): 426, 541

2.4.19. The phenyl substituted Nickel porphyrins were prepared by the same procedure described above NiTPP(Br)

Ni(T(*m*-NO_2)PP) : λ_{max} (nm) (dichloromethane): 413, 526

Ni(T(*o*-CH_3)PP) : λ_{max} (nm) (dichloromethane): 412, 525

Ni(T(*m*-CH_3)PP) : λ_{max} (nm) (dichloromethane): 413, 526

Ni(T(*p*-CH_3)PP) : λ_{max} (nm) (dichloromethane): 414, 528

Ni(T(*m*-OCH_3)PP) : λ_{max} (nm) (dichloromethane): 412, 526

Ni(T(*p*-OCH_3)PP) : λ_{max} (nm) (dichloromethane): 418, 530

2.4.20. CoTPP(Br) : The complex was synthesised by the method of Adler et al.[12] It was chromatographed on silica gel by using benzene as eluent. The purity of the product was checked by TLC and UV-visible spectra. λ_{max} (nm) (dichloromethane): 411, 529

Similarly, $CoTPP(Br)_2$, $CoTPP(Br)_3$ and $CoTPP(Br)_4$ were synthesised by the same procedure as described above.

$CoTPP(Br)_2$: λ_{max} (nm) (dichloromethane): 413, 531

$CoTPP(Br)_3$: λ_{max} (nm) (dichloromethane): 415, 547

$CoTPP(Br)_4$: λ_{max} (nm) (dichloromethane): 420, 557

2.4.21. The phenyl substituted cobalt complexes were prepared by the same procedure as described above. The purity of the complexes were checked by TLC and UV-visible spectra.

Co(T(*o*-Cl)PP) : λ_{max} (nm) (dichloromethane): 409, 527

Co(T(*m*-Cl)PP) : λ_{max} (nm) (dichloromethane): 409, 527

Co(T(*p*-Cl)PP) : λ_{max} (nm) (dichloromethane): 416, 529

Co(T(*o*-CH_3)PP) : λ_{max} (nm) (dichloromethane): 409, 528

Co(T(*m*-CH_3)PP) : λ_{max} (nm) (dichloromethane): 410, 527

Co(T(*p*-CH_3)PP) : λ_{max} (nm) (dichloromethane): 412, 527

Co(T(*o*-Br)PP) : λ_{max} (nm) (dichloromethane): 410, 530

Co(T(*m*-Br)PP) : λ_{max} (nm) (dichloromethane): 411, 528

Co(T(*p*-Br)PP) : λ_{max} (nm) (dichloromethane): 412, 527

Co(T(*m*-NO_2)PP) : λ_{max} (nm) (dichloromethane): 410, 527

Co(T(*m*-F)PP) : λ_{max} (nm) (dichloromethane): 409, 526

Co(T(*m*-OCH_3)PP) : λ_{max} (nm) (dichloromethane): 409, 528

Co(T(*p*-OCH_3)PP) : λ_{max} (nm) (dichloromethane): 413, 530

2.5. INSTRUMENTATION:

2.5.1 CYCLIC VOLTAMMETRIC MEASUREMENTS :

Cyclic voltammograms were obtained with a three electrode system using a PAR model 174 polarographic analyser and a universal programmer model 175 coupled with a digigraphic recorder. The working electrode was a Beckman platinum rod and a platinum strip served as the auxiliary electrode. A commercial saturated Calomel Electrode (SCE) was used as the reference electrode and was separated from the bulk of the solution by a fritted glass septum. Deaeration was accomplished by bubbling N_2 gas through the solution for about 8–10 minutes prior to the recording. Nitrogen blanketed the solution during the recordings.

2.5.2. EPR MEASUREMENTS:

EPR spectra were obtained at room temperature as well as at liquid nitrogen temperature with E109(Varian) X-band spectrometer at 100 KHz modulation. For liquid nitrogen measurements a Cold Finger Dewar has been employed. Oxidation were carried out in EPR tube by dropping $SbCl_5$. All measurements were done after deaerating by bubbling N_2 gas through the solution in the tube. The g values were determined by using DPPH as reference (g =2.0036).

REFERENCES

1. H. O. House, Feng, Edith and N. P. Peet, *J. Org. Chem.* **36**(16), 2371-2374(1971).
2. A. D. Adler, F. R. Longo, J. D. Finarelli, J. Goldmacher, J. Assour, and L. Karsakoff, *J. Org. Chem.* **32**, 476 (1967).
3. G. M. Badger, R. A. Jones, and R. L. Laslet, *Aust. J. Chem.* **17**, 1028 (1964).
4. E. Samuels, R. Shuttleworth, and T. S. Stevens, *J. Chem. Soc.(C).* 145(Pt-1) (1968).
5. H. J. Callot, *Bulletin de la Society 'Chinnique de France'*, 7-8, (1974).
6. J. S. Lindsey and R. W. Wagner, *J. Org. Chem.* **54**, 828-836 (1989).
7. D. W. Thomas and A. E. Martell, *J. Am. Chem. Soc.* **78**, 1335-1338 (1956).
8. D. W. Thomas and A. E. Martell, *J. Am. Chem. Soc.* **78**, 1338-1343 (1956).
9. K. Uneo and A. E. Martell, *J. Phys. Chem.* **60**, 934-938 (1956).
10. A. Bettelheim, B. A. White, S. A. Raybuck, and R.W. Murray, *Inorg. Chem.* **26**, 1009-1017 (1987).
11. J. G. Erdman, V. G. Ramsay, N. W. Kalenda, and W. E. Hanson, *J. Am. Chem. Soc.* **78**, 5844-5847 (1956).
12. A. D. Adler, F. R. Longo, F. Kampus and *J. Kim, J. Inorg. Nucl. Chem.* **32**, 2443 (1970).

CHAPTER 3

CV AND EPR STUDIES OF THE OXIDATION PRODUCTS OF VOTPP AND SUBSTITUTED VOTPP

CHAPTER – 3

3.1. INTRODUCTION

Generally, a metalloporphyrin possessed a D_{4h} symmetry where the two highest π - molecular orbitals a_{1u} and a_{2u} are close lying and are nearly degenerate. The energy difference between them is about 0.5 eV or less. These energy levels are affected by the nature of the central metal ion as well as the type of substituents on the porphyrin ring[6]. MTPP (M = metal atom) generally have a_{2u} ground state[7]. One electron oxidation of such system generates π - cation having the unpaired spin density more on the nitrogen atoms of the porphyrin ring. Thus, it gives a triplet state, which can be studied by EPR.

On the other hand the effect on the energy levels will be reflected in the redox potentials. Therefore, cyclic voltammetric study of the substituted metalloporphyrins will give us the information about the changes in the redox potentials[4,5].

3.2. CYCLIC VOLTAMMETRY OF SOME SUBSTITUTED VANADYL MESO - TETRA PHENYL PORPHYRINS

The effect on the redox potentials due to the substituents on the periphery of porphyrin ring is available in literature[1,8-10]. But no proper information on the redox potentials of substituted vanadyl meso-tetraphenyl porphyrins is available in the literature. One can study the effect on the redox behaviour by substituting the exo-positions (i.e.α and β) of the pyrrole ring or different substituents on the phenyl rings.

Even substituents on both the pyrrole and phenyl ring can be done. However, the effect on the redox potentials is more pronounced if the substitution is in the pyrrole ring rather than the phenyl ring[8].

With this background information we investigated redox behaviour of some substituted vanadyl meso-tetraphenyl porphyrins using cyclic voltammetric technique.

3.3. CYCLIC VOLTAMMETRY OF VANADYL MONO-, DI, TRI AND TETRA BROMO MESO -TATRAPHENYL PORPHYRINS.

A. RESULTS

(i) VOTPP(Br) : The voltammogram of 10^{-3} M VOTPP(Br) in CH_2Cl_2 show two reversible one – electron oxidations (Fig.3.1.1). The first oxidation potential is 1.22V and the second oxidation potential is 1.46V (table 3.1). Their corresponding ΔE values are 0.18V and 0.17V respectively.

(ii) VOTPP(Br_2) : The voltammogram of 10^{-3} M VOTPP(Br_2) in CH_2Cl_2 is presented in the figure 3.1.2. Two reversible one-electron transfer oxidations are exhibited in the voltammogram. Oxidation potentials are 1.26V and 1.5V with their ΔE values 0.19V and 0.20V (table 3.1) respectively.

(iii) VOTPP(Br_3) : Successive one electron transfer oxidation of VOTPP(Br_3) 10^{-3} M solution in CH_2Cl_2 is presented in the figure 3.1.3. The oxidation potentials are 1.26V and 1.49V and $\Delta E_1 = 0.19V$ and $\Delta E_2 = 0.20V$ (table 3.1)

(iv) VOTPP(Br_4): 10^{-3} M solution of VOTPP(Br_4) in CH_2Cl_2 give two reversible one electron transfer oxidations with oxidation potentials 1.26V and 1.47V. Their ΔE values are 0.17V and 0.18V (table 3.1).

B. DISCUSSION

Except for the VOTPP(Br) no appreciable change in the oxidation potentials are observed. The first oxidation potentials for VOTPP(Br_2), VOTPP(Br_3) and VOTPP(Br_4) are same. There is very negligible change in the second oxidation potentials. It is to be noted that the oxidation potentials are shifted more towards positive potential in compared to that of the VOTPP. The first oxidation potentials are shifted by 0.22 ± 0.04V while the second oxidation potentials are shifted by 0.24 ± 0.04V. Electrophilic substitutions in the pyrrole ring of the porphyrin macrocycle have effect on the oxidation potential of the metalloporphyrin and shift the oxidation potentials to higher positive values. The constancy of Δ_{ox} ($\approx$ 0.22 ± 0.04V) is maintained. From these observations one can conclude that oxidations occur in the porphyrin ligand. The oxidation process is represented by the following scheme:

$$[VO(TPP)Xn] \underset{+e}{\overset{-e}{\rightleftharpoons}} [VO(TPP)Xn]^{+}$$

(1.12 - 1.26) V vs. SCE

$$+e \uparrow\downarrow -e$$

$$[VO(TPP)Xn]^{2+}$$

(1.47 - 1.50) V vs. SCE

where X = Br, n = 1 to 4

3.4. CYCLIC VOLTAMMETRY OF VO(T(*o*-X)PP),VO(T(*m*-X)PP), VO(T(*p*-X)PP))]VO, X = Cl, Br, F and NO_2

A. RESULTS

All complexes mentioned above show similar voltammograms. The voltammograms consists of two one- electron oxidation waves (figure 3.1.4). Their cyclic voltammetric results are summerised in the table 3.1. All potentials are measured against standard SCE.

VO(T(*o*-Cl)PP) : E_p^a (I) is 1.32V and E_p^a (II) is 1.46V while their ΔE values are 0.12V, 0.11V and $E_{1/2}$ values are 1.25V and 1.40V respectively. This gives the value of Δ_{ox} = 0.15V.

VO(T(*m*-Cl)PP) : E_p^a values are 1.25V and 1.47V while that $E_{1/2}$ values are 1.22V and 1.44V. ΔE values are 0.07V and 0.12V. The ΔE_{ox} = 0.22V.

VO(T(*p*-Cl)PP) : E_p^a values are 1.23V and 1.46V while that $E_{1/2}$ values are 1.16V and 1.39V respectively. ΔE values are 0.14V and 0.14V.

VO(T(*o*-Br)PP); VO(T(*p*-Br)PP) and VO(T(*m*-F)PP) : Their voltammetric data are summarised in the table 3.1.

For VO(T(*m* - NO_2)PP), the first and the second oxidation potentials are 1.34V and 1.58V respectively. Their $E_{1/2}$ values are 1.28V and 1.51V while ΔE values are 0.12V and 0.13V respectively.

B. DISCUSSION

All VOTPP substituted by halogens in the phenyl ring show similar voltammograms. Their oxidation potentials do not vary much. In fact very small changes are observed. Ortho – substituted show largest positive oxidation potentials shift. Meta and para substituted potentials show lesser positive shifts. Of the three substitutions lowest potential shift is shown by the *p*-substituted one. Variations are observed in the first oxidation potentials with very little variation in the second oxidation potentials. Both the first and the second oxidations for all these complexes occur in the ligand.

The oxidation potentials of VO(T(*m*-NO_2)TPP) are higher than any of the vanadyl porphyrins we have undertaken for the measurements. Comparing with the oxidation potentials of VOTPP, the first oxidation potential is shifted by 0.289V while the second oxidation by 0.288V. Shifts are quite uniform and large. As –NO_2 is a strong electron-withdrawing group; the oxidation potentials are shifted positively to higher potentials making oxidation difficult. The oxidation process is represented as

$$[VO(T(p\text{-}X)\ PP)] \underset{+e}{\overset{-e}{\rightleftharpoons}} [VO(T(p\text{-}X)\ PP)]^{+}$$

$E_1/_2$ (I)

+e ⇅ -e

$[VO(T(p\text{-}X)PP)]^{2+}$

$E_1/_2$(II)

where X = Cl, Br, F and NO_2

Similarly, meta and ortho substituted porphyrins takes place in the same reaction pathway.

3.5. CYCLIC VOLTAMMETRY OF VO(T(*o*-X)PP) , VO(T(*m*-X)PP) and VO(T(*p*-X)PP), X = CH_3, OCH_3

A. RESULTS

Voltammograms consists of two reversible successive one – electron transfer oxidation waves are obtained for all six vanadyl porphyrins (figure 3.1.5). The oxidation potentials of OCH_3 substituted and CH_3 substituted porphyrins are lower than those halogens substituted VOTPP complexes. The results are summarised in the table 3.1. The first and the second oxidations for VO(T(*m* - OCH_3)PP) are 1.16V and 1.35V and for VO(T(*p* - OCH_3)PP) are 1.10V and 1.29V respectively. Their $E_{1/2}$ values are 1.10V, 1.30V and 1.04V, 1.23V respectively. Their ΔE values are 0.12V,

0.11V and 0.12V, 0.12V respectively. All the methyl substituted vanadyl porphyrins, the first oxidation potentials are almost the same i.e. 1.17 ± 0.01V and the second oxidation potentials are 1.41± 0.01V. But their $E_{1/2}$ values differ. For para substituted the values are 1.07V and 1.32V, for meta 1.09V and 1.33V while for ortho 1.12V and 1.36V.

B. DISCUSSION

There are differences in $E_{1/2}$ values of VO(T(*m* - OCH_3)PP) and VO(T(*p* - OCH_3)PP) . The $E_{1/2}$ values are higher for the former. In the case of *p*, *m* and *o*-CH_3 substituted VOTPP, the oxidation potentials do not exhibit any variations. Their $E_{1/2}$ values show some variations. It changes from 1.32V to 1.36V from para to ortho. Of the two substitutions viz. OCH_3 and CH_3, the former is more electron donating while the later is a weak electron donating group. But no difference in the oxidation potentials are observed. The $E_{1/2}$ value is the largest when the substitution is in the ortho position. The reason for this may be due to more steric hindrance, which increases the energy barrier for phenyl ring rotation. Thus, the phenyl ring contribution to the resonance reduces. In other words, the phenyl ring is more out of plane of the porphyrin ring when the substitution is in the ortho position. In contrast, the oxidation potentials are decreased when the substitution is in the para position. This is because phenyl ring is more in plane with the porphyrrin macrocycle, hence more resonance contribution.

Of all the complexes, the lowest $E_{1/2}(1)$ value is observed for VO(T(*p* - OCH_3)PP) followed by VO(T(*p* - CH_3)PP). In general the oxidation steps can be represented by the following scheme:

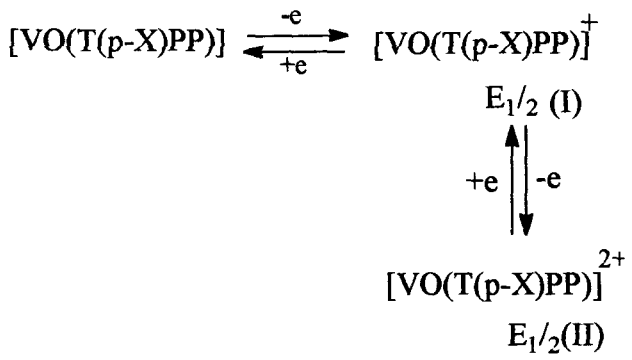

where X = CH_3 and OCH_3.

Meta and ortho substituted vanadyl porphyrins takes place in the same reaction pathway.

3.6. EPR OF SOME SUBSTITUTED VANADYL MESO -TETRAPHENYL PORPHYRINS OXIDISED WITH $SbCl_5$.

3.6.1. EPR OF THE OXIDATION OF VOTPP

To compare the oxidation products of the substituted VOTPP, we carried out the room temperature EPR measurements of VOTPP oxidation with $SbCl_5$. In the course of our measurements we observed some EPR signals, which were not reported in the literature[2] earlier. Thus, we discuss here the room temperature EPR of the oxidation of VOTPP with $SbCl_5$.

A. EPR MEASUREMENTS

Oxidations are carried out in the EPR tube. To the solution of VOTPP in CH_2Cl_2 (10^{-3} M), $SbCl_5$ is added dropwise using 1mm (ID) capillary. Addition of $SbCl_5$ as well as the EPR measurements are all done after deaerating the solution by bubling N_2 gas.

B. RESULTS AND DISCUSSION

The spectra of VOTPP oxidation with $SbCl_5$ are presented in the figure 3.2.1(a-f). With the first drop of $SbCl_5$ the spectrum (3.2.1a) is obtained which changed to spectra (3.2.1b) and (3.2.1c) on addition of more $SbCl_5$. Further addition of $SbCl_5$ produced the spectrum (3.2.1d) which turned to spectrum (3.2.1e) and spectrum (3.2.1f) on excess addition of $SbCl_5$. Spectrum (3.2.1a) shows splitting of lines which on further addition of $SbCl_5$ exhibit additional lines on both ends (figure 3.2.1b) and subsequently followed inversion of the intensity of lines. The oxidation steps can be represented as follows:

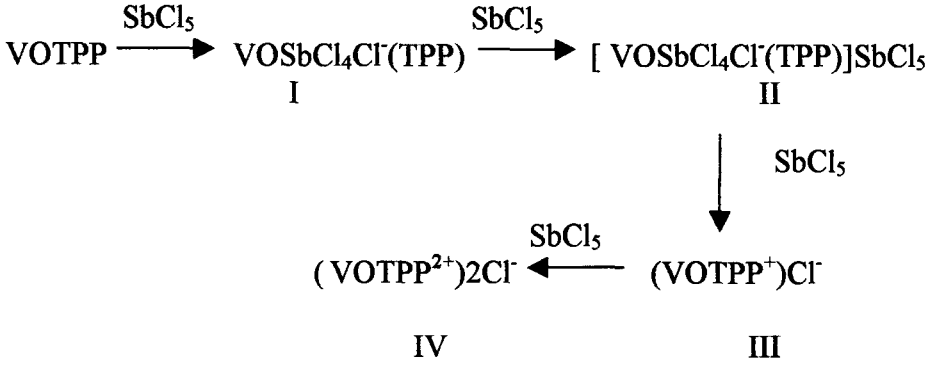

The pre-oxidised species I and II are observed at room temperature (figure 3.2.1(a, b & c)). The EPR signal of the species III i.e. $VOTPP^{+}$ (supposed to be triplet state with S = 1) does not vanish completely at room temperature but broadens out. This is observable at higher modulation as a broad signal (figure 3.2.1(e)). We have not measured it at 77K because reports on the EPR of the triplet state of VOTPP are available in the literature[3]. The formation of mono cation is further supplemented by IR spectrum[12,13] which shows a new band at 1272.76 cm^{-1}. The authenticity of the IR spectra of mono cation is checked by IR spectra of $SbCl_5$ solution 10^{-2}M) in CH_2Cl_2 which do not show any accountable band around 1272-1290cm^{-1}. The spectrum (3.2.1f) is due to the dication i.e. $VOTPP^{2+}$ (species IV). The coupling constant (80Gauss) of the $VOTPP^{2+}$ is slightly lesser than that of the unoxidised VOTPP. The broad triplet state signal at room temperature is not reported in the literature. This points to a considerable unpaired electron spin density in a_{1u}. Thus the ground state of VOTPP is not purely in a_{2u} state. However, it requires more careful theoretical calculations.

3.6.2. EPR OF THE OXIDISED VO(T(*m*-NO_2)PP)

It is observed that most of the substituted VOTPP undergo oxidations similar to that of VOTPP.

A. RESULTS

Oxidation of [VO(T(*m*-NO_2)PP)] with $SbCl_5$ produces $[VO(T(m\text{-}NO_2)PP)]^{+}$ giving rise to a very broad EPR signal at room temperature (Figure 3.2.3(a)). On freezing it to 77K gives a triplet state spectrum (figure 3.2.3(b)). Half-field signal characteristic

of ^{51}V nucleus is observed at g = 3.75 (figure 3.2.3(d)). On checking the reversibility no demetallation is observed.

B. DISCUSSION

The low temperature (77K) spectra are quite similar to the one we observed earlier for the vanadyl meso-porphyrin[14]. In the light of this similarity we adopted the same Hamiltonian which is reported elsewhere (also presented in the appendix B). Diagonalisation of the Hamiltonian is done considering the system to be axial symmetry and powder spectrum is obtained by averaging over all angular orientations using Gaussian quadrature method. The value of A and D are varied so as to match the experimentally obtained spectrum.

For an axially symmetric systems

$D_{x'x'} = D_{y'y'} = -D_{z'z'}/2$ ..... (3.1)

And $D_{II} = D_{x'x'} = D_{y'y'} = -D_{z'z'}/2$ ..... (3.2)

$D_{z'z'}$ (in MHz) = $1.298 \times 10^4 g^2/R^3$ .....(3.3)

where R is express in Angstrom

And $g^2 = (g_{II}^2 + 0.5g_{\perp}^2)$ .....(3.4)

Thus, a simulated spectrum (figure 3.2.3(c)) is obtained which fairly matches with the experimentally obtained spectrum. Using the experimental parameters and considering the dipolar coupling between the two electrons as the only major factor or dominant factor for the zero – field splitting interaction, an inter – electron distance of

3.619 ± 0.03Å is obtained. Considering a larger D value i.e. D = 0.04cm^{-1} an inter-electron distance of 3.575 ± 0.05Å is obtained. For D = 0.036cm^{-1} an inter-electron distance of 3.73 ± 0.05Å is obtained. Surprisingly no appreciable change in the simulated spectrum is obtained. This points to a possibility of having a considerable unpaired electron spin density in a_{1u} although the density is more in a_{2u} for MTPP (M = metal ion) system. Non vanishing EPR spectrum of the π - cation at room temperature suggest that there is a considerable unpaired π - electron spin density in a_{1u}. This may be the reason for observing large ΔE values in the voltammogram. The value of ΔE is rather large for one-electron transfer oxidation. At the moment we do not have any theoretical backing for this view but such admixture of states do occur in Co porphyrins. However, it is to be noted that shorter inter – electron distance (3.619 ± 0.030Å) points to a more dominant a_{2u} ground state.

3.6.3. EPR OF THE OXIDATION OF VOTPP(Xn), (X = Br, n = 1 to 4)

The room temperature EPR spectra of brominated VOTPP show same type of EPR spectra. The oxidation steps can be represented by the same scheme as that of the VOTPP oxidation. The formation of mono cation in all cases is supported by UV-visible spectra (figure 3.3.1) as well as by IR spectra. In the case of VOTPP(Br_4) the mono cation is characterised by appearance of a new band at 1266cm^{-1}. The formation of cation and the reversibility is checked by neutralising the $SbCl_5$ using dimethylamine (figure 3.3.1). The room temperature EPR of the oxidation of VOTPP(Br_4) is the same as that of the VOTPP oxidation (figure 3.2.4(A-D)). The low

temperature EPR spectrum of the oxidised VOTPP(Br) with $SbCl_5$ is presented in the figure 3.2.2. The EPR data are presented in the table 3.2. From the spectrum we obtained g_{II} =1.920, $g_{\perp}$ = 1.969, $A_{\perp}$ = 2.450 and half - field signal at g = 3.7.

A. RESULTS

Oxidation of all four brominated vanadyl TPP with $SbCl_5$ follows the same pattern as that of TPPVO and VO(T(*m*-NO_2)PP). Since no differences in the EPR spectra are observed, we present the room temperature EPR spectra of VOTPP(Br_4) and the low temperature EPR spectrum VOTPP(Br).

Room temperature oxidation of VOTPP(Br_4) with $SbCl_5$ exhibit spectrum (3.2.4A) (with 2 drops of $SbCl_5$) followed by spectrum (3.2.4B) (with 6-8 drops of $SbCl_5$). Further addition of $SbCl_5$ yield spectra (3.2.4C) and (3.2.4D) on excess of $SbCl_5$.

The triplet state EPR spectrum of VOTPP(Br) is presented in the figure 3.2.2. The EPR data are presented in the table 3.2. The spectrum does not differ from the triplet spectrum of VO(T(*m*-NO_2)PP). The following EPR parameters are obtained:

At room temperature g = 1.98 and at 77K g_{II}= 1.92, $g_{\perp}$ = 1.969, A_{II} = 4.260 (Gauss) and $A_{\perp}$ = 2.540 (Gauss)

B. DISCUSSION

The pre-oxidised complexes I and II yield the spectra (3.2.4A) and (3.2.4B) respectively. The spectrum (3.2.4C) corresponds to the complex III, which is a triplet state. At room temperature the EPR signal does not vanish completely and is

observable at higher modulation. The formation of the cation is supplemented by IR bands 1266cm^{-1}.

The triplet state of $[VOTPP(Br)]^+$ exhibit the spectrum quite similar to that of $VO(T(m\text{-}NO_2)PP)]^+$. The EPR parameters do not vary much. An inter – electron distance of 3.619 ± 0.030Å is obtained.

The oxidation steps of $VOTPP(Br_4)$ is represented as

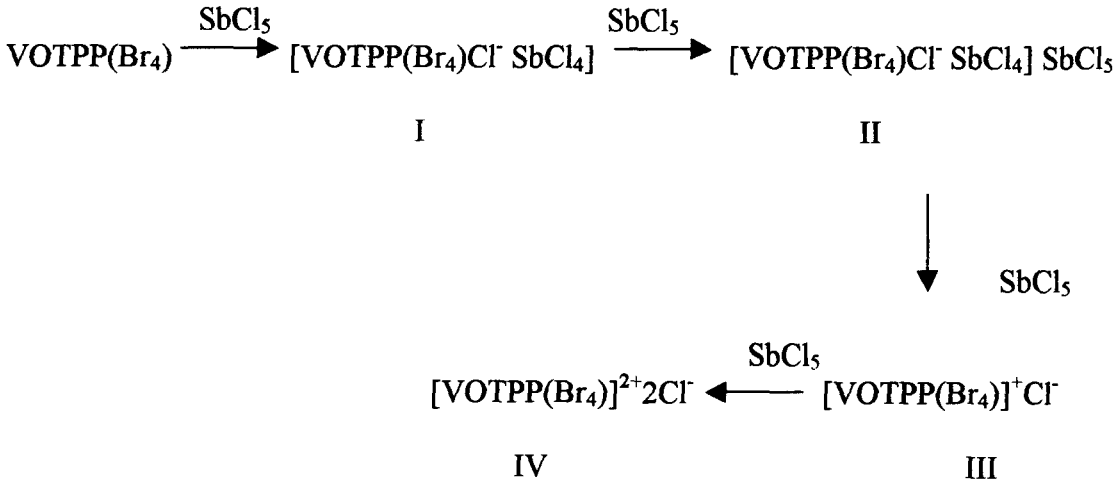

3.6.4. EPR OF THE OXIDATION OF VO(T(*p*-X)PP), VO(T(*m*-X)PP) and VO(T(*o*-X)PP), X = Cl, Br, F, CH_3, OCH_3

A. **EPR measurements:** All complexes show similar EPR spectra at room temperature. The triplet states are generated at room temperature, since the spectra do not vanishes. Then we freeze it down to 77K.

B. RESULTS

All triplet state spectra are similar with that of the triplet state spectra of VOTPP and VO(T(*m*-NO_2)PP). EPR results are summarized in the table 3.2. Triplet state EPR spectra of VO(T(*o*-Cl)PP) and VO(T(*o*-CH_3)PP) at room temperature as well as at 77K are presented here along with their half-field spectrum(figure 3.2.5 and 3.2.6).

C. DISCUSSION

For all the complexes, two g – values are observed at 77K ($g_{\parallel}$ and $g_{\perp}$). Analysis of these spectra are done in the same manner as we have done for VO(T(*m*-NO_2)PP). Theoretical back ground of the analysis is given in the appendix B. The EPR spectra and their parameters are not affected significantly by different substituents. Using the EPR data inter-electron distances between the unpaired electron on the metal atom and the unpaired electron on the ligand of the different vanadyl porphyrins are obtained. The values are as given below:

3.619Å for VO(T(*m*-NO_2)PP)

3.625Å for VO(T(*m*-F)PP)

3.603Å for VO(T(*o*-Cl)PP)

3.613Å for VO(T(*m*-Cl)PP)

3.610Å for VO(T(*p*-Cl)PP)

3.623Å for VO(T(*o*-Br)PP)

3.618Å for VO(T(*p*-Br)PP)

3.619Å for VOTPP(Br)

3.629Å for VO(T(*o*-CH_3)PP)

3.656Å for VO(T(*m*-CH_3)PP)

3.632Å for VO(T(*m*-OCH_3)PP)

No significant change in the inter-electron distance is observed. Thus, we can take an average distance of 3.623 ± 0.030Å. In fact this distance is shorter than the one reported for VO(meso) (3.88 ± 0.05Å). This points to an a_{2u} ground state.

3.7. UV-VIS CHARACTERISATION OF THE OXIDATION AND REDUCTION OF SOME VANADYL PORPHYRINS

To characterise the oxidations and subsequent reductions of VOTPP(X_n) where X = Br, n = 1 to 4 and VO(T(*p*-X)PP), VO(T(*m*-X)PP) and VO(T(*o*-X)PP), X=Cl, Br, F, NO_2, CH_3 and OCH_3, UV-vis measurements are done in CH_2Cl_2 using $SbCl_5$ as oxidant and dimethylamine as the reducing agent. The results are summarised in the table 3.3.

For most of the complexes, soret band is blue shifted on oxidation and Q bands become very broad. For VO(T(m-NO_2)PP), VOTPP(Br) no change are observed. VOTPP(Br) and VOTPP(Br_3) show 1nm red shifts. The blue shift for VOTPP(Br_4) is 1nm while for VO(T(*o*-Cl)PP) and VO(T(*m*-Cl)PP) it is 2nm. The largest blue shift is observed for VO(T(*o*-CH_3)PP), which is 9nm while VO(T(*m*-CH_3)PP) and VO(T(*p*-

CH_3)PP) shifts are 7nm and 4nm respectively. For VO(T(*m*-F)PP), VO(T(*m*-OCH_3)PP) and VO(T(*o*-Br)PP) and VO(T(*p*-Br)PP) the shifts are 8nm. No particular trends for electron donating and electron withdrawing substitutions are observed. Therefore, on the basis of the shift in soret band no generalisation can be made.

3.8 CONCLUSION

From the cyclic voltammetric study of the substituted vanadyl meso-tetraphenyl porphyrins, we observed the followings:

(i) Electrophilic substitutions in the exo-positions (i.e. α, β positions) of the pyrrole ring shift the oxidation potentials to more higher positive potentials. In the case of VOTPP(X_n) where X = Br and n = 1 to 4, oxidation potentials are shifted by 0.22V to 0.26V vs. SCE for the first oxidation potential and by 0.23V to 0.27V vs. SCE for the second oxidation. No linearity in the shift is observed.

(ii) Substitutions in the phenyl ring with electron-withdrawing groups shift the oxidation potentials to higher positive potentials. In the case of VO(T(*p*-X)PP), VO(T(*m*-X)PP) and VO(T(*o*-X)PP) where X= Cl, Br, F and NO_2, the shifts for the first oxidation is by 0.22V to 0.34V vs. SCE while the shifts for the second oxidation is by 0.29V to 0.36V vs. SCE. The largest shift is observed for VO(T(*m*-NO_2)PP). Ortho substitutions show higher potential shifts because of the steric hindrance while para substitutions show the least.

(iii) Substitution in the phenyl ring with electron donating group lower the potential shift but the oxidation potentials are higher than the oxidation potentials of the unsubstituted VOTPP. The potentials are shifted by 0.01V to 0.18V vs. SCE for

the first oxidation and by 0.07V to 0.22V vs. SCE for the second oxidation. The lowest shifts are observed for VO(T(*p*-OCH_3)PP) and the highest shifts are observed for VO(T(*o*-CH_3)PP).

For all the redox couples, the ΔE values are observed to be quite large for one – electron transfer redox process.

No significant changes due to substitutions are observed in the EPR spectra. EPR parameters show different values but overall spectra show almost the same pattern. On the average an inter-electron distance of 3.623 $\pm$ 0.030Å is obtained. The shorter distance points to an a_{2u} ground state for the substituted VOTPP. However, there seems to be non-negligible a_{1u} ground state.

Formation of the cations is supported by IR spectra as well as by the UV-visible spectra.

Table 3. 1

Redox potentials (VOLTS vs. SCE) for VOTPP, VOTPP(X_n), X = Br, n = 1 to 4 and VO(T(*o*-X)PP), VO(T(*m*-X)PP), and VO(T(*p*-X)PP), X = Cl, Br, NO_2, CH_3 and OCH_3 in CH_2Cl_2 ($\approx 10^{-3}$ M) using TBAP as supporting electrolyte. Scan rate 100mV/s (at room temperature).

Compound	$E_p^a(I)$	$E_p^a(II)$	$E_p^c(I)$	$E_p^c(II)$	ΔE_1	ΔE_2	$E_{1/2}(I)$	$_{1/2}(II)$
TPP[a]	1.00	1.22	1.32	0.94	0.32	0.10	0.97	1.27
TPP(Br)	1.22	1.46	1.28	1.05	0.18	0.18	1.14	1.37
TPP(Br_2)	1.26	1.50	1.29	1.06	0.19	0.20	1.16	1.40
TPP(Br_3)	1.26	1.49	1.29	1.07	0.19	0.20	1.17	1.39
TPP(Br_4)	1.26	1.47	1.29	1.09	0.17	0.18	1.17	1.38
T(*o*-Cl)PP	1.32	1.46	1.35	1.18	0.14	0.11	1.25	1.40
T(*m*-Cl)PP	1.25	1.47	1.35	1.18	0.07	0.12	1.22	1.44
T(*p*-Cl)PP	1.23	1.46	1.32	1.09	0.14	0.14	1.16	1.39
T(*o*-Br)PP	1.30	1.43	1.30	1.16	0.14	0.13	1.23	1.37
T(*p*-Br)PP	1.22	1.44	1.33	1.11	0.11	0.11	1.16	1.38
T(*m*-F)PP	1.27	1.51	1.34	1.11	0.16	0.17	1.19	1.42
T(*m*-OCH_3)PP	1.16	1.35	1.24	1.04	0.12	0.11	1.10	1.30
T(*p*-OCH_3)PP	1.10	1.29	1.17	0.98	0.12	0.12	1.04	1.23
T(*o*-CH_3)PP	1.18	1.42	1.30	1.06	0.12	0.12	1.12	1.36
T(*m*-CH_3)PP	1.17	1.41	1.25	1.01	0.17	0.17	1.09	1.33
T(*p*-CH_3)PP	1.17	1.42	1.22	0.97	0.21	0.20	1.07	1.32
T(*m*-NO_2)PP	1.34	1.58	1.45	1.23	0.12	0.13	1.28	1.51

[a]reference 1

Table 3.2.

EPR parameters of the oxidation of VOTPP(Br), VO(T(*o*-X)PP), VO(T(*m*-X)PP) VO(T(*p*-X)PP), X = Cl, F, Br, NO_2, CH_3 and OCH_3 with $SbCl_5$ in CH_2Cl_2 ($\approx 10^{-3}$ M)

Compound	R(Å)	Oxidized g value at room temp.	Oxidized g value at room temperature		Oxidized A(G) value at low temperature	
			$g_{\parallel}$	$g_{\perp}$	$A_{\parallel}$	$A_{\perp}$
T(*m*-NO_2)PP	3.619	1.987	1.919	1.975	3.560	1.950
T(*m*-F)PP	3.625	1.994	1.929	1.996	0.404	0.055
T(*o*-Cl)PP	3.603	1.987	1.919	1.965	4.800	2.935
T(*m*-Cl)PP	3.613	1.994	1.922	1.976	3.280	1.854
T(*p*-Cl)PP	3.610	1.998	1.925	1.974	3.370	2.050
T(*o*-Br)PP	3.623	1.995	1.937	1.989	0.849	0.576
T(*p*-Br)PP	3.618	1.992	1.920	1.976	3.389	0.506
TPP(Br)	3.619	1.988	1.920	1.969	4.260	2.540
T(*o*-CH_3)PP	3.629	1.992	1.974	1.916	4.390	2.050
T(*m*-CH_3)PP	3.656	1.987	1.958	1.994	0.900	0.850
T(*m*-OCH_3)PP	3.632	1.979	1.937	1.979	2.103	1.559

Table 3.3

UV-vis data of Unoxidised, Oxidised and Reduced products of VOTPP, VOTPP(X_n), X = Br, n = 1 to 4, VO(T(*o*-X)PP), VO(T(*m*-X)PP) and VO(T(*p*-X)PP) in CH_2Cl_2 containing 0.5M $SbCl_5$(at room temperature)

	λ, nm				
	Unoxidised		Oxidation	Reduction of the oxidised species with dimethylamine	
Porphyrin	Soret	Q	Soret	Soret	Q
TPP[a]	423	547			
TPP(Br)	423	548	424	423	502(sh), 548
TPP(Br_2)	425	549	416, 425	426	514(sh), 550
TPP(Br_3)	427	558	428	428	554, 607
TPP(Br_4)	430	591	426, 429(sh)	432	556, 605
T(*o*-Cl)PP	421	546	410	422, 437(s)	500(sh), 546
T(*m*-Cl)PP	422	548	420(sh), 444	422, 476	511, 546
T(*p*-Cl)PP	422	546	417	422, 437(sh)	504(sh), 547
T(*o*-CH_3)PP	422	546	413, 424(sh)	421, 477	510(sh), 546
T(*m*-CH_3)PP	422	547	415	423	502(sh), 547
T(*p*-CH_3)PP	423	548	419, 478(sh)	424	502(sh), 548
T(*m*-NO_2)PP	423	546	423, 439(sh)	424, 440(s)	502(sh), 548, 603
T(*m*-F)PP	421	545	413, 502(s)	421, 436	502(sh), 545
T(*m*-OCH_3)PP	423	547	415	424	502(sh), 546
T(*p*-OCH_3)PP	428	550	427	427	550
T(*o*-Br)PP	423	548	415	423, 437(s)	548
T(*p*-Br)PP	423	547	415	424	547

[a]reference 15

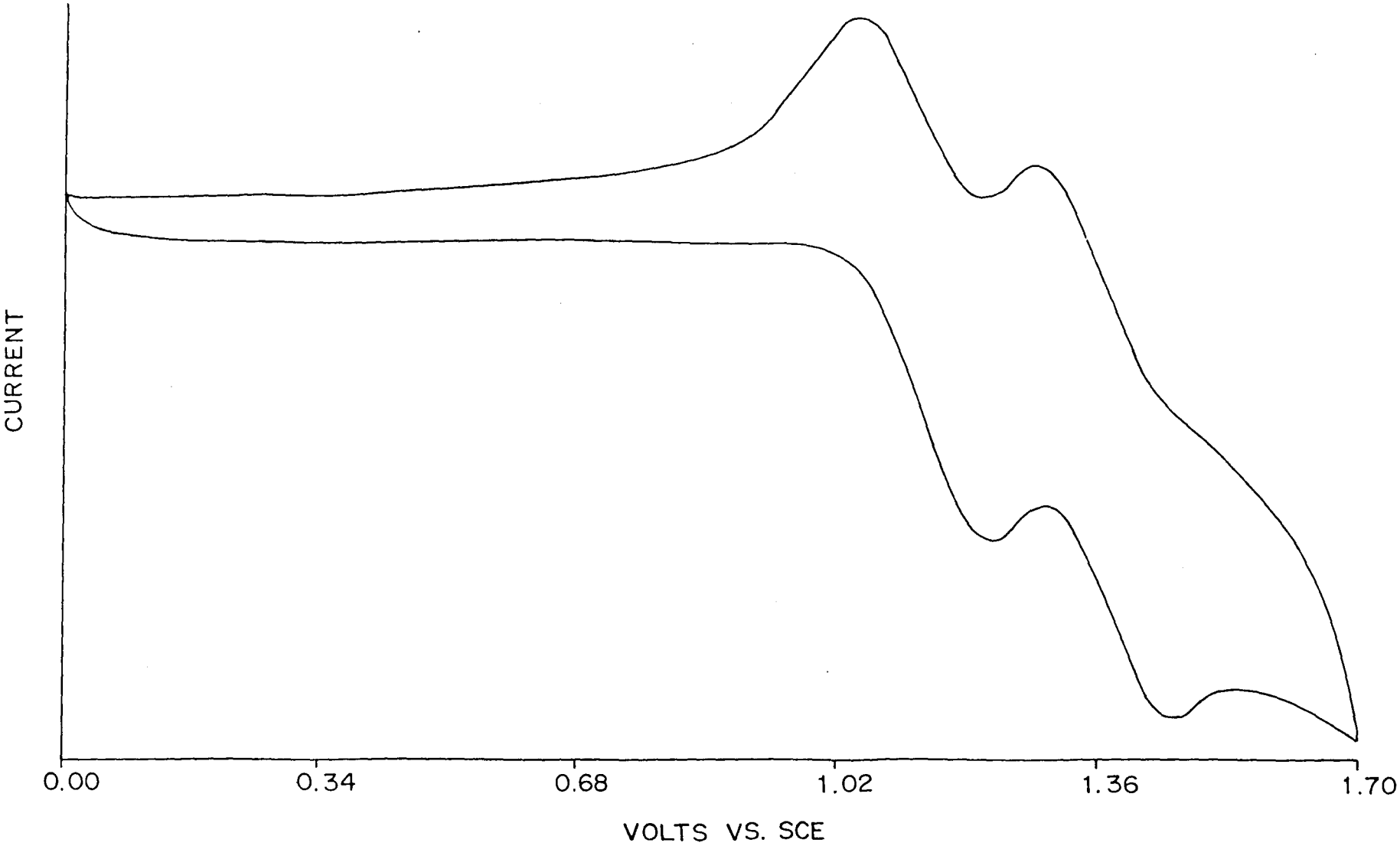

Figure 3.1.1. Cyclic voltammogram of VOTPP(Br) in CH_2Cl_2 containing 0.1 M TBAP at room temperature. Scan rate 100 mV/s

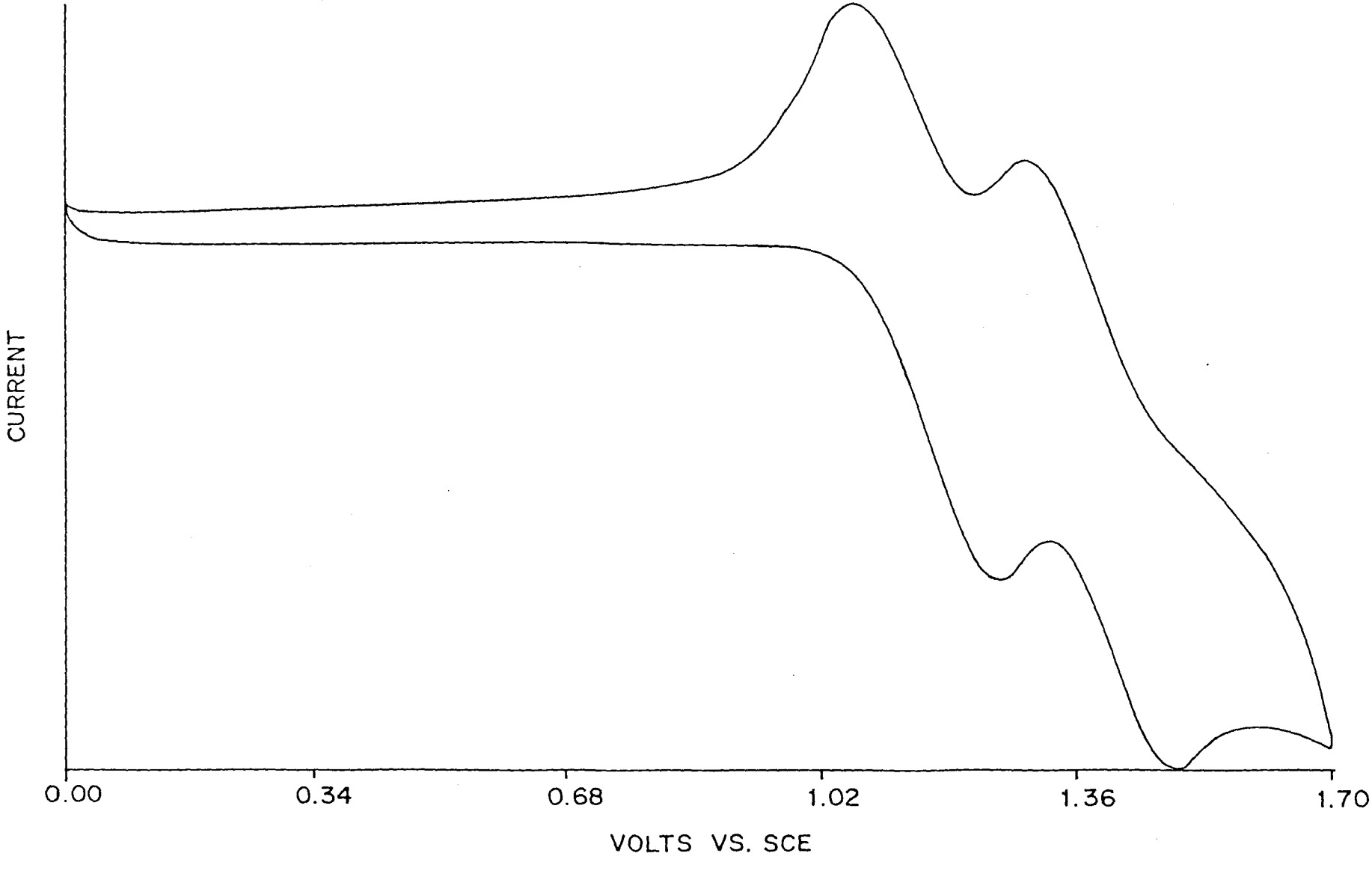

Figure 3.1.2. Cyclic voltammogram of VOTPP(Br_2) in CH_2Cl_2 containing 0.1 M TBAP at room temperature. Scan rate 100 mV/s

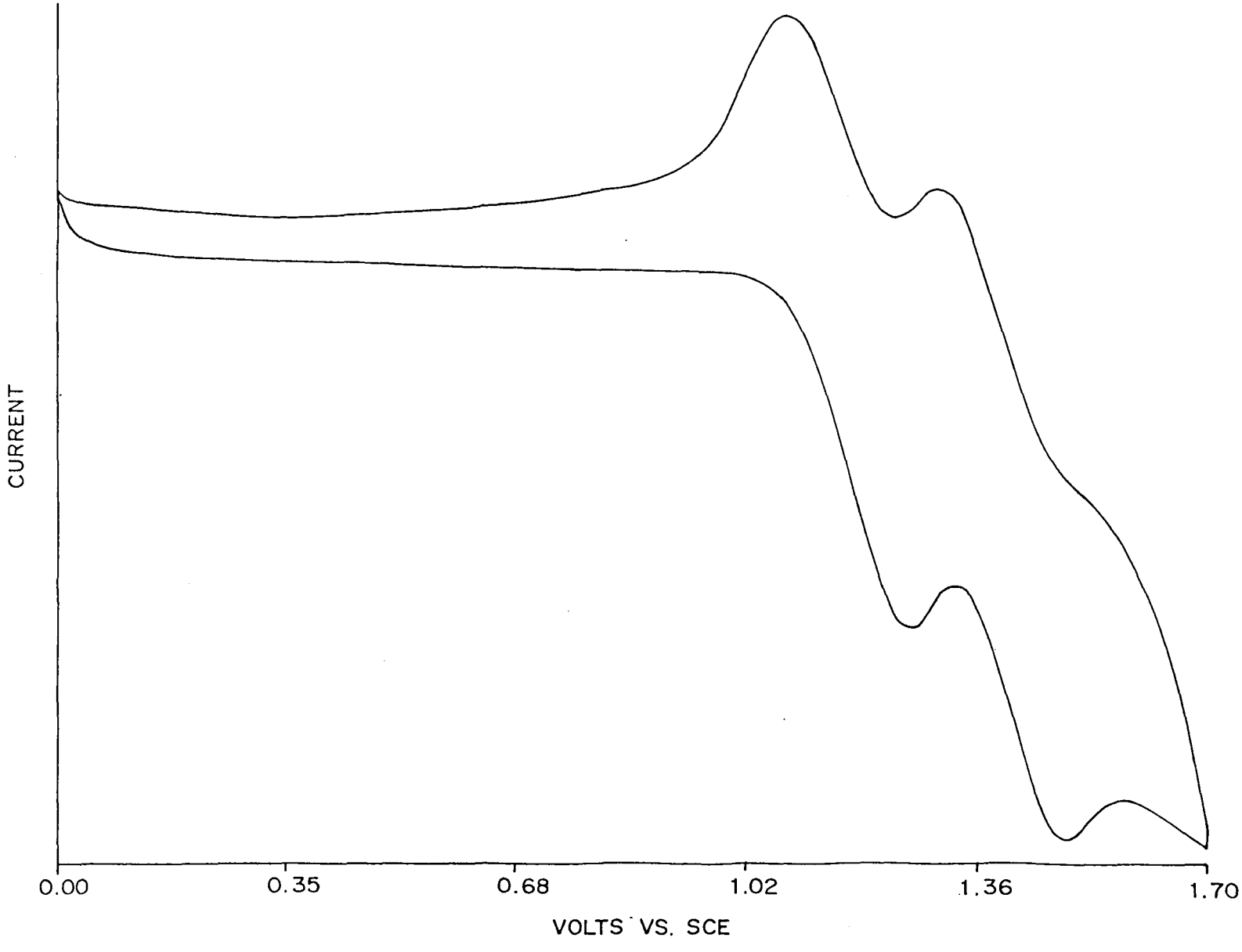

Figure 3.1.3. Cyclic voltammogram of VOTPP(Br_3) in CH_2Cl_2 containing 0.1 M TBAP at room temperature. Scan rate 100 mV/s

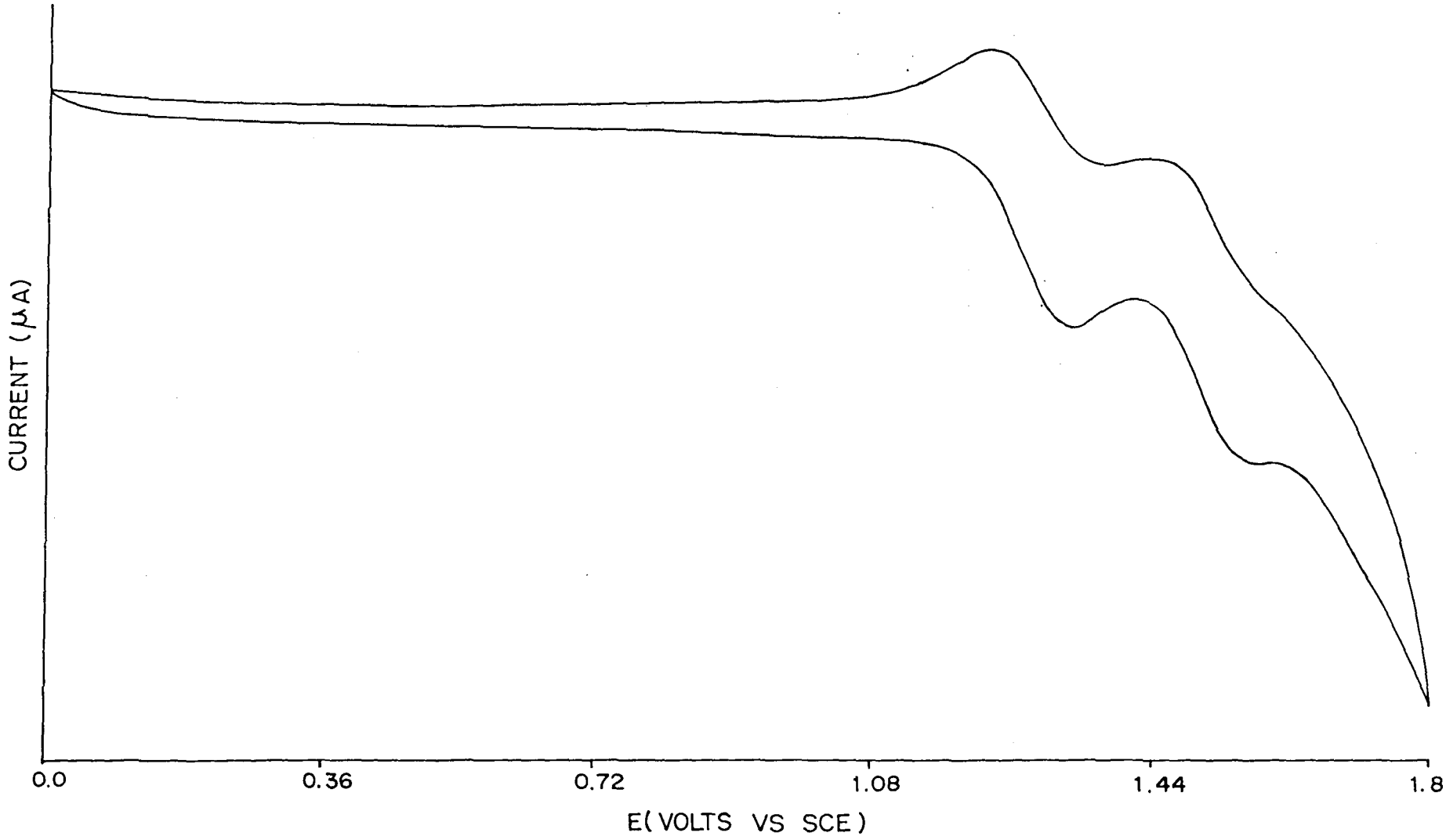

Figure 3.1.4. Cyclic voltammogram of VO(T(*m*-NO_2)PP) in CH_2Cl_2 containing 0.1 M TBAP at room temperature. Scan rate 100 mV/s

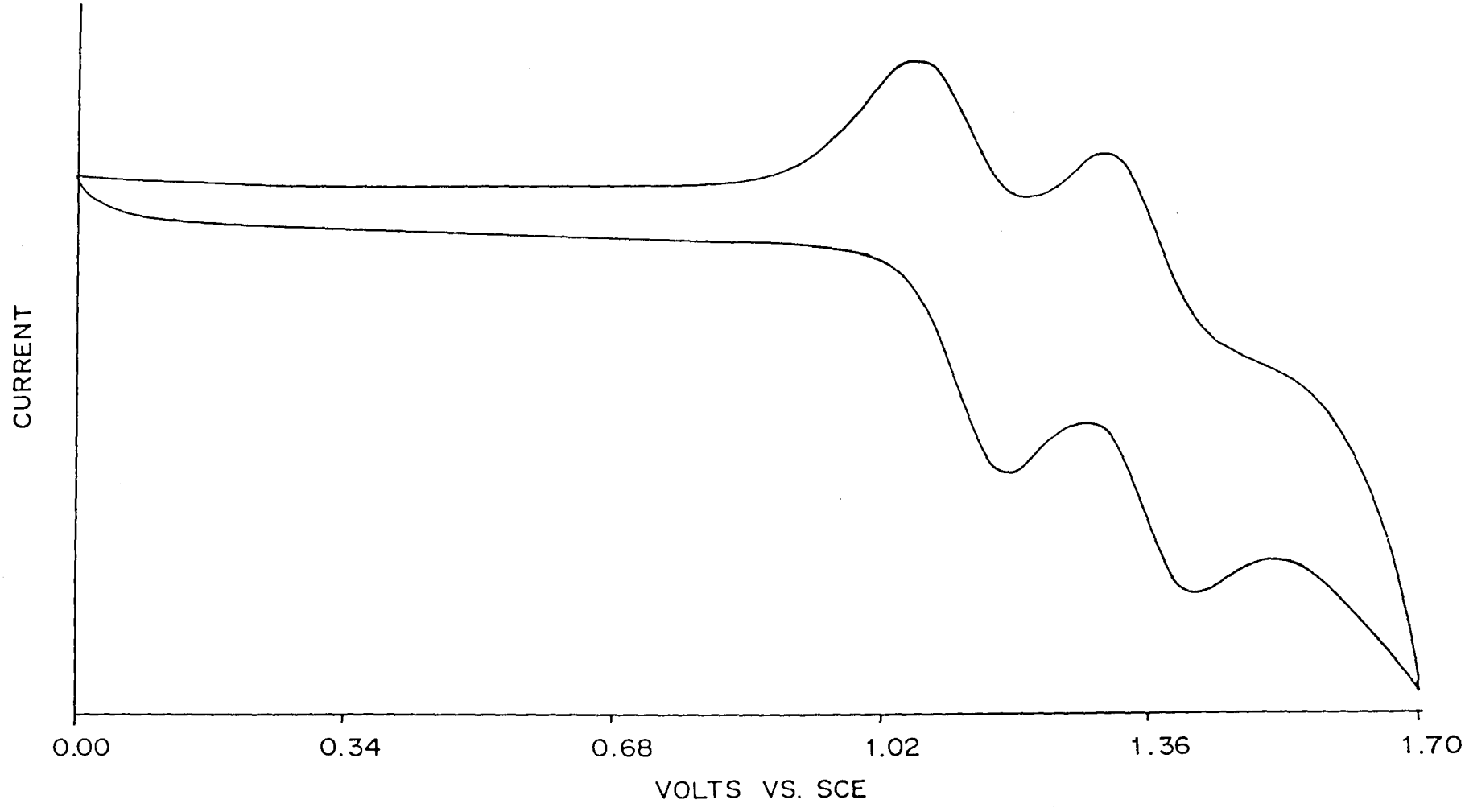

Figure 3.1.5. Cyclic voltammogram of VO(T(*o*-CH_3)PP) in CH_2Cl_2 containing 0.1 M TBAP at room temperature. Scan rate 100 mV/s

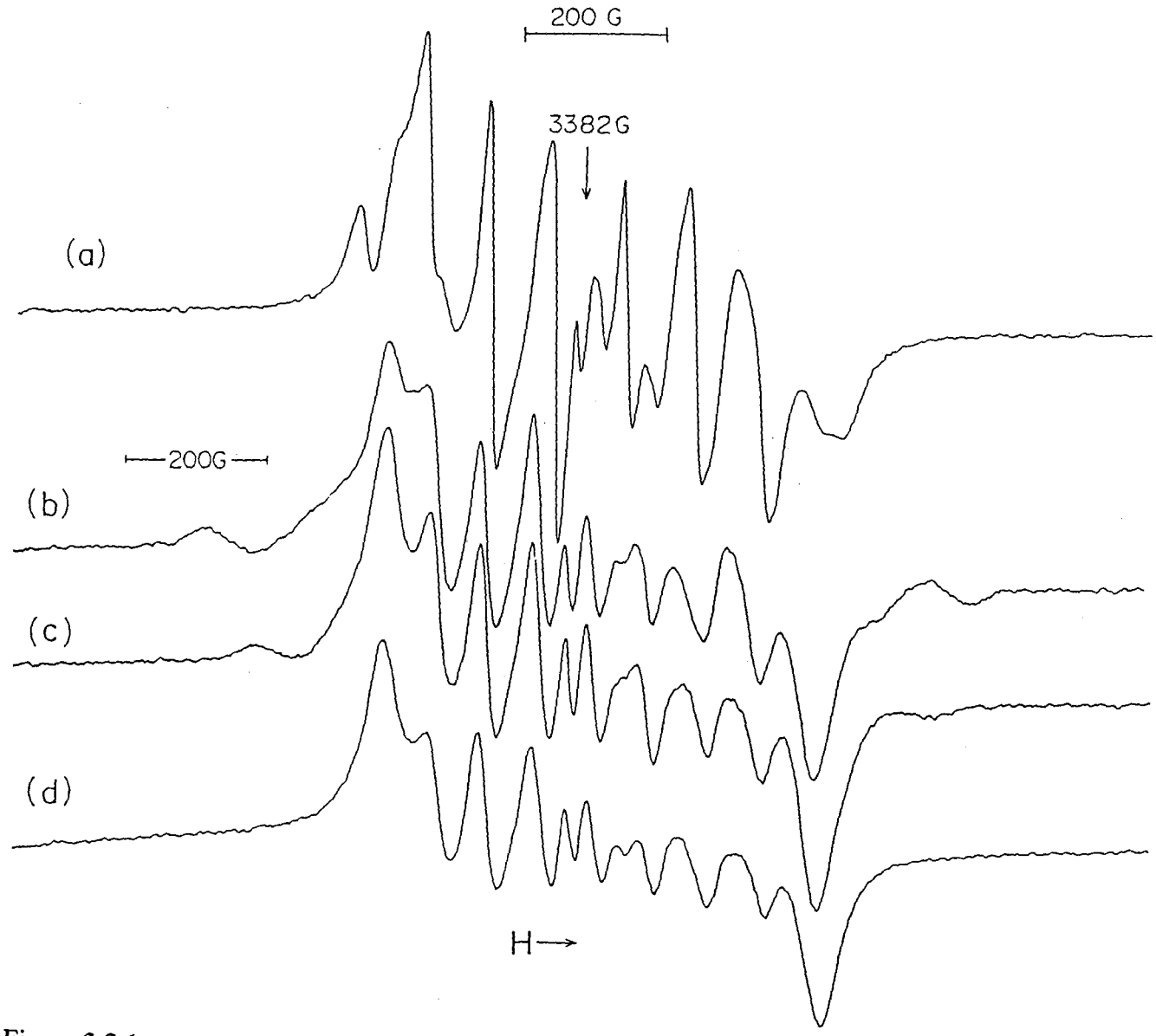

Figure 3.2.1. X – band EPR spectra of VOTPP in CH_2Cl_2 oxidised with $SbCl_5$ (a) species I , (b), (c) and (d) species II at room temperature

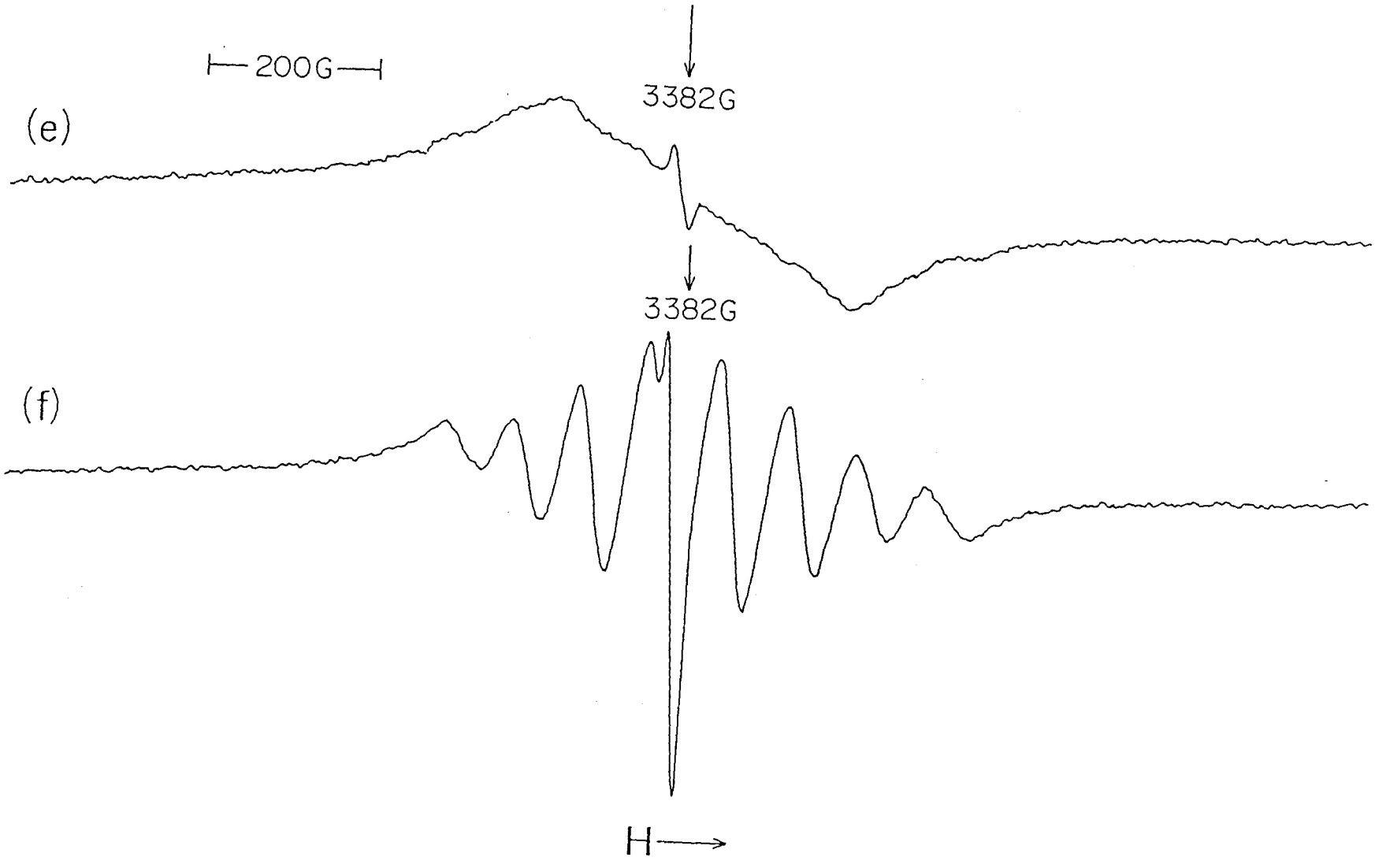

Figure 3.2.1. X – band EPR spectra of VOTPP in CH_2Cl_2 oxidised with $SbCl_5$ (e) species III and (f) species IV at room temperature

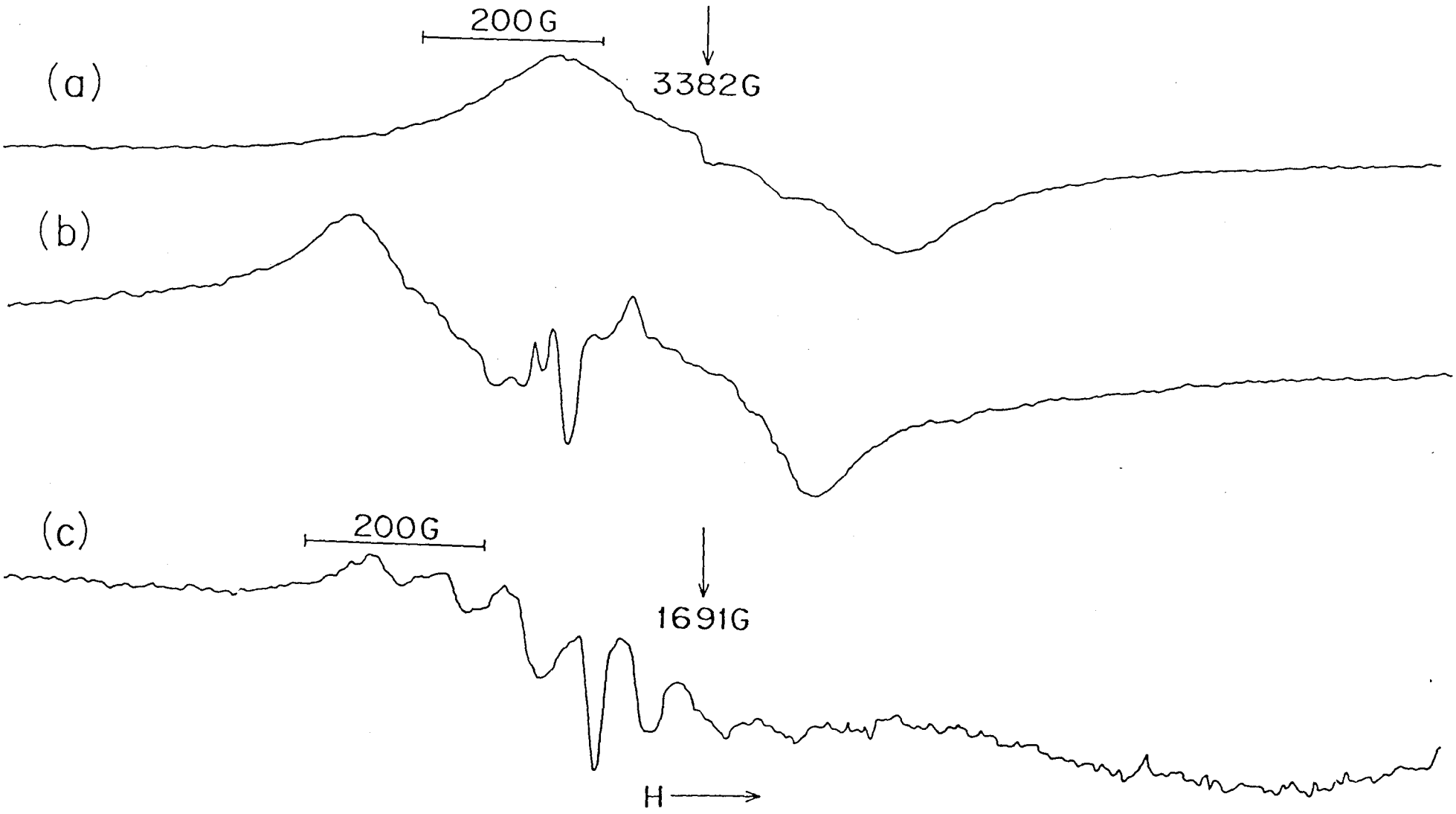

Figure 3.2.2. X– band EPR spectra of VOTPP(Br) in CH_2Cl_2 oxidised with $SbCl_5$
(a) at room temperature, (b) at 77K and (c) Half – field spectrum

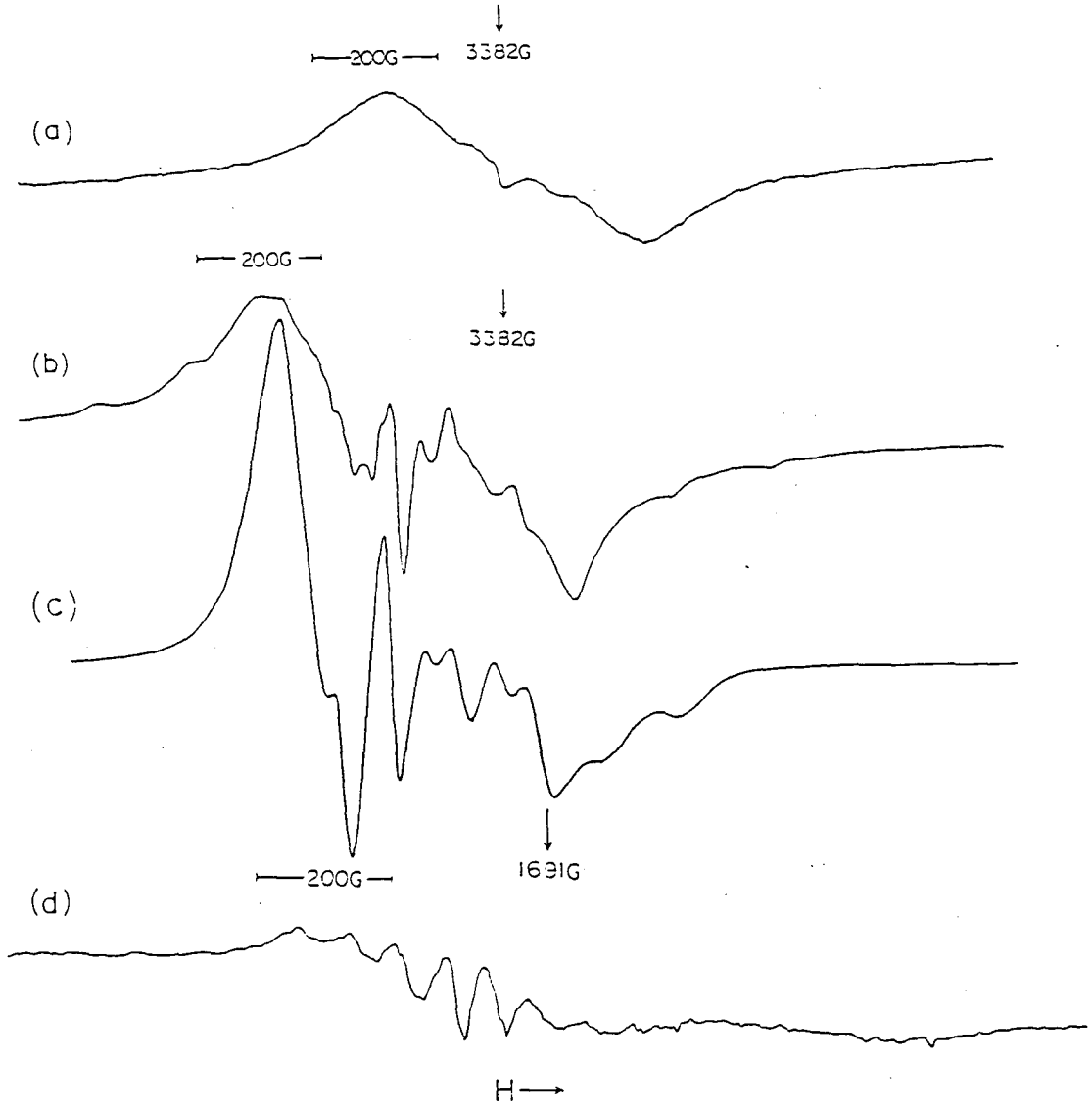

Figure 3.2.3. X– band EPR spectra of VO(T(*m*-NO_2)PP) in CH_2Cl_2 oxidised with $SbCl_5$ (a) at room temperature , (b) at 77K, (c) computer simulated spectrum and (d) Half - field spectrum

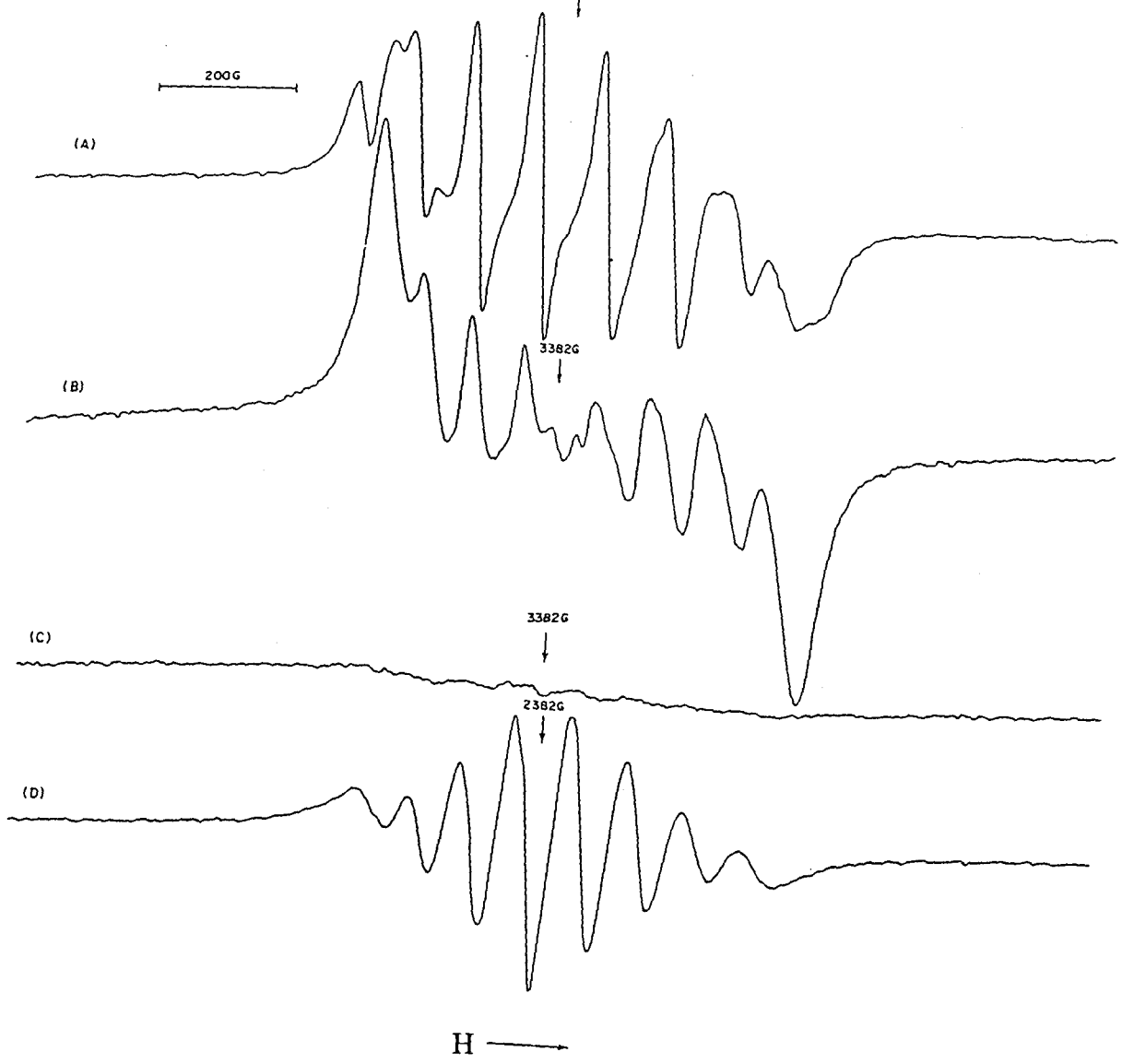

Figure 3.2.4. X – band EPR spectra of VOTPP(Br_4) in CH_2Cl_2 oxidised with $SbCl_5$ (A) 2 drops of $SbCl_5$, (B) 6-8 drops of $SbCl_5$, (C) 12 drops of $SbCl_5$ and (D) excess of $SbCl_5$ at room temperature

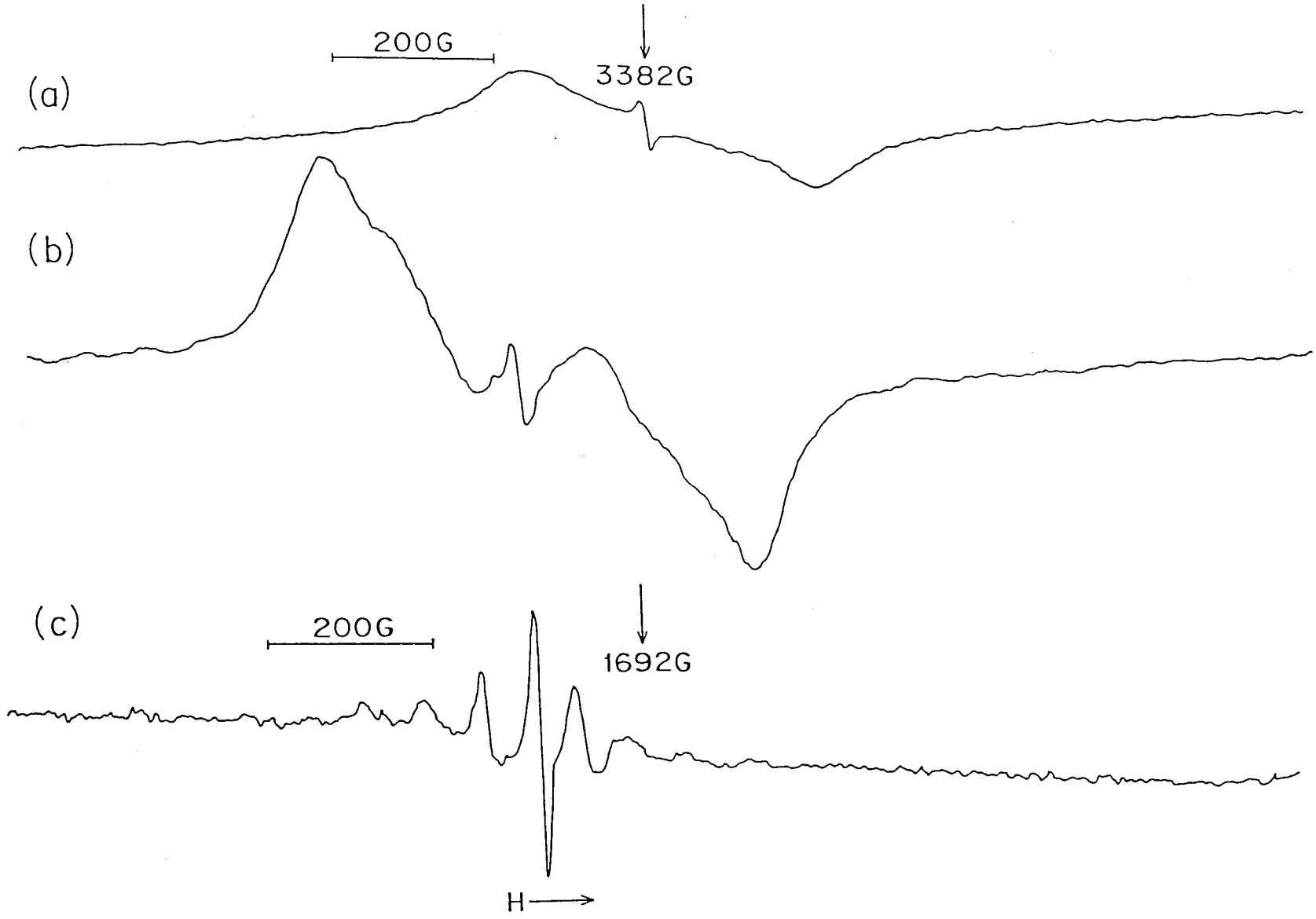

Figure 3.2.5. X – band EPR spectra of VO(T(*o*-Cl)PP) in CH_2Cl_2 oxidised with $SbCl_5$ (a) at room temperature, (b) 77K, (c) Half - field spectrum

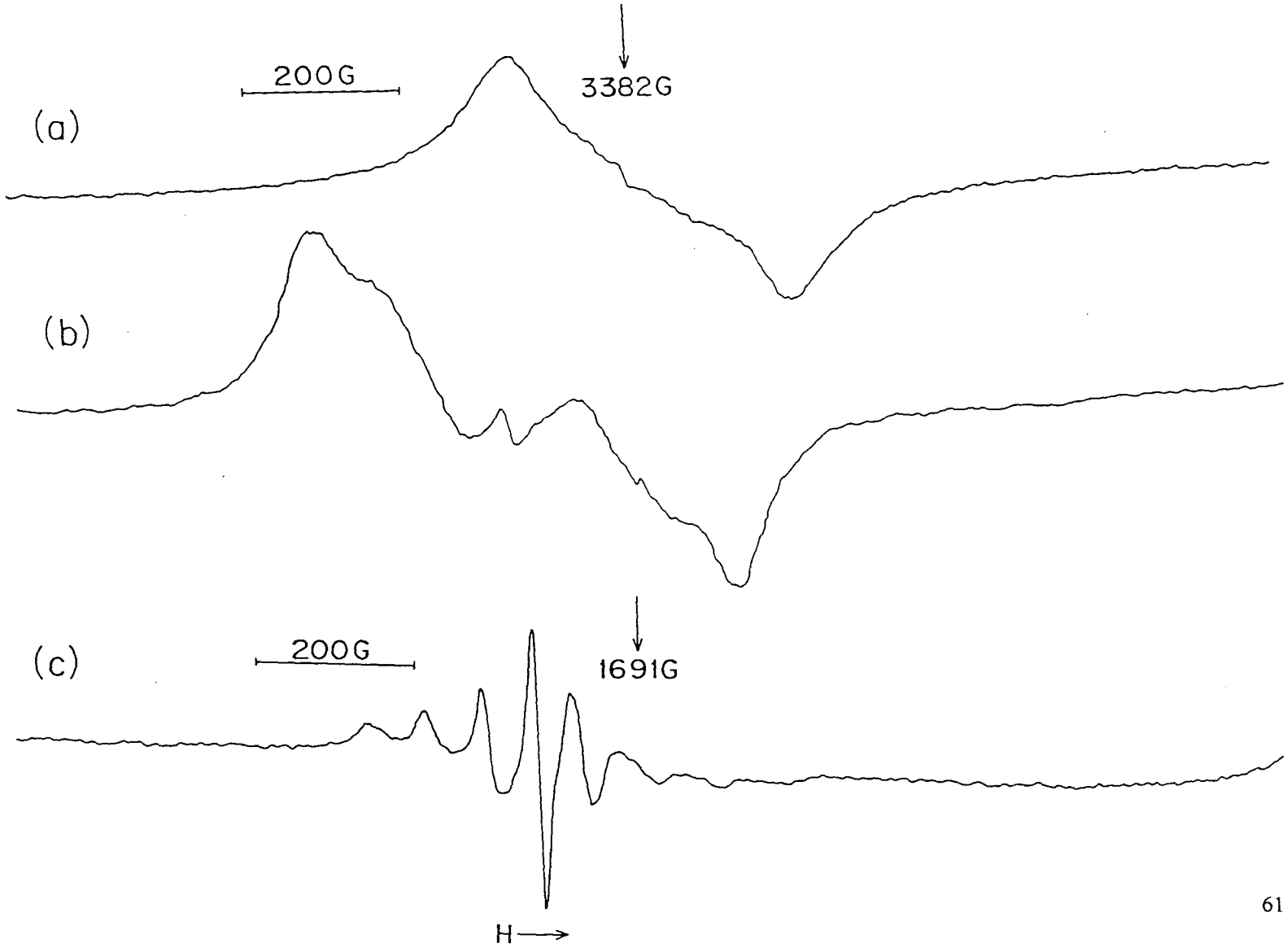

Figure 3.2.6. X – band EPR spectra of VO(T(*o*-CH_3)PP) in CH_2Cl_2 oxidised with $SbCl_5$ (a) at room temperature , (b) 77K, and (c) Half - field spectrum

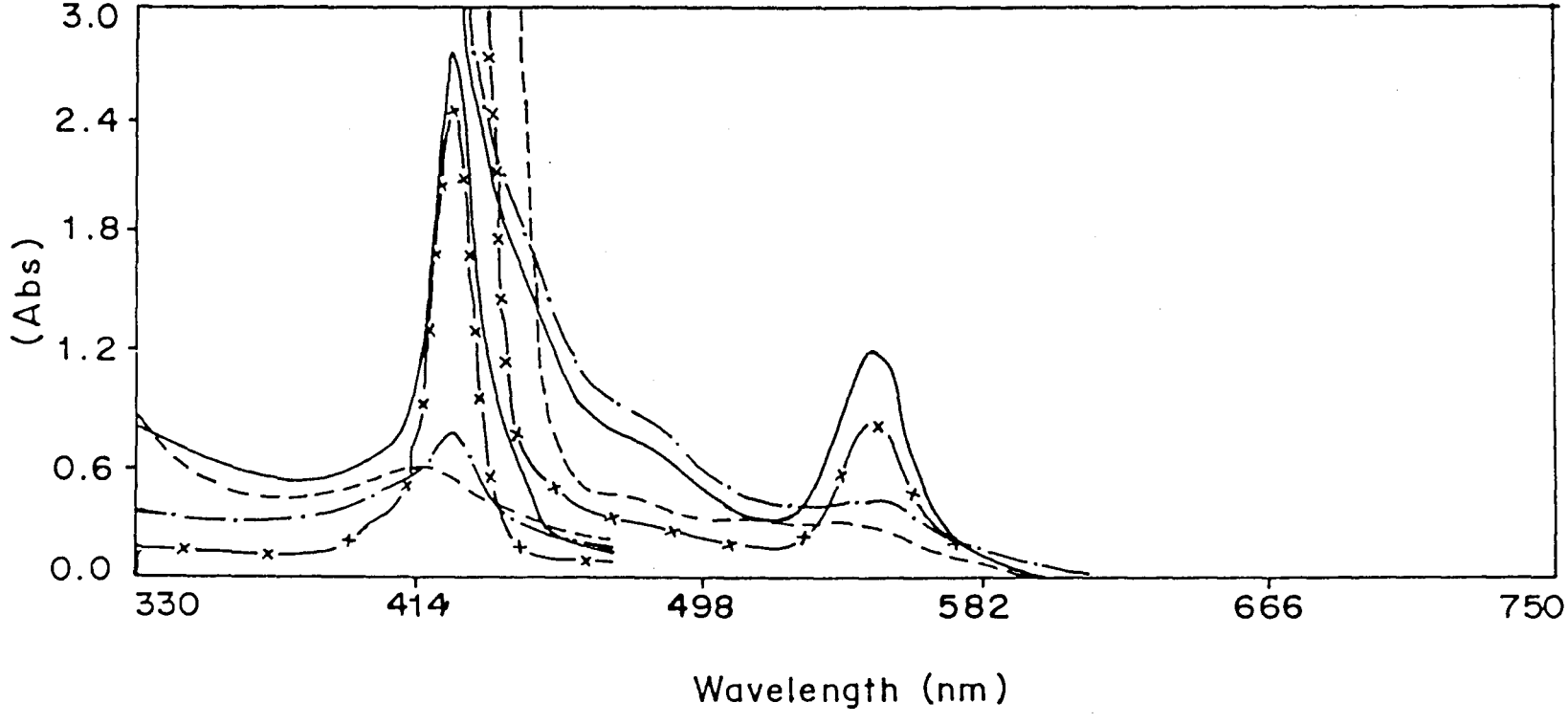

Figure 3.3.1. Visible absorption spectra of VOTPP(Br) in CH_2Cl_2 Unoxidised — · —·, Oxidised (with 0.1 M $SbCl_5$) —·—·, - - - - and Reduced (with dimethylamine)——

REFERENCES

1. C. M. Newton and D. G. Davis, *J. Magn. Resonance*, **20**, 446 (1975).
2. G. E. Selyutin, A. A. Shkylaev and V. T. Anufrienko, *Dokl. Akad. Nauk, SSR*, **255**, 390 (1980).
3. M. Hoshino, S. Konishi, M. Imamura, S. Watanabe and Y. Hama, *Chem. Phys. Lett.* **102**, 259 (1983).
4. R. H. Felton, in " The porphyrins", Edited by Dolphin (Academic press, New York, 1979), Vol. V. p. 53.
5. D. G. Davis, in " The porphyrins", Edited by Dolphin (Academic press, New York, 1979), Vol. V. p. 127.
6. J. Subramanian, in " Porphyrins and metalloporphyrins", Edited by K.M. Smith (Elsevier, Amsterdam, 1975), p. 555.
7. J. Fajer, D. C. Borg, A. Foreman, D. Dolphin and R. H. Felton, *J. Am. Chem. Soc.* **92**, 3451 (1970).
8. K. M. Kadish and M. M. Morrison, *Inorg. Chem.* **15**, 930 (1976).
9. A. Giraudeau, H. J. Callot and M. Gross, *Inorg. Chem.* **18**, 201 (1979).
10. L. A. Bottomley, L. Olson, K. M. Kadish, in " Electrochemical and spectrochemical studies of Biological redox component", Edited by K. M. Kadish (ACS advances, Washington, 1982), p. 279.
11. K. M. Kadish, D. Sazou, C. Araullo, Y. M. Liu, A. Saoiabi, M. Ferhart and R. Guilard, *Inorg. Chem.* **27**, 2313 (1988).

12. E. T. Shimomura, M. A. Phillippi, H. M. Goff, W. F. Schulz and C. A. Reed, *J. Am. Chem. Soc.* **103**, 6778 (1981).

13. A. S. Hinman, B. J. Pavelich and K. McGarty, *Can. J. Chem.* **66**, 1589 (1988).

14. J. Subramanian, V. P. Shedbalkar, A. Lemtur and R. Chakravorty, T.N. Saloi, *J. Phys. Chem.* **100**, 4770 (1996).

15. C.S. Bencosme, C. Romero and S. Simoni, Inorg. Chem. **24**, 1603 (1985).

CHAPTER 4

CV AND EPR STUDIES OF SOME Ni PORPHYRINS

CHAPTER - 4

4.1. INTRODUCTION

Synthesis and study of Ni(I) complex in non-porphyrin macrocycles are already available in the literature[1-4]. The stabilization of Ni(I) state in different porphyrin macrocycles are well known[5-14]. At present synthesis and isolation of Ni(I) porphyrins are not available in the literature. During the synthesis of porphyrins and metalloporphyrins, we stumbled upon Ni(I) porphyrins. Synthesis of Ni(I) porphyrins are already described in chapter 2

Both Ni(I) and Cu(II) are d^9 system having nuclear spin 3/2. But there are some differences in oxidation potentials of CuTPP and NiTPP. Their absorption wavelength (λ_{max}) of the soret band are also different. These differences can be seen from the data presented in the table 4.1. Thus, Ni(I) porphyrins exhibit EPR spectra similar to that of the Cu porphyrins.

Note: To ascertain the genuiness of the Ni complexes (Salts) viz. Nickel acetate and Nickel chloride which we used for the synthesis of Nickel porphyrins, we checked by different analytical methods, compared with the Copper acetate and Copper chloride and found that these metal compounds were Nickel acetate and Nickel chloride. There is also a difference in the synthesis of CuP and NiP. Using Cu acetate, metallation completes in 15 to 20 minutes. But metallation of Ni, using Nickel acetate and nickel chloride takes much longer time.

Table 4.1.

Compound	UV – visible data Soret band (λ max nm)	Electro-chemical oxidation potentials $E_{1/2}$ V Vs. SCE (1)	(2)	Reference
CuTPP	419	0.90	1.16	15 - 17
NiTPP	417	1.10	1.40	15 - 17
Cu(T(*p*-OCH_3)PP)		0.86		18
Ni(T(*p*-OCH_3)PP)		0.96		19
Ni(T(*p*-CH_3)PP)		1.01		19
Ni(T(*p*-NO_2)PP)		1.23 (metal)		19

4.2. CYCLIC VOLTAMMETRY OF [Ni(py)TPP(X_n)], (X = Br, n = 1 to 4)

A. RESULTS

All four bromo NiTPP complexes show similar voltammograms. Two broad redox waves are observed (figure 4.1.1) containing (TBA)PF_6 as supporting electrolyte. The results are summarised in table 4.2. The $E_{1/2}$ values increases from 1.32 V to 1.46V. The ΔE values vary from 0.10V to 0.29V. Similar redox waves are

not observed containing TBAP as supporting electrolyte in CH_2Cl_2. We observed a broad redox wave. The effect of supporting electrolyte has been observed by Chang et al.[20]

B. DISCUSSION

Approximate electro-chemical data are calculated although the redox waves are broad. The Δ_{ox} values are more or less constant (0.32 $\pm$ 0.04V). Both redox waves exhibit large ΔE values, which are quite large for one – electron transfer process. The values are ΔE_1 = 0.160 to 0.29V and ΔE_2 = 0.10 to 0.24V. The peak current ratio i_{pa}/i_{pc} $\approx$2 in all cases. This is a clear indication that each redox process involves more than one – electron transfer. Therefore, we can not strickly adhere to the oxidation potentials obtained. However, we can accommodate the values with some reservations. By doing so we observed that the oxidation potentials are increased by 0.07V to 0.22V vs. SCE for the first oxidation and increased in the second oxidation potentials by 0.08V to 0.28V vs. SCE. We have not observed the metal oxidation. We feel that the metal oxidation waves are overlapped with that of the ligand oxidation waves. One point we can draw out of these results is that the electron-withdrawing substitutions in the exo-positions of the pyrrole ring of the porphyrin macrocycle shifts the oxidation potentials to more higher positive values.

4.3. CYCLIC VOLTAMMETRY OF Ni(py)(T(*o*-X)PP), Ni(py)(T(*m*-X)PP), Ni(py)(T(*p*-X)PP), X = F, NO_2, CH_3, OCH_3

A. RESULTS

The voltammograms of Ni(py)(T(*o*-CH_3)PP), Ni(py)(T(*p*-CH_3)PP), Ni(py)(T(*p*-OCH_3)PP) and Ni(py)(T(*m*-NO_2)PP) are presented in figure 4.1.2-5 and the oxidation potentials are presented in the table 4.2. Three redox couples are observed for Ni(py)(T(*p*-CH_3)PP) and Ni(py)(T(*p*-OCH_3)PP). For the rest two broad redox waves are observed. Increased in the oxidation potentials are observed for Ni(py)(T(*o*-CH_3)PP) and Ni(py)(T(*m*-F)PP) in compare to that of the NiTPP. Ni(py)(T(*o*-CH_3)PP) the potentials are increased by 0.15V for the first oxidation and 0.28V vs. SCE for the second oxidation. For Ni((py)(T(m-F)PP) potentials are increased by 0.11V for the first oxidation and 0.09V vs. SCE for the second oxidation. For the rest of the complexes decrease in potentials are observed. However, difference in potentials are very small.

B. DISCUSSION

In all the above mentioned Nickel porphyrins except Ni(py)(T(*p*-CH_3)PP) and Ni(py)(T(*p*-OCH_3)PP two broad oxidation and reduction waves are observed and are not very well resolved. Their ΔE values are quite large for one-electron redox processes. Their $i_{pa}/i_{pc} \approx 2$ which is an indication that these processes involve more than one – electron transfer. Due to poor resolution we cannot effectively assign the different oxidation species.

Voltammograms are more resolved in the case of Ni(py)(T(*p*-CH_3)PP) and Ni(py)(T(*p*-OCH_3)PP). Their voltammograms consist of three redox couples and are one-electron reversible processes except the third redox couple. The ΔE values of their third redox couple are 0.17V and 0.14V vs. SCE. Further, its $i_{pa}/i_{pc} > 1$ and is indicative of involving more than one – electron transfer process. This analysis is drawn from the voltammogram of Ni(py)(T(*p*-OCH_3)PP) which clearly exhibit three redox couples. Therefore, the third couple is possibly an overlap of two couples, one for Ni(III) and the other from the dication. However, this is simply an assumption in the absence of proper resolution and requires further careful measurements. Thus, voltammogram of Ni(py)(T(*p*-OCH_3)PP) may be represented by the following oxidation steps:

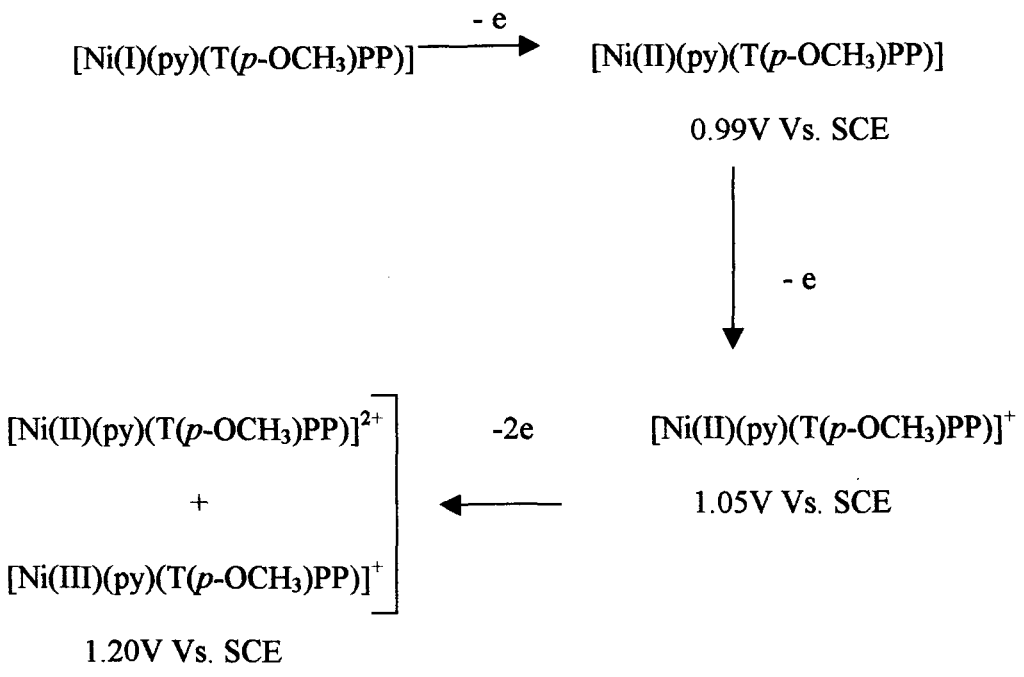

In the absence of proper resolution oxidation steps are represented as follows:

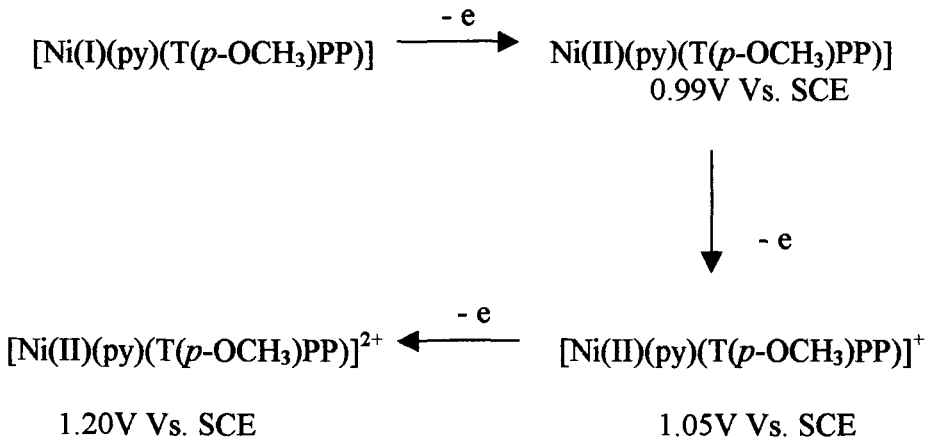

4.4. EPR OF SOME NICKEL PORPHYRINS

A. RESULTS

EPR measurements of Ni(I)(py)(TPP)(X_n) where X=Br, n = 1 to 4 and [Ni(I)(py)(T(*m*-NO_2)PP)] are done both in the room temperature as well as at the liquid nitrogen temperature. Measurements are also done for the oxidation of NiP with $SbCl_5$ at both temperature. All spectra of unoxidised NiP show four lines spectrum at room temperature. The results are summarised in the table 4.3. The values of g ranges from 2.125 to 2.134 (at room temperature). The hyperfine coupling constant is around 92G (at room temperature). The room temperature spectrum of Ni(py)TPP(Br_2) show a better resolution with some superhyperfine lines (figure 4.2.2(ia)). But these lines are not well resolved at room temperature. At liquid nitrogen temperature superhyperfine lines are well resolved (figure 4.2.2(ib)) having coupling constant. $A_{shp} \approx 16G$.

B. DISCUSSION

The four lines spectrum at room temperature arises out of an unpaired electron on the metal atom and the nuclear spin 3/2. At room temperature superhyperfine lines are visible only in the case of [Ni(py)TPP(Br_2)]. We will discuss only two representative compounds since all of them show similar spectra. Since [Ni(py)TPP(Br_2)] show superhyperfine lines at room temperature, we will discuss this spectrum. The superhyperfine coupling are almost isotropic i.e. $A_{II}^N \cong A_{\perp}^N$ and is equal to 16G. Since Ni(I) is a d^9 system we consider it to have D_{4h} symmetry (although it is having an axial ligand). Using EPR data we calculated the molecular

orbital coefficients α, α', β and β_1 of equation (3) and (4) of the appendix B. Thus, the following values are obtained for [Ni(py)TPP(Br_2)]. The in-plane σ bond between Ni and N is quite strong and show more of covalent character with $\alpha = 0.79$ and $\alpha' = 0.70$. The in – plane π - bonding $\beta_1 = 0.999$ which is very small. The out - of plane π - bonding between the metal ion and the ligand is also very small with $\beta = 0.999$. Both are almost equal to 1 and are quite negligible. From these parameters, we see that there exist strong σ - bond between the metal ion and the N of the ligand. But the in-plane and out – of plane π - bonding show ionic. In presence of the axial ligand one can consider the situation as in the case of the vanadyl. This is a situation where Ni ion is slightly out of plane of the porphyrin ring due to axial ligand (py). In that case the unpaired electron may lie in d_{xy} orbital and this does not take part in bonding with N of the porphyrin ligand. Since we observed Ni(I) state, we suggest two possibilities viz. there may be some amount of bonding between the axial ligand (py) and the metal and that the unpaired electron in the d_{xy} orbital polarizes the charge on the nitrogen of the porphyrin which results in generating superhyperfine coupling. The other possibility is that the in – plane π - bonding may not be negligible making more difficult to observe the superhyperfine coupling. We do not observe readily the superhyperfine coupling as in the case of copper porphyrins (observable even at room temperature). In the case of NiP the super hyperfine is observed at higher concentration. Ironically, these are possibilities only and are needed to be verified by calculating the coefficient of the molecular orbitals. However, our contention is that

the Ni(I) in the porphyrin is stabilised by the strong axial ligand (py). Kadish et al [14]. have reported the electro – reduction of [Ni(T(*p*-Me_2)N)F_4PP)] and have shown by EPR the presence of Ni(I) for [Ni(T(*p*-Me_2)N)F_4PP)]$^-$ in pyridine under N_2 atmosphere. Similar observations are made in DMF under N_2 and in THF under CO.

On oxidation with $SbCl_5$ the four lines as well as the superhyperfine structure are replaced by a single line EPR spectrum centering at g= 2.019 (at room temperature) figure 4.2.2(iia). The oxidized spectrum at low temperature is presented in figure 4.2.2(iib) The unoxidised low temperature computer simulated EPR spectra is also presented in figure 4.2.2(ic). Since the oxidation potentials of the metal (Ni(I) $\rightarrow$ Ni(II) and the porphyrin ring are very close, oxidations occur almost at the same range. Thus, a single line EPR spectra are produced at room temperature and at low temperature ($g_{||}$ very faint) which corresponds to [Ni(II)(py)TPP(Br_2)]$^+$. Since Ni(II) is diamagnetic, no EPR signal is observed. The single line EPR spectrum is due to the oxidation of the porphyrin ring. Apart from slight increased in the oxidation potentials due to electrophilic substitutions in the pyrrole ring, no accountable difference are observed in the EPR spectra.

Both the unpaired and oxidised EPR of [Ni(py)(T(*m*-NO_2)PP)] show similar pattern as that of the [Ni(py)TPP(Br_2)] system. No appreciable difference are observed.

4.5. UV-VIS. SPECTRA OF SOME NICKEL PORPHYRINS

UV-vis measurements are done to diagnose the axial ligation, oxidations and reversibility of oxidations. The soret band and the visible band are expected to be red shifted due to axial ligand. Not much differences are observed except for the soret band (which is slightly red shifted)(see table 4.4.). In fact spectra look very normal. Similar trend is observed for Ni(pip)TPP. UV – vis spectrum of the monoadduct Ni(Pip)TPP is practically indistinguishable from the spectrum of NiTPP. This is because the diamagnetic Ni(II) ion is too small for the porphyrin hole. Thus, it can take one or two axial ligand in solution when excess of ligand is present. Addition of ligand increases the co-ordination number as well as the effective size of the ion. This may be the reason why metallation took long time and occurred when excess of pyridine is used.

On careful inspection we also observed hypsochromic shift in the spectra of Nickel porphyrin (although not much). This indicates the re-enforcement in metal to porphyrin back – bonding.

Oxidations are done using $SbCl_5$ and the reversibility are checked by neutralizing $SbCl_5$ with dimethylamine. These spectra are presented in the figure 4.3.1-3. Oxidation spectra show splitting in the soret band. One of them is blue shifted while the main soret band is red shifted. The visible band is also red shifted and a new broad and strong band is developed between 600nm and 900nm. Interestingly one difference is observed in the spectra of the NiTPP without the axial ligand and the one with the axial ligand. The difference in the later show split in the soret band on oxidation while

the former do not. Same trend is observed in the case of DMF ligation. As the oxidation proceeds, the intensity of the metal band slowly diminishes and new broad band emerges in the region 600nm – 900nm. This is an indication of the ligand oxidation. Neutralisation of the oxidised NiP regenerates the original form (figure 4.3.1-3)

4.6. CONCLUSION

The Cyclic voltammetric studies indicate the oxidation of Ni(I) → Ni(II). This step is manifested in the voltammograms of Ni(py)(T(*p*-CH_3)PP) and Ni(py)(T(*p*-OCH_3)PP). However, Ni(II) → Ni(III) oxidation is not observed due to poor resolution. This step will be possible because of the back bonding between the Ni ion and the porphyrin ligand. Besides, it can also accommodate the sixth ligand. Electrophilic substitutions in the α and β positions of the pyrrole ring of the porphyrin leads to higher oxidation potentials. Electrophilic substitutions in the meta position of the phenyl ring of the porphyrin also increases the oxidation potentials significantly due to the steric hindrance. Substitution by NO_2 group in the meta position of the phenyl ring of the porphyrin also increases the oxidation potentials quite significantly. The lowest oxidation potentials are observed for para substitution. On the other hand nucleophilic substitution in the phenyl ring of the porphyrin reduces the oxidation potentials and is more significant in the meta and para positions. Perhaps it is the electron-donating group that stabilizes the Ni(I) state by means of charge transfer such that the voltammograms show three redox couples in which Ni(I)→ Ni(II) oxidations is quite clear.

The UV-vis spectra show the oxidation of the porphyrin ligand. The spectra of the neutral NiP show the presence of the axial ligand to a certain extent (although not very significantly). The spectra exhibit splitting of the soret band and a new band emerges between 600nm – 900 nm indicating the ligand oxidation.

The EPR spectra of the unoxidised Nickel porphyrins show Ni(I) state with superhyperfine structure. The molecular orbital parameters show strong in-plane σ bonding between the metal and the nitrogen of porphyrin ligand. Oxidation with $SbCl_5$ indicates Ni(I) $\rightarrow$ Ni(II) oxidation and the ligand oxidation.

Table 4.2

Redox potentials (VOLTS vs. SCE) for NiTPP, Ni(py)TPP(X_n), X = Br, n = 1 to 4 and Ni(py)(T(*o*-X)PP), Ni(py)(T(*m*-X)PP), Ni(py)(T(*p*-X)PP), X = F, NO_2, CH_3, OCH_3 in CH_2Cl_2 ($\approx 10^{-3}$ M) using TBA(PF_6) as supporting electrolyte. Scan rate 100mV/s (at room temperature)

Compound	$E_p^a(I)$	$E_p^a(II)$	$E_p^a(III)$	$E_p^c(I)$	$E_p^c(II)$	$E_p^c(III)$	ΔE_1	ΔE_2	ΔE_3	$E_{1/2}(I)$	$E_{1/2}(II)$	$E_{1/2}(III)$
TPP[a]	1.01	1.34		1.31								
TPP(Br)	1.08	1.43		1.22	0.92		0.16	0.21		1.00	1.32	
TPP(Br_2)	1.11	1.42		1.18	0.93		0.19	0.24		1.02	1.30	
TPP(Br_3)	1.22	1.47		1.37	0.93		0.29	0.10		1.08	1.42	
TPP(Br_4)	1.23	1.52		1.40	0.99		0.25	0.11		1.11	1.46	
T(*o*-CH_3)PP	1.16	1.52		1.15	0.80		0.36	0.36		0.98	1.34	
T(*m*-CH_3)PP	1.00	1.37		1.18	0.86		0.14	0.19		0.93	1.28	
T(*p*-CH_3)PP	0.97	1.12	1.20	1.12	1.04	0.88	0.09	0.10	0.17	0.92	1.08	1.20
T(*m*-OCH_3)PP	0.99	1.27		1.04	0.93		0.07	0.23		0.96	1.15	
T(*p*-OCH_3)PP	0.91	1.05	1.20	1.06	0.96	0.85	0.07	0.08	0.14	0.88	1.01	1.13
T(*m*-NO_2)PP	0.99	1.30		1.06	0.90		0.08	0.23		0.95	1.18	
T(*m*-F)PPP	1.12	1.43		1.24	0.97		0.14	0.19		0.04	1.33	

[a] reference 7

Table 4.3.

EPR parameters of Ni(py)TPP(X_n), X = Br, n = 1 to 4 and Ni(py)(T(*m*-NO_2)PP) at room temperature and at low temperature

Compound	Unoxidized g value at room temperature	Unoxidized g value at low temperature		Oxidized g value at room temperature	Oxidized g value at low temperature		Unoxidized A(G) value room temperature		Unoxidized A(G) value at room temperature
		$g_{\parallel}$	$g_{\perp}$		$g_{\parallel}$	$g_{\perp}$	$A_{\parallel}$	$A_{\perp}$	
NiTPP(Br)	2.134	2.247	2.078	2.019	2.297	1.98	92.58	205.28	36.23
NiTPP(Br_2)	2.128	2.238	2.073	2.019	2.288	1.98	88.55	205.53	30.06
NiTPP(Br_3)	2.127	2.237	2.072	2.019	2.287	1.98	87.32	206.55	26.69
NiTPP(Br_4)	2.125	2.234	2.071	2.019	2.286	1.98	86.65	207.03	26.46
Ni(T(*m*-NO_2)PP)	2.129	2.225	2.081	2.018	2.221	1.98	94.00	169.26	54.24

Table 4.4

UV - vis data of Unoxidised, Oxidised and Reduced products of NiTPP, Ni(py)TPP(X_n), X = Br, n = 1 to 4, Ni(py)(T(*o*-X)PP), Ni(py)(T(*m*-X)PP) and Ni(py)(T(*p*-X)PP), X= Cl, F, Br, NO_2, CH_3 and OCH_3 in CH_2Cl_2 containing 0.1M TBAP and 0.5M $SbCl_5$(at room temperature)

	λ, nm					
	Unoxidised		Oxidation		Reduction of the oxidised species with dimethylamine	
Porphyrin	Soret	Q	Soret	Q	Soret	Q
TPP[a]	414	525, 555	350, 410	512, 606, 641,648,750	414	522, 600, 762
TPP(Br)	416	527	417, 443	531, 660	416	527
$TPP(Br_2)$	419	527	418, 451	532, 670	420	527, 648
$TPP(Br_3)$	420	532	422, 455	538, 678	422	531, 650
$TPP(Br_4)$	426	541	426, 456	542, 678	425	541
$TPP(Br_8)$[b]	344	561, 592				
T(*m*-NO_2)PP	413	526	410	526, 606, 642, 610	413	526
T(*o*-CH_3)PP	412	525	412, 483	526, 640	412	525
T(*m*-CH_3)PP	413	526	400	526, 639, 758	414	527
T(*p*-CH_3)PP	414	528	411, 482	526, 639, 784	414	528
T(*p*-CH_3)PP[a]	418	502, 537 570	422, 431	558, 603, 720	418	549, 600, 722
T(*m*-OCH_3)PP	412	526	400, 482	525, 644, 789	414	526
T(*p*-OCH_3)PP	418	530	425	525, 658, 894	419	530

[a]reference 7 (in presence of TBAP), [b]reference 20

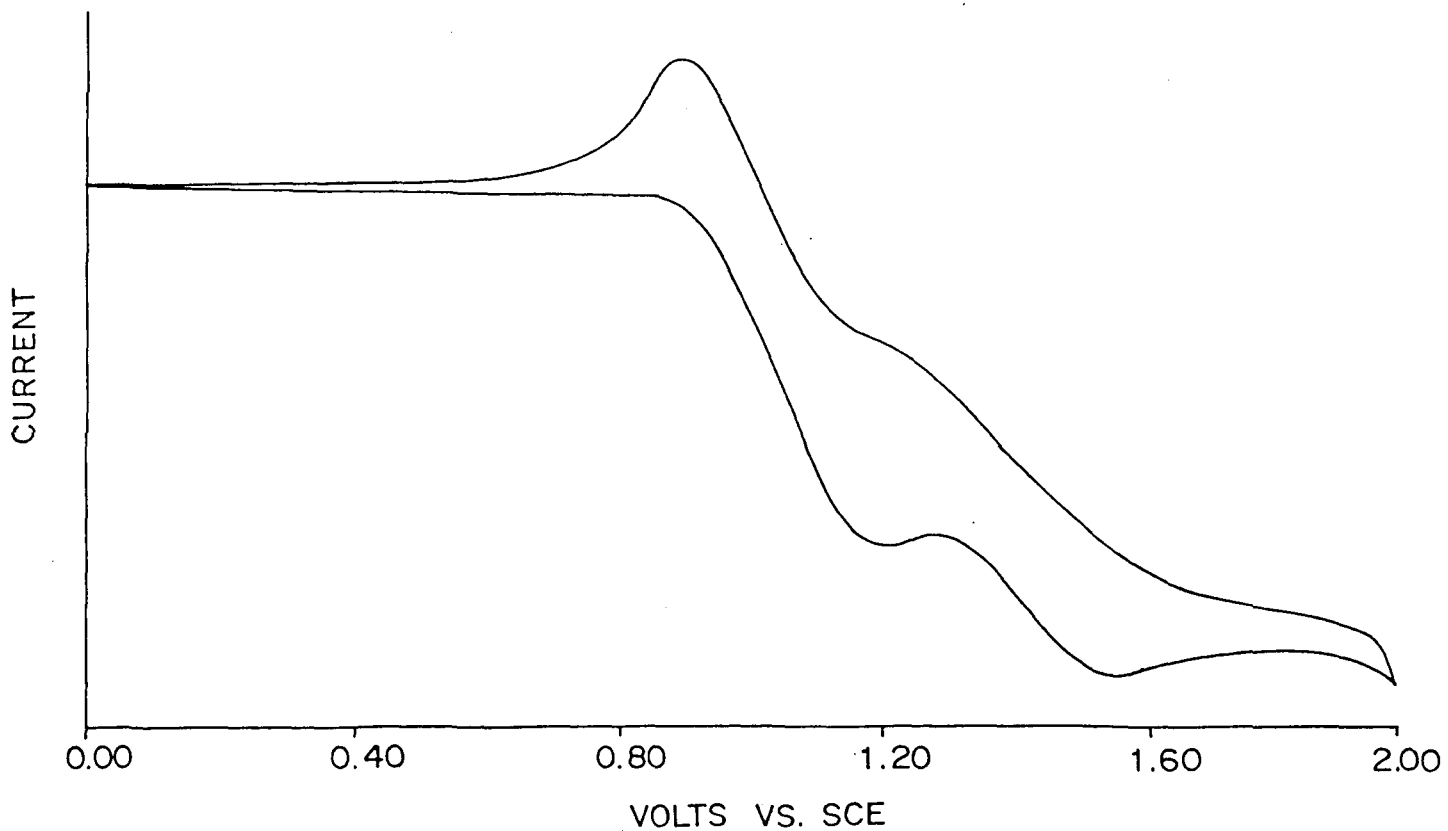

Figure 4.1.1. Cyclic voltammogram of Ni(py)TPP(Br_2) in CH_2Cl_2 containing 0.1 M TBA(PF_6) at room temperature. Scan rate 100 mV/s

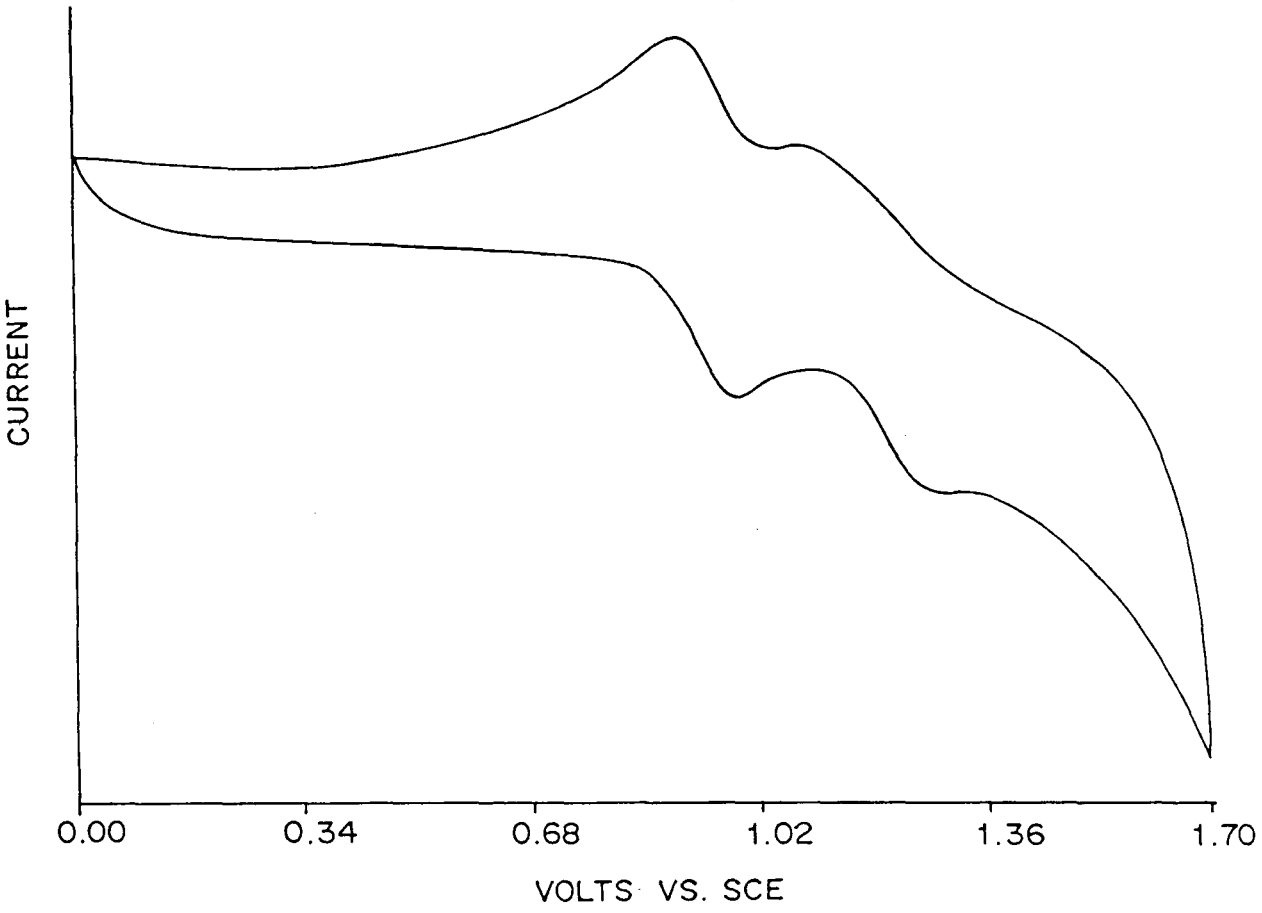

Figure 4.1.2. Cyclic voltammogram of Ni(py)(T(*m*-NO_2)PP) in CH_2Cl_2 containing 0.1 M TBA(PF_6) at room temperature. Scan rate 100 mV/s

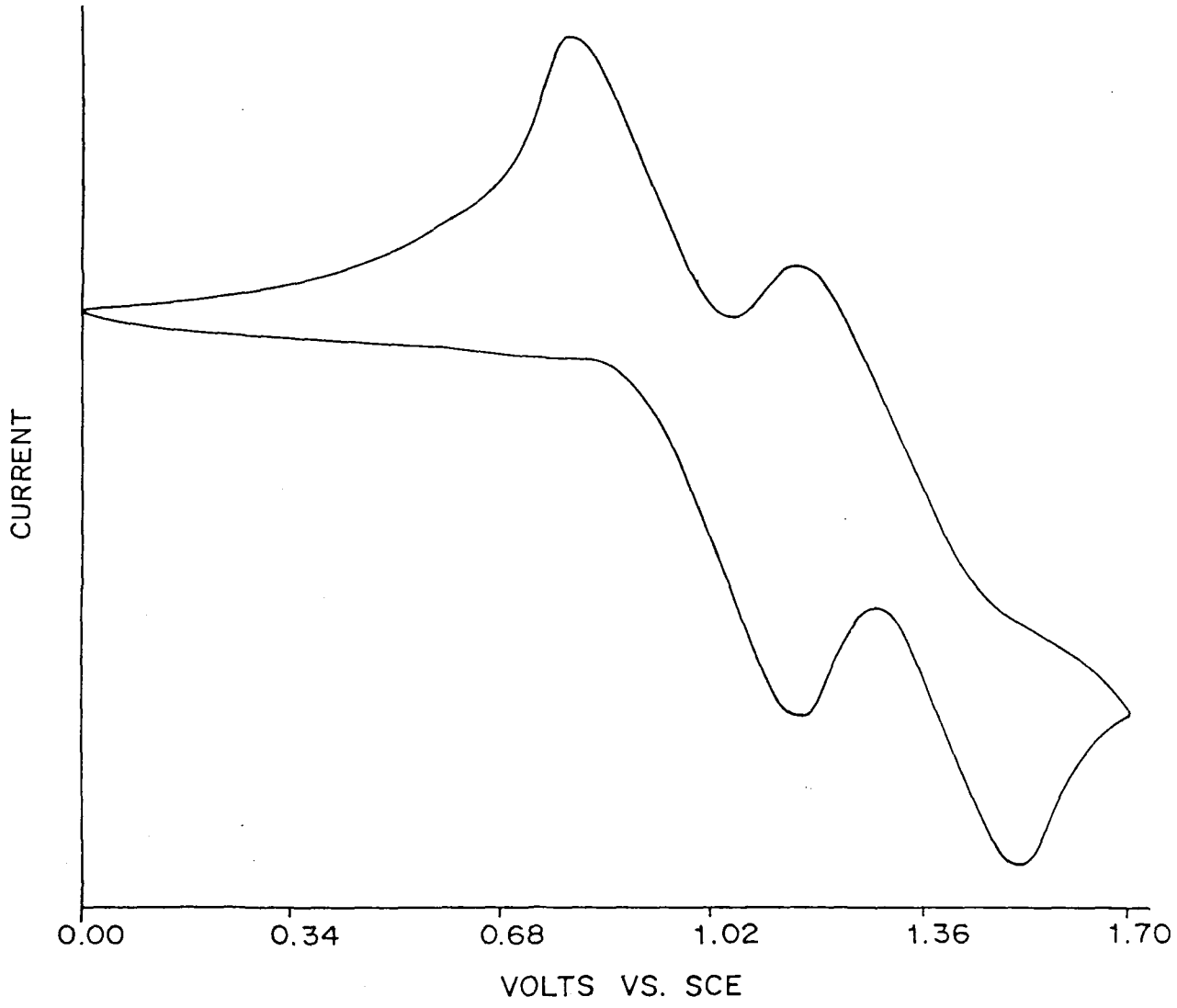

Figure 4.1.3. Cyclic voltammogram of Ni(py)(T(*o*-CH_3)PP) in CH_2Cl_2 containing 0.1 M TBA(PF_6) at room temperature. Scan rate 100 mV/s

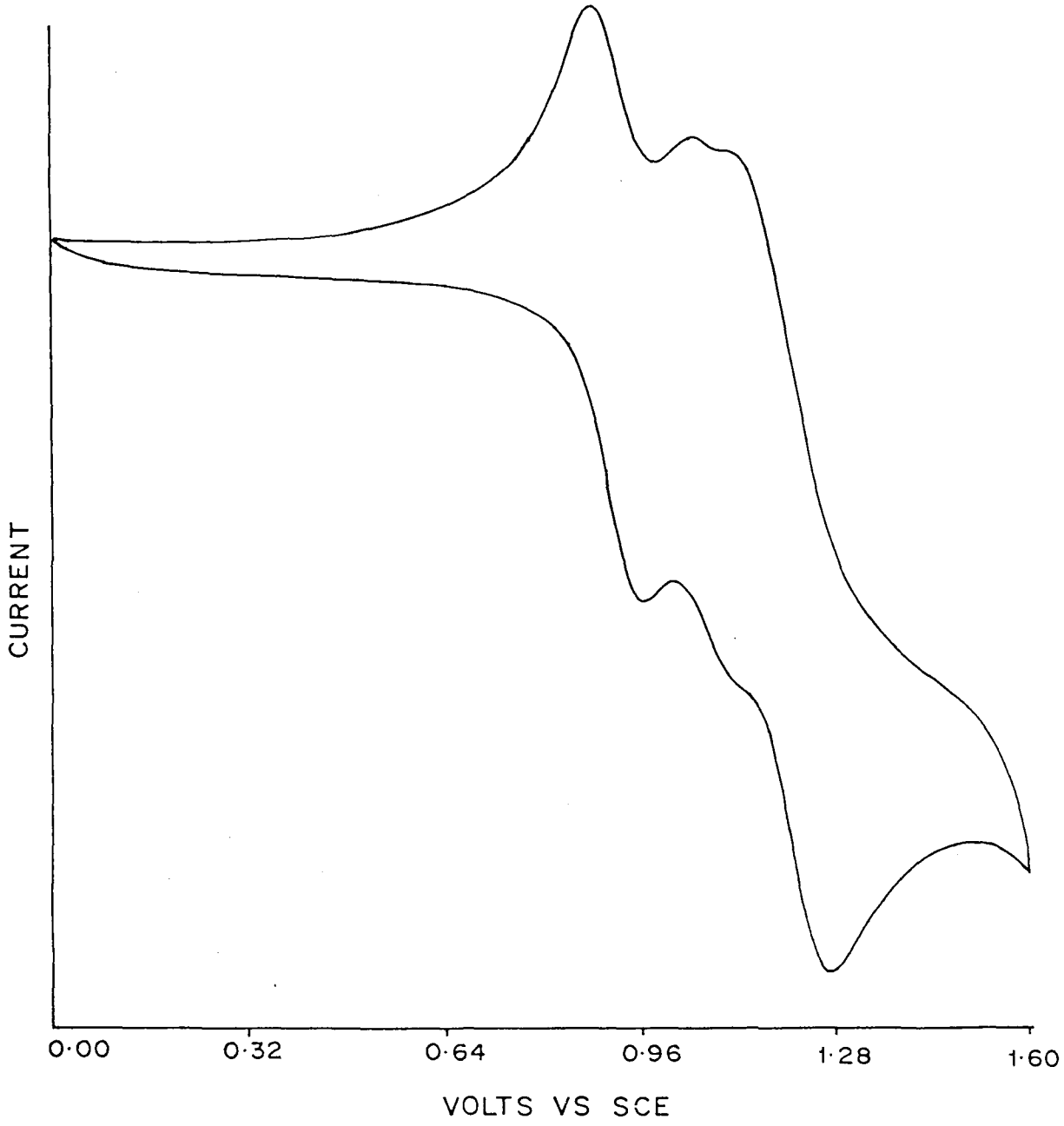

Figure 4.1.4. Cyclic voltammogram of Ni(py)(T(*p*-CH_3)PP) in CH_2Cl_2 containing 0.1 M TBA(PF_6) at room temperature. Scan rate 100 mV/s

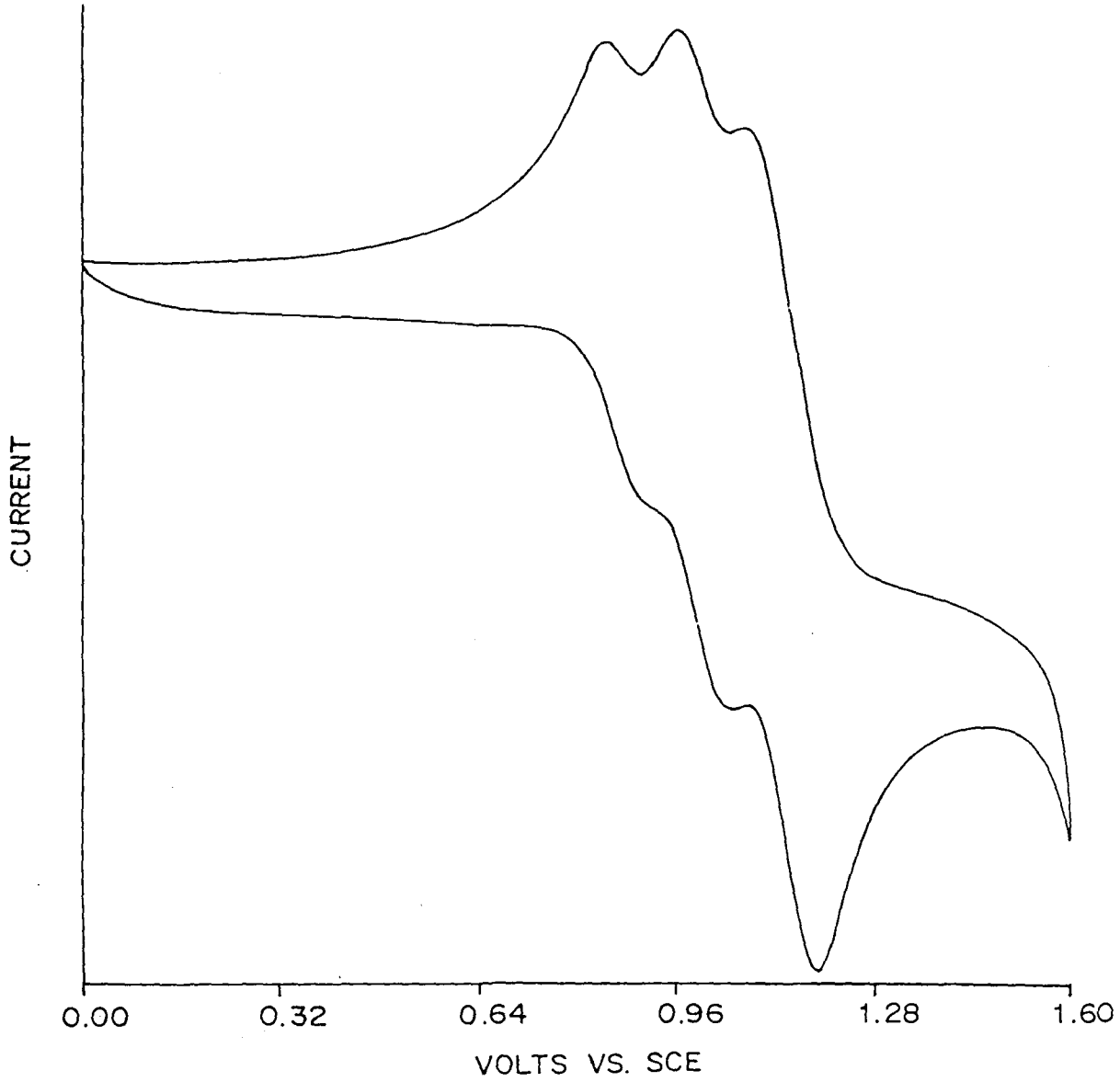

Figure 4.1.5. Cyclic voltammogram of Ni(py)(T(*p*-OCH_3)PP) in CH_2Cl_2 containing 0.1 M TBA(PF_6) at room temperature. Scan rate 100 mV/s

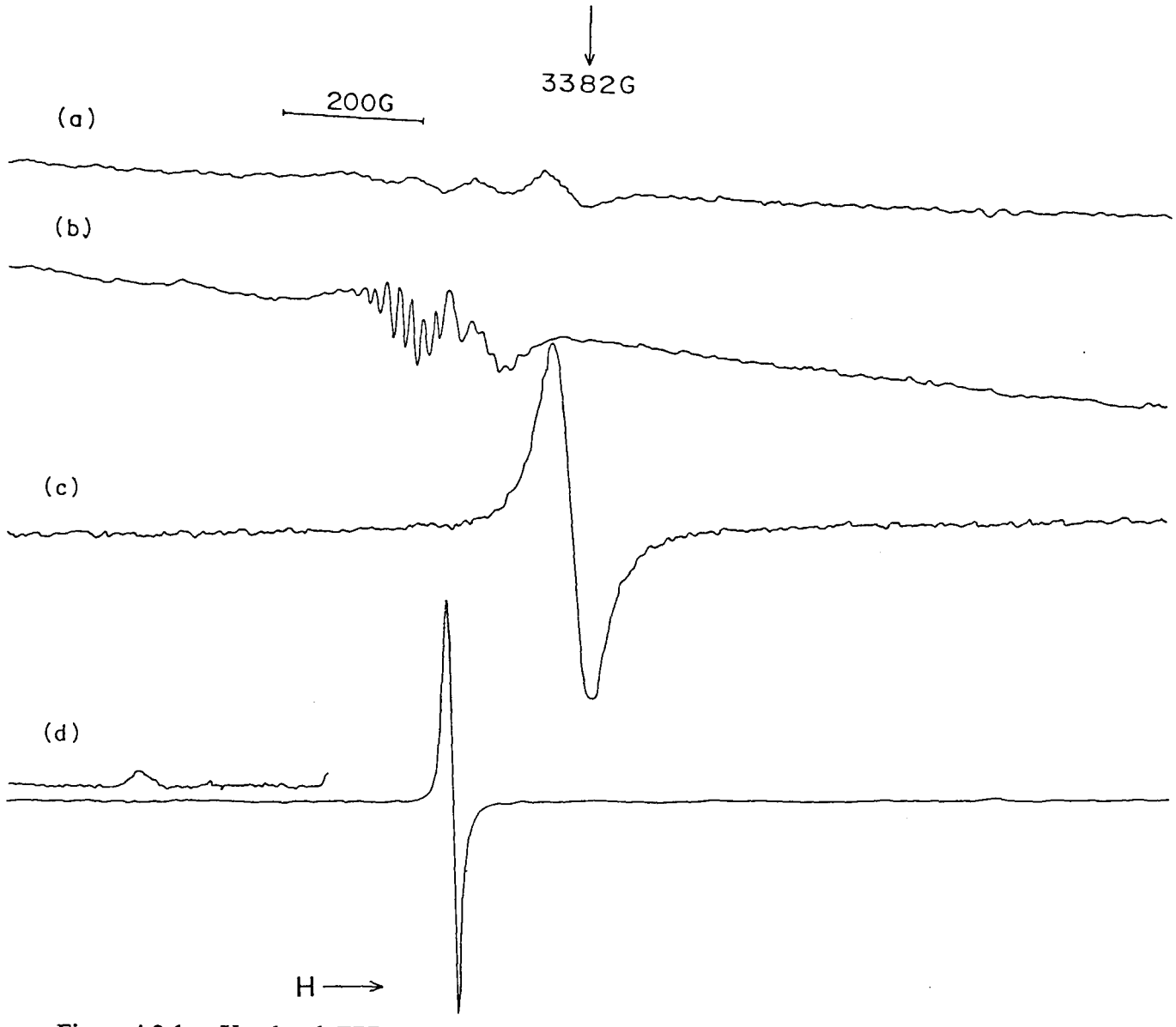

Figure 4.2.1. X – band EPR spectra of Ni(py)TPP(Br) in CH_2Cl_2 (a) Unoxidised at room temperature , (b) Unoxidised at 77K, (c) Oxidised (with $SbCl_5$) at room temperature and (d) Oxidised (with $SbCl_5$) at 77K.

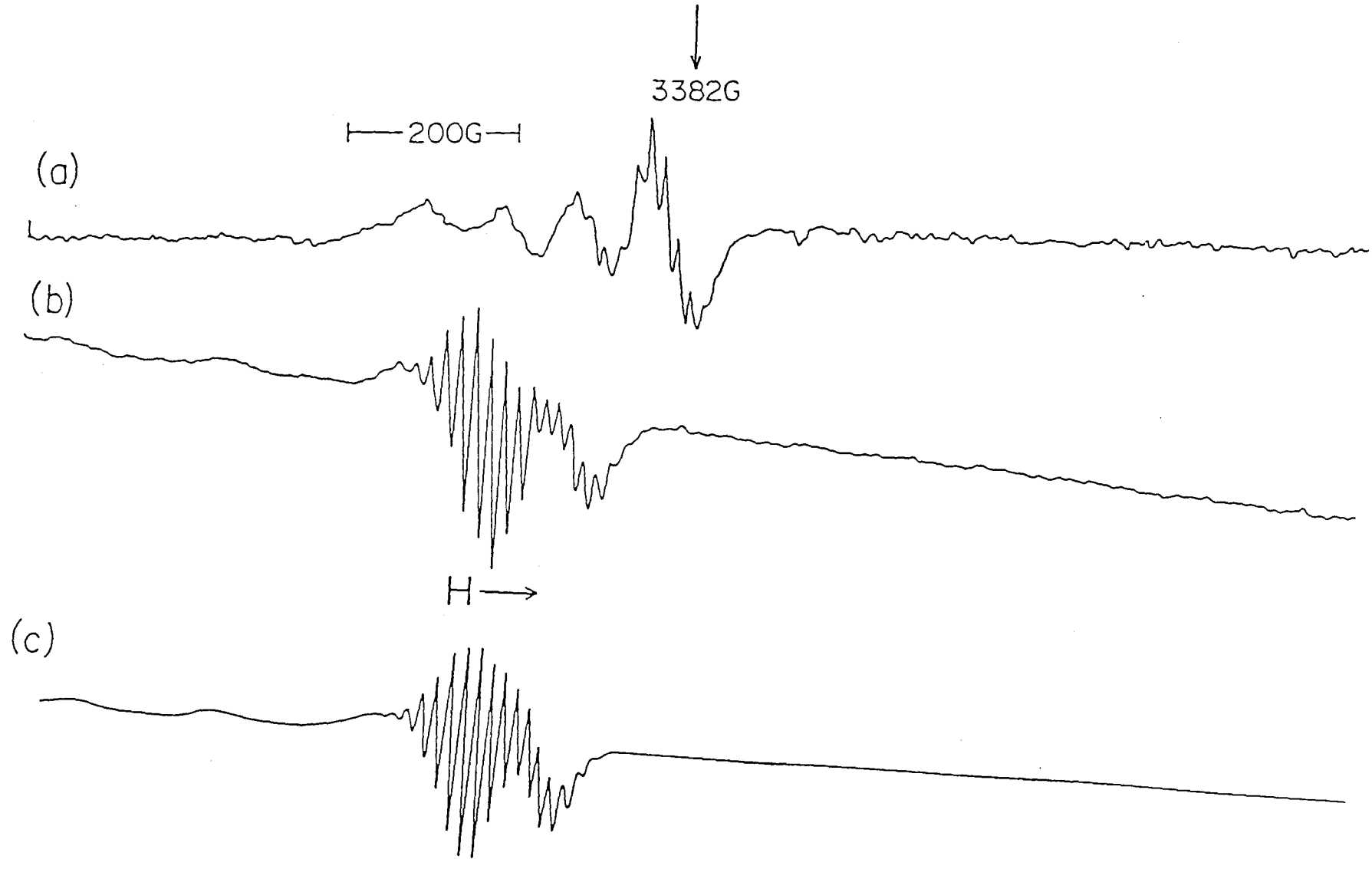

Figure 4.2.2(i). X – band EPR spectra of Ni(py)TPP(Br_2) in CH_2Cl_2 (a) Unoxidised at room temperature , (b) Unoxidised at 77K and (c) Computer simulated spectrum

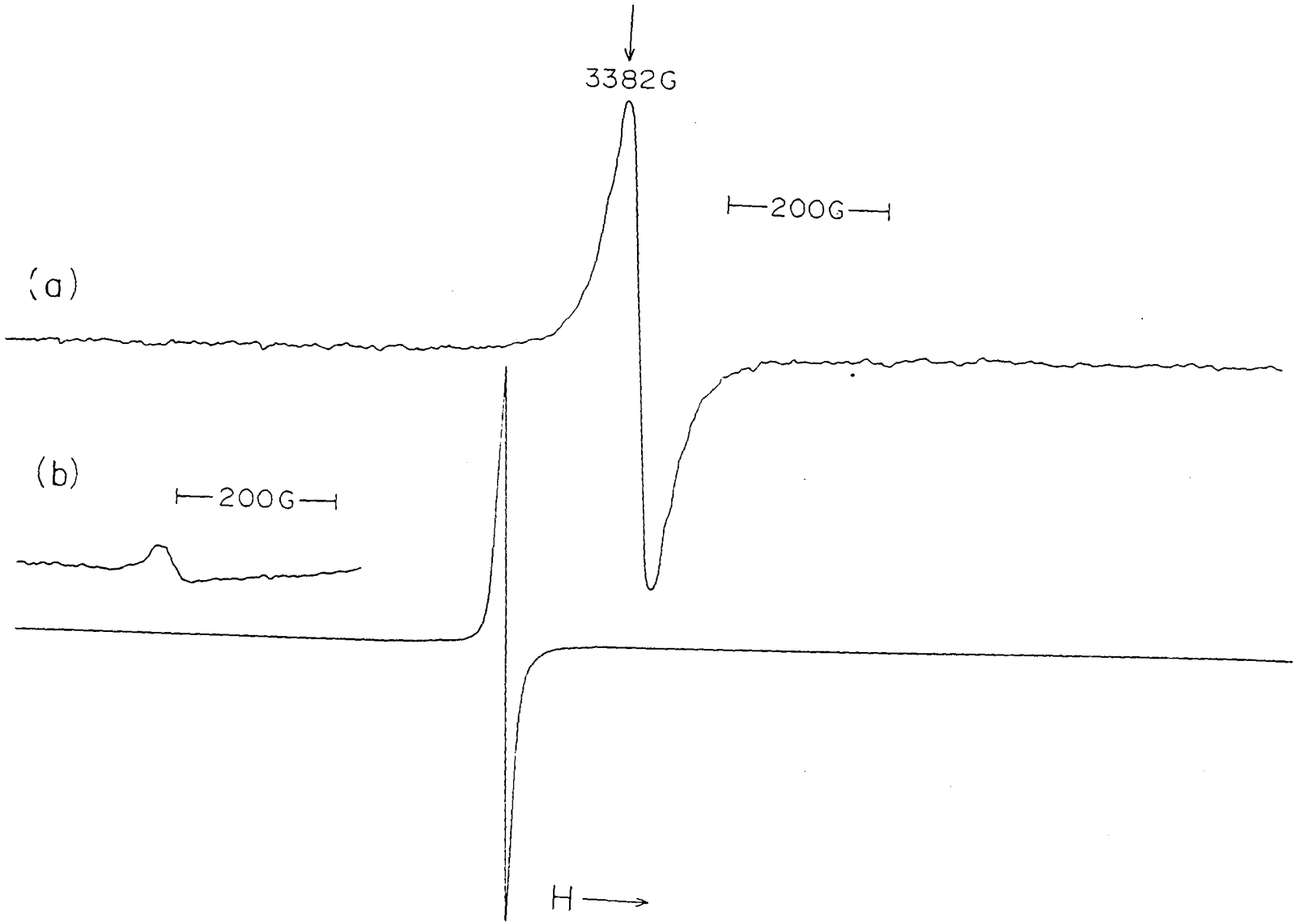

Figure 4.2.2(ii) X – band EPR spectra of Ni(py)TPP(Br_2) in CH_2Cl_2 oxidised with $SbCl_5$ (a) at room temperature and (b) at 77K

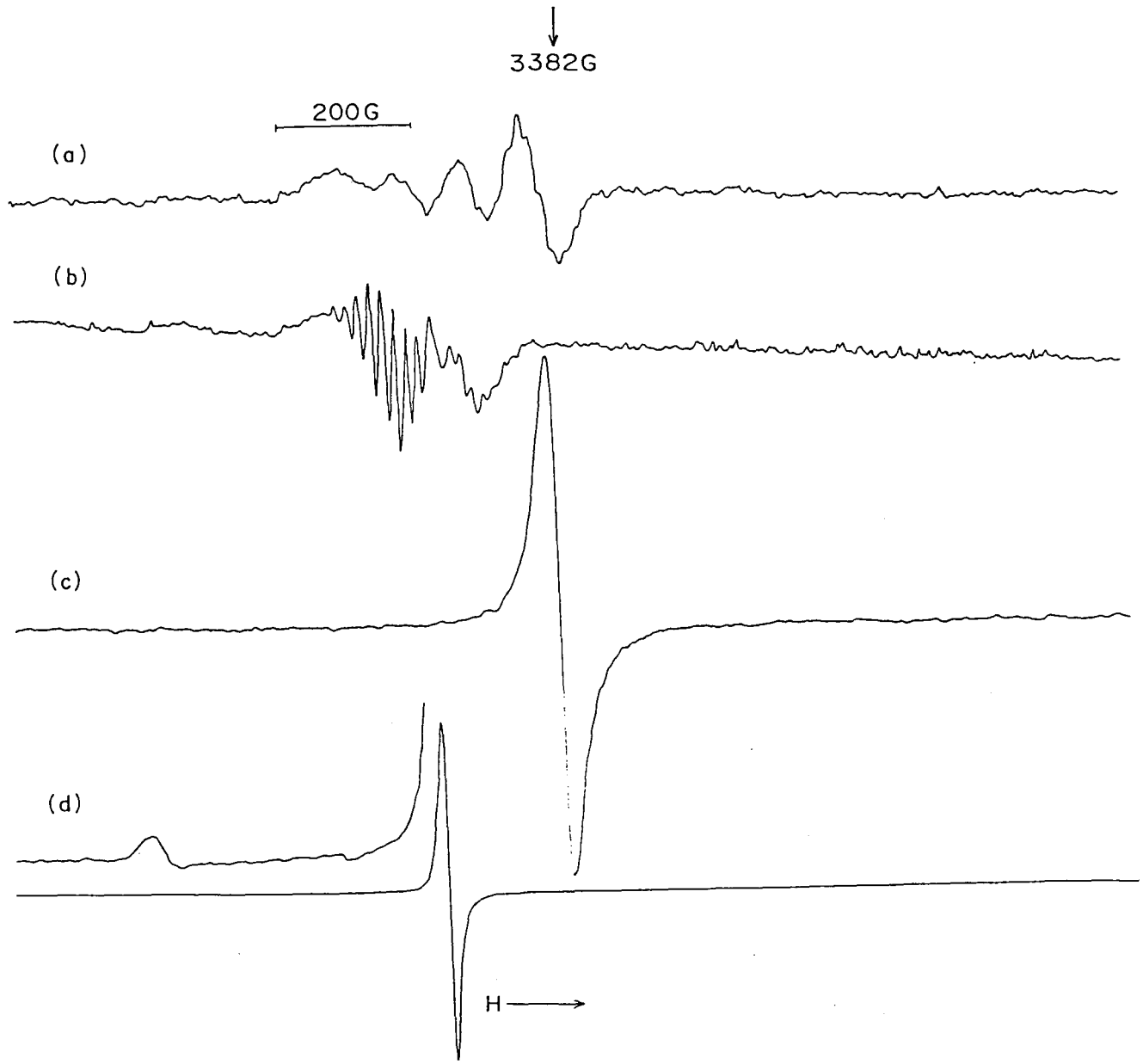

Figure 4.2.3. X – band EPR spectra of Ni(py)TPP(Br_3) in CH_2Cl_2 (a) Unoxidised at room temperature , (b) Unoxidised at 77K, (c) Oxidised (with $SbCl_5$) at room temperature and (d) Oxidised (with $SbCl_5$) at 77K

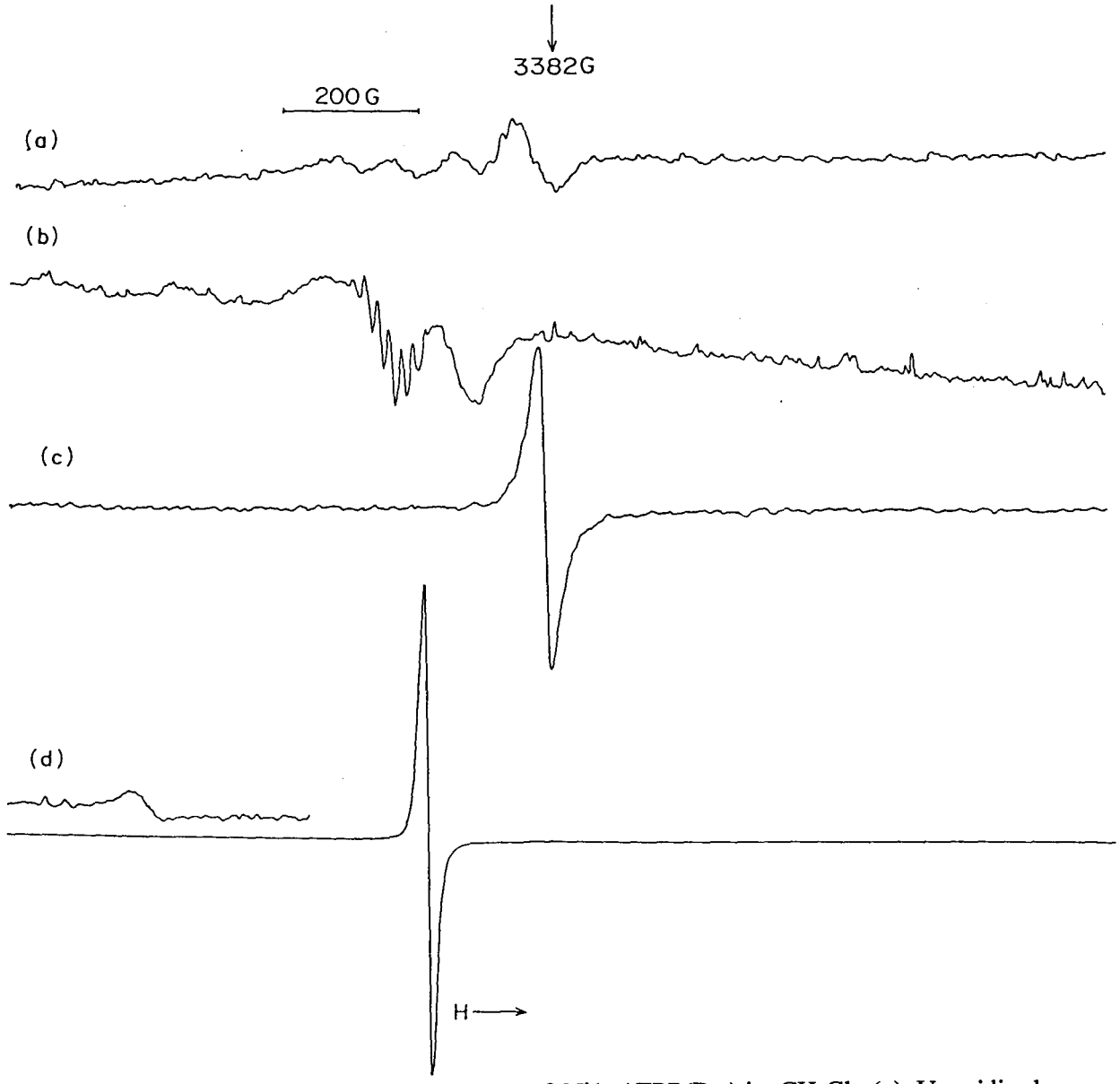

Figure 4.2.4. X – band EPR spectra of Ni(py)TPP(Br_4) in CH_2Cl_2 (a) Unoxidised at room temperature , (b) Unoxidised at 77K, (c) Oxidised (with $SbCl_5$) at room temperature and (d) Oxidised (with $SbCl_5$) at 77K

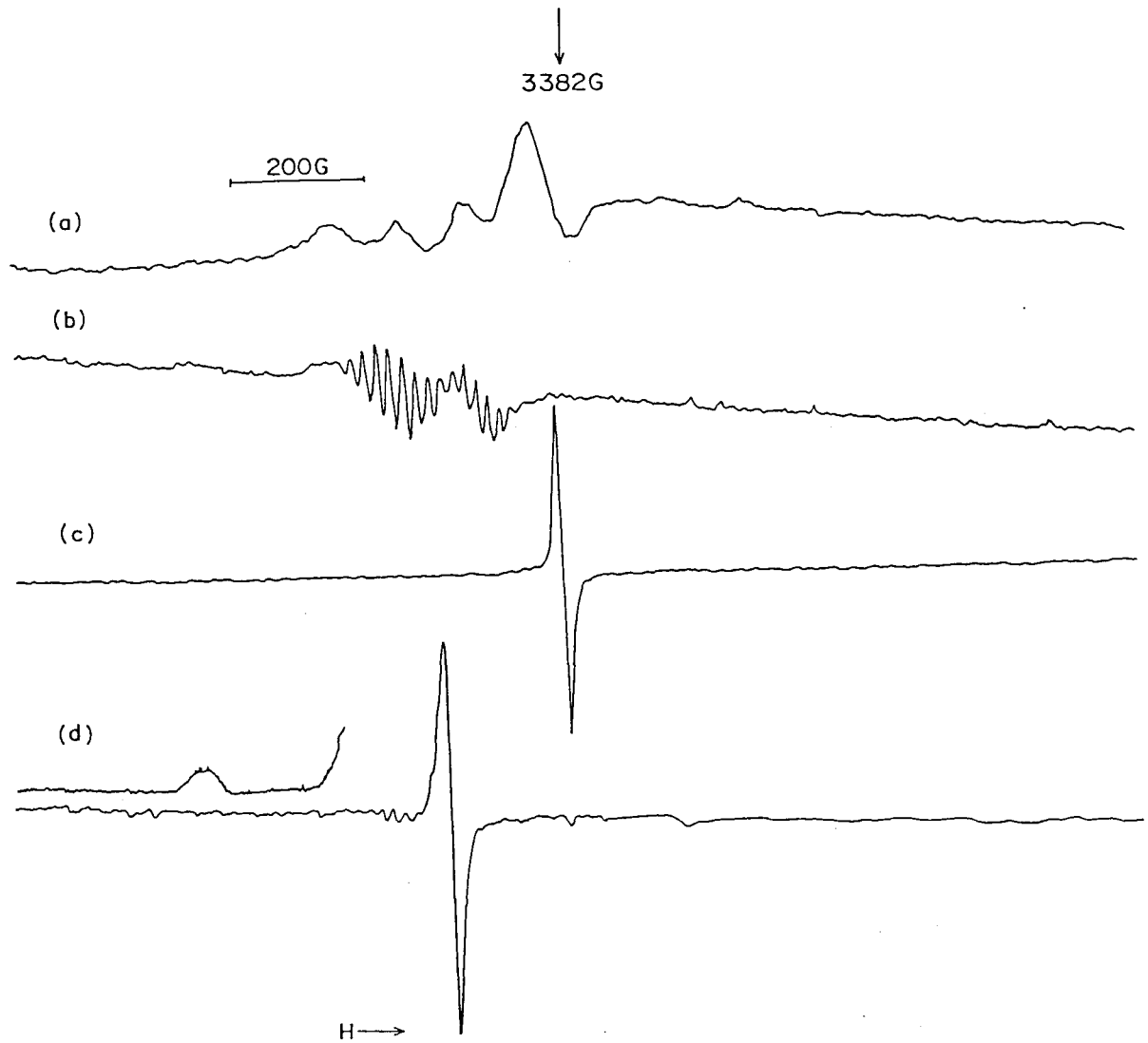

Figure 4.2.5. X– band EPR spectra of Ni(py)(T(m-NO_2)PP) in CH_2Cl_2 (a) Unoxidised at room temperature , (b) Unoxidised at 77K, (c) Oxidised (with $SbCl_5$) at room temperature and (d) Oxidised (with $SbCl_5$) at 77K

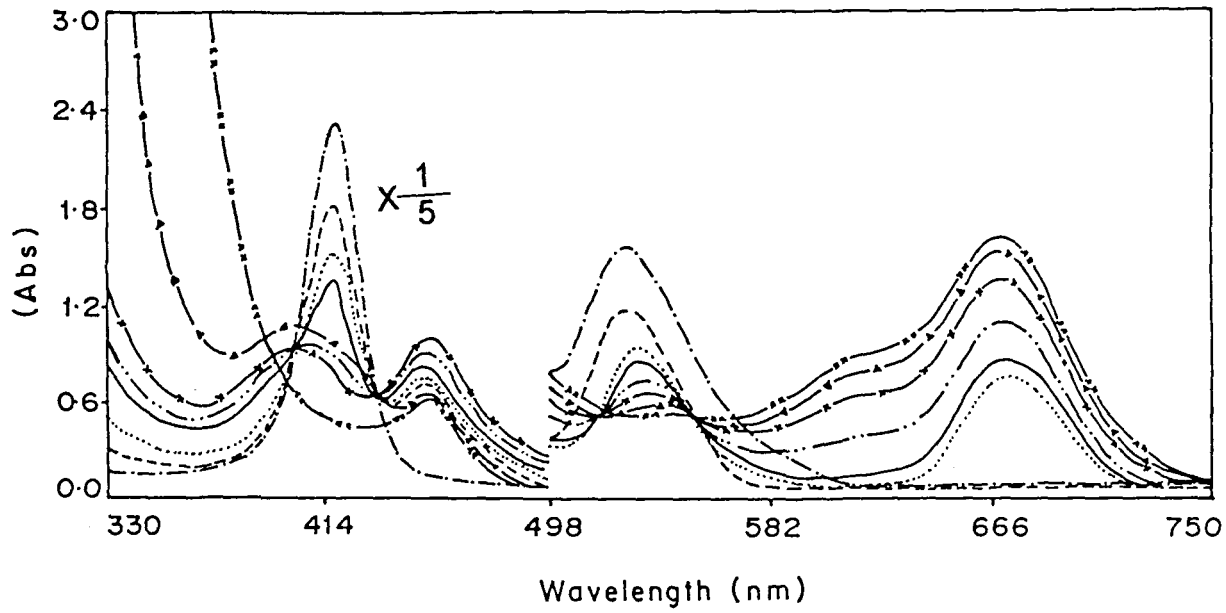

Figure 4.3.1. Visible absorption spectra of Ni(py)TPP(Br_2) in CH_2Cl_2 Unoxidised - - -, Oxidised (with 0.1 M $SbCl_5$)·····, ——, — ·· — ··, — · —·, —◀ —◀, —·· —·· and Reduced (with dimethylamine) — · — ·

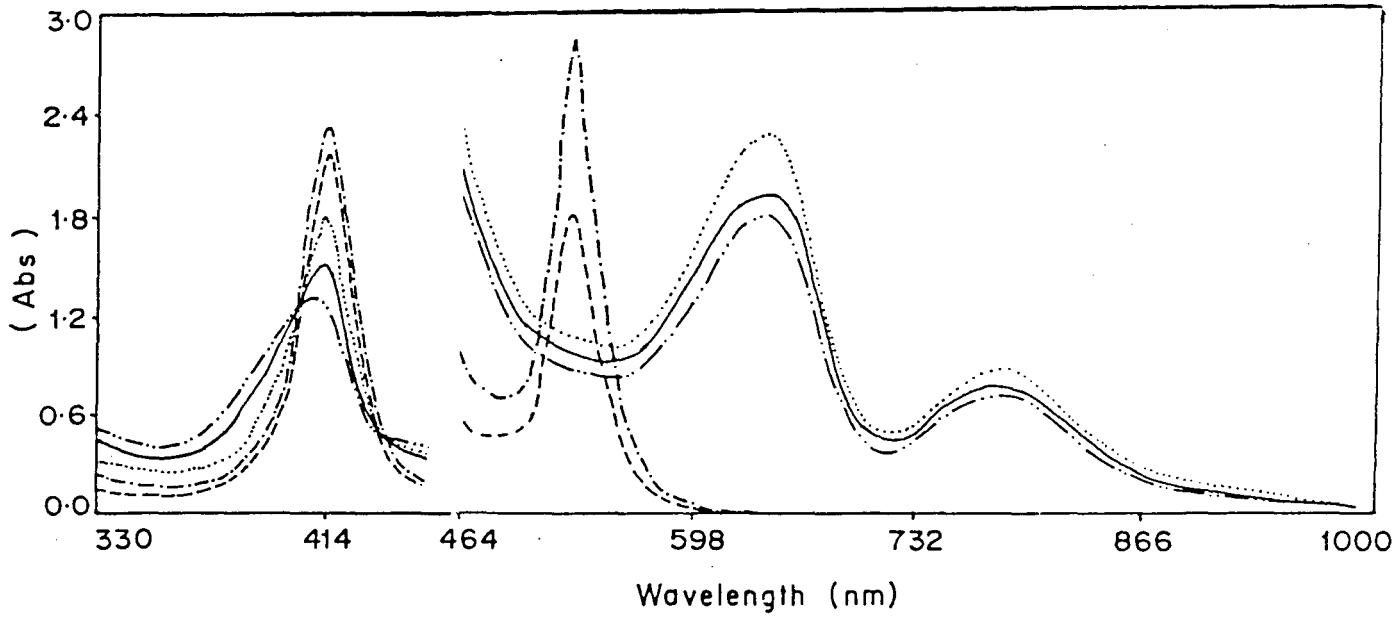

Figure 4.3.2. Visible absorption spectra of Ni(py)(T(p - CH_3)PP) in CH_2Cl_2 Unoxidised - - - - -, Oxidised (with 0.1 M $SbCl_5$) ·····, ——, — ·· — ·· , and Reduced (with dimethylamine) — · — ·

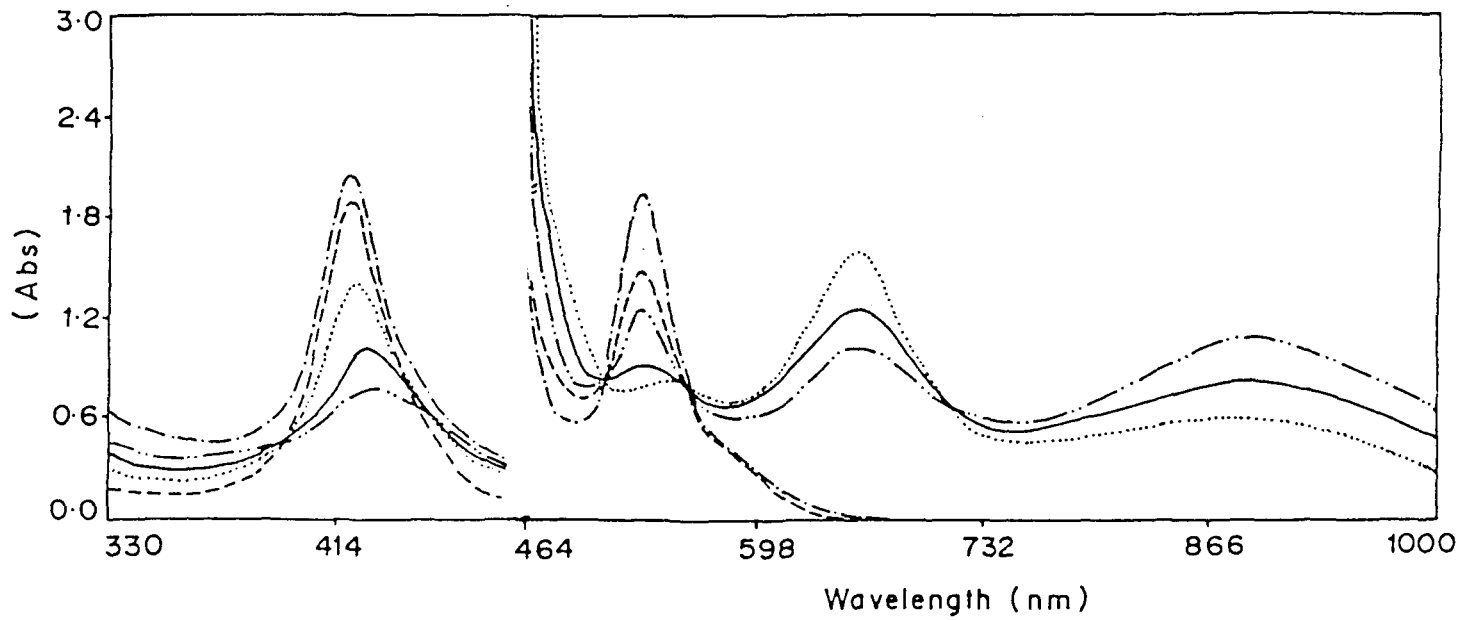

Figure 4.3.3. Visible absorption spectra of Ni(py)(T(p -OCH_3)PP) in CH_2Cl_2 Unoxidised - - - - -, Oxidised (with 0.1 M $SbCl_5$) ·····, ——, — ·· — ··, and Reduced (with dimethylamine) — · — ·

REFERENCES

1. F. V. Lovecchio, E. S. Gore and D. H. Busch, *J. Am. Chem. Soc.* **96**, 3109 (1974).
2. R. R. Gagne and D. M. Ingle, J. Am. Chem. Soc. **102**, 1444 (1980).
3. R. R. Gagne and D. M. Ingle, Inorg. Chem. **20**, 420 (1981).
4. B. G. Maiya, Y. Deng, K. M. Kadish, *J. Am. Chem. Soc. Dalton Trans.* 3571 (1990).
4. K. M. Kadish, *Prog. Inorg. Chem.* **34**, 435 (1987).
5. K. M. Kadish and M. M. Morrison, *Inorg. Chem.* **15**, 980 (1987).
6. D. Chang, T. Malinski, A. Ulman and K.M. Kadish, *Inorg. Chem.* **23**, 817 (1984). (1984).
7. K. M. Kadish, D. Sazou, Y. M. Liu, A. Saoiabi, M. Ferhat and R. Guilard, *Inorg. Chem.* **27**, 1198 (1988).
8. K .M. Kadish, D. Sazou, G. B. Maiya, B. C. Han, Y. M. Liu, A. Saoiabi, M. Ferhat and R. Guilard, *Inorg. Chem.* **28**, 2542 (1989).
9. A. M. Stolzenberg and M. T. Stershic, *J. Am. Chem. Soc.* **110**, 6391 (1988).
10. A. M. Stolzenberg and M. T. Stershic, *Inorg. Chem.* **26**, 3082 (1987).
11. M. W. Renner, A. Foreman, J. Fajer, D. Simpson and K. M. Smith and K. M. Barkigia, *Biophys. J.* **53**, 2771**a** (1988).
12. D.Lexa, M. Momenteau, J. Mispetter and J. M. Saveant, *Inorg. Chem.* **28**, 30 (1989).

13. K. M. Kadish, M. M. Franzen, B. C. Han, C. Araullo-McAdams and D. Sazou, *J. Am. Chem. Soc.* **113**, 512 (1991).

14. R. H. Felton and H. Linschitz. *J. Am. Chem. Soc.* **88**, 1113 (1966).

15. A. Wolberg and J. Manassen, *J. Am. Chem. Soc.* **92**, 2982 (1970).

16. A. Stanienda and G. Biebl, *Phys. Chem.* (Frankfurt am Main) **52**, 254 (1967).

17. A. Wolberg, *Isr. J. Chem.* **12**, 1031 (1974).

18. K. M. Kadish and M. Morrison, *Inorg. Chem.* **15**, 483 (1976).

19. P.Bhyrappa and V. Krishnan, *Inorg. Chem.* **30**, 239 (1991).

CHAPTER 5

CYCLIC VOLTAMMETRIC STUDIES OF SOME Co PORPHYRINS

CHAPTER 5

5.1 INTRODUCTION

Extensive physico chemical studies are done for cobalt porphyrins. EPR and electrochemical studies are also done quite extensively[1-15,17-19]. Inspite of the extensive physico chemical reports in the literature, a systematic study on the redox behaviour of some substituted cobalt meso-tetraphenyl porphyrins is required. Thus, we are prompted to carry out this work. Our interest in the substituted CoTPP is as follows: Cobalt ion in the porphyrin ring is electroactive. Subjecting CoP to oxidation both cobalt ion as well as the porphyrin ring are oxidised. This will give us some information on the oxidation potentials of the metal ion as well as the porphyrin ligand. If there is strong metal - ligand interaction both the metal ion and the ligand oxidations will be affected due to substitutions in the porphyrin ring. Therefore, metal ligand interactions will be reflected in the voltammograms i.e. in the oxidation potentials.

A. RESULTS

The voltammograms are presented in the figure 5.1.1- 7 and the results are summarised in the table 5.1. All voltammograms show three one-electron redox couples. The oxidation potentials of CoTPP are cited as reference in the table 5.1. from the literature.

B. DISCUSSION

All voltammograms of Cobalt porphyrins exhibit three one-electron oxidation processes. Interestingly, no change in the oxidation potentials of the metal oxidation (first oxidation) is observed. The first oxidation wave is due to Co(II) → Co(III). The difference in the metal oxidation is very small (0.06V). The lowest potential 0.72V is observed for Co(T(*p*-OCH_3)PP) while the large potential 0.87V is observed for Co(T(*m*-F)PP). The highest potential differs by 0.09V only. If we incorporate the error, the difference will be negligible. This means the substitutions in the porphyrins ring do not have profound effect on the metal ion. On the other hand we observe changes in the second and the third oxidation potentials. These oxidation potentials correspond to the first and the second oxidations of the porphyrin ring. The first oxidation of the ring varies from 0.094V for Co(T(*p*-OCH_3)PP) to 1.17V for Co(T(*o*-Cl)PP). For CoTPP(Xn) where X = Br, n = 1 to 4, the first ligand oxidation potential increases from mono bromo to tetra bromo CoTPP. However, the change is not linear. The increase in the second ligand oxidation is higher. The same trend is observed for the electrophilic substitution in the phenyl ring. The highest shift (+ ve) is observed for Co(T(*m*-F)PP). Substitution by electron - donating groups either in the pyrrole ring or phenyl ring lower the oxidation potentials but not lower than that of the CoTPP.

5.2. UV-VIS SPECTRA OF SOME COBALT PORPHYRINS

To diagnose the oxidation and reduction optical absorption measurements are carried out. Oxidations are done with $SbCl_5$ while the reduction of the oxidized species is done by adding dimethylamine. Optical absorption spectra are presented in the figure 5.2.1-3 and the results are summarised in the table 5.2.

RESULTS AND DISCUSSION

UV-vis spectra of the unoxidised cobalt porphyrins do not exhibit significant changes. Red shifts are observed in the soret band and the visible band of CoTPP(X_n), where X = Br and n = 1 to 4. The shift for monobromo to tetrabromo is in the range 1 to 10nm. It indicates that electrophilic substitution in the pyrrole ring does effect the electronic energy levels. For Co(T(*p*-Cl)PP), Co(T(*p*-CH_3)PP), Co(T(*p*-Br)PP) and Co(T(*p*-OCH_3)PP) shifts are marginal. This indicates that the substitutions in the phenyl ring do not effect the electronic energy levels substantially (for both electrophilic and nucleophilic substitution).

Oxidation of Co(II)TPP to Co(III)TPP split in the soret band is observed (table 5.2). On oxidation of Cobalt porphyrins we observed splitting in the soret band only for Co(T(*p*-Cl)PP) and Co(T(*p*-Br)PP). On the other hand on oxidations the visible band broadens out and new bands emerge in the region 500 to 750nm indicating ring oxidations.

Reductions of the oxidised products with dimethylamine show the original spectra but all bands are red shifted considerably. The shifts are quite significant and equal. This may be due to the complexation by dimethylamine.

5.3 CONCLUSION

Electrophilic substitution in the pyrrole ring increases the oxidation potentials of the porphyrin ring but do not exhibit any significant change in the metal oxidation. The trend is same in the case of phenyl ring substitutions (affects are smaller). The metal ligand interaction is not reflected substantially in the oxidation potentials of the metal ion although some effects are indicated in the ligand oxidations.

Table 5.1.

Redox potentials (VOLTS vs. SCE) for CoTPP, CoTPP(X_n), X=Br, n = 1 to 4, Co(T(*o*-X)PP), Co(T(*m*-X)PP) and Co(T(*p*-X)PP), X = Cl, F, Br, NO_2, CH_3, OCH_3in CH_2Cl_2 ($\approx 10^{-3}$ M) using TBAP as supporting electrolyte. Scan rate 100mV/s (at room temperature)

Compound	$E_p^a(I)$	$E_p^a(II)$	$E_p^a(III)$	$E_p^c(I)$	$E_p^c(II)$	$E_p^c(III)$	ΔE_1	ΔE_2	ΔE_3	$E_{1/2}(I)$	$E_{1/2}(II)$	$E_{1/2}(III)$
TPP[a]	0.78	0.97	1.16									
TPP(Br)	0.75	1.02	1.19	1.05	0.87	0.56	0.19	0.14	0.14	0.65	0.94	1.12
TPP(Br_2)	0.77	1.07	1.25	1.14	0.96	0.63	0.14	0.11	0.11	0.70	1.02	1.19
TPP(Br_3)	0.79	1.10	1.27	1.15	0.98	0.64	0.15	0.12	0.12	0.71	1.04	1.21
TPP(Br_4)	0.81	1.11	1.28	1.16	0.99	0.67	0.14	0.12	0.12	0.74	1.05	1.22
T(*o*-CH_3)PP	0.84	1.08	1.32	1.15	0.94	0.66	0.18	0.14	0.17	0.75	1.01	1.24
T(*m*-CH_3)PP	0.78	1.04	1.25	1.10	0.90	0.58	0.20	0.14	0.15	0.68	0.97	1.18
T(*p*-CH_3)PP	0.74	0.97	1.17	1.09	0.90	0.52	0.22	0.07	0.09	0.63	0.94	1.13
T(*o*-Cl)PP	0.80	1.17	1.36	1.21	1.06	0.51	0.28	0.11	0.15	0.66	1.12	1.29
T(*m*-Cl)PP	0.78	1.13	1.33	1.22	1.02	0.59	0.19	0.11	0.11	0.68	1.08	1.28
T(*p*-Cl)PP	0.75	1.07	1.26	1.20	1.01	0.62	1.23	0.15	0.07	0.06	0.69	1.04
T(*o*-Br)PP	0.81	1.17	1.36	1.25	1.08	0.55	0.26	0.09	0.11	0.68	1.12	1.31
T(*m*-Br)PP	0.73	1.09	1.32	1.22	1.00	0.52	0 .21	0.10	0.10	0.63	1.04	1.27
T(*m*-F)PP	0.87	1.12	1.33	1.30	0.99	0.49	0.38	0.13	0.13	0.68	1.06	1.26
T(*m*-NO_2)PP	0.73	1.05	1.27	1.12	0.91	0.55	0.17	0.14	0.16	0.68	0.98	1.19
T(*m*-OCH_3)PP	0.79	1.05	1.25	1.11	0.91	0.59	0.19	0.14	0.14	0.69	0.98	1.18
T(*p*-OCH_3)PP	0.72	0.94	1.12	1.04	0.85	0.62	0.10	0.08	0.09	0.67	0.90	1.08

[a] reference 17

Table 5.2

UV-Vis. data of Unoxidised, Oxidised and Reduced products of CoTPP, CoTPP(X_n), X=Br , n=1 to 4, Co(T(*o*-X)PP), Co(T(*m*-X)PP) and Co(T(*p*-X)PP) , X = Cl, F, Br, NO_2, CH_3 and OCH_3 in CH_2Cl_2 containing 0.1M TBAP and 0.5M $SbCl_5$(at room temperature)

	λ, nm					
	Unoxidised		Oxidation		Reduction of the oxidized species with dimethylamine	
Porphyrin	Soret	Q	Soret	Q	Soret	Q
TPP[a]	410	528				
TPP[b]	427	540				
$[Co(III)TPP]^{2+b}$			415, 455	597, 662		
$[Co(III)TPP]^{3+b}$			352, 417, 455	564		
TPP(Br)	411	529	428	601	429	541
$TPP(Br_2)$	413	531	432	531, 615	430	545
$TPP(Br_3)$	415	547	436	553, 631	436	547
$TPP(Br_4)$	420	557	439	639	438	552
$TPP(CN)_4$[c]	434	626				
T(*o*-Cl)PP	409	527	425	538, 672, 602	430	540
T(*m*-Cl)PP	409	527	427	539, 601, 660	428	540
T(*p*-Cl)PP	416	519	427, 444	540, 607, 662	419,428	512, 542, 644
T(*o*- CH_3)PP	409	528	426	541, 603, 663	428	540
T(*m*- CH_3)PP	410	527	426	603, 651	428	541, 574
T(*p*- CH_3)PP	412	527	420	528, 610, 644	429	542, 576
T(*o*-Br)PP)	410	530	427	541, 609, 673	430	542
T(*m*-Br)PP	411	528	428	540, 604, 663	428	541
T(*p*-Br)PP	412	527	424, 446	541, 609, 662	427	541, 573
T(*m*-NO_2)PP	410	527	425	540, 558	428	540, 571
T(*m*-F)PP	409	526	425	540, 595, 664	426, 481	539
T(*m*-OCH_3)PP	409	528	426	532, 593, 663	424	540
T(*p*-OCH_3)PP	413	530	430	542, 665	433	543, 581

[a]reference 7, [b]In presence of 0.5M TBAP; [c]reference 16

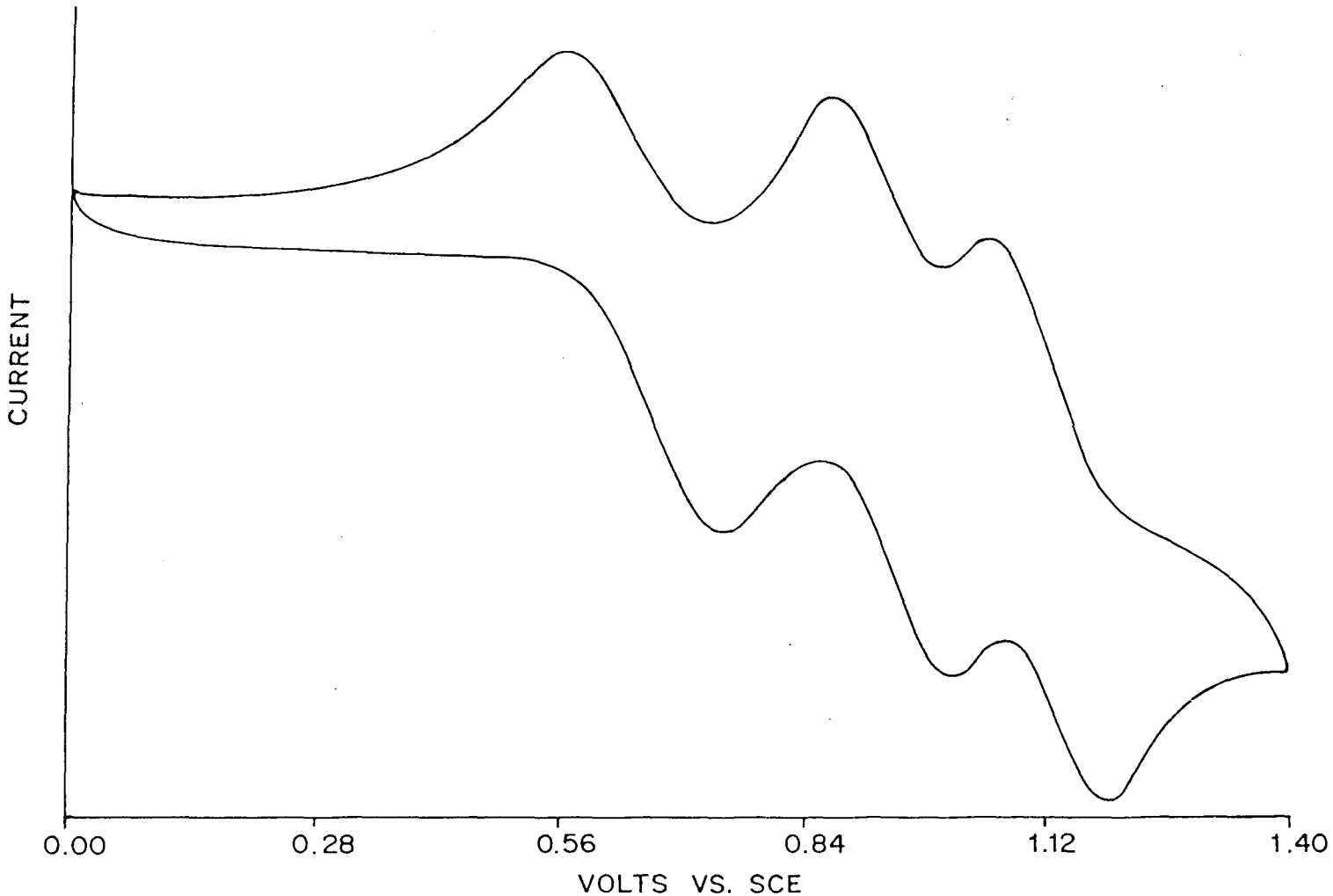

Figure 5.1.1. Cyclic voltammogram of CoTPP(Br) in CH_2Cl_2 containing 0.1 M TBAP at room temperature. Scan rate 100 mV/s

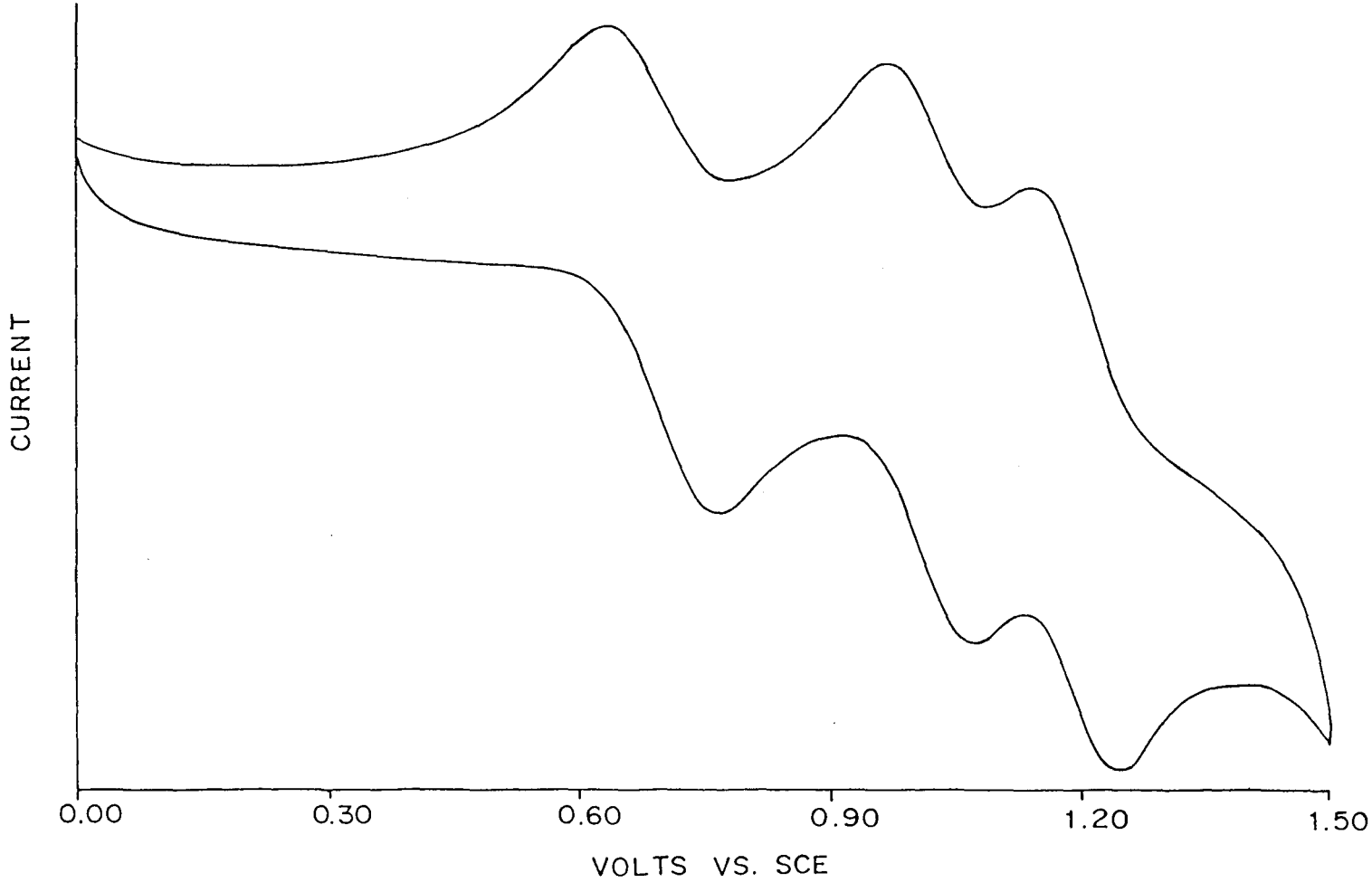

Figure 5.1.2. Cyclic voltammogram of $CoTPP(Br_2)$ in CH_2Cl_2 containing 0.1 M TBAP at room temperature. Scan rate 100 mV/s

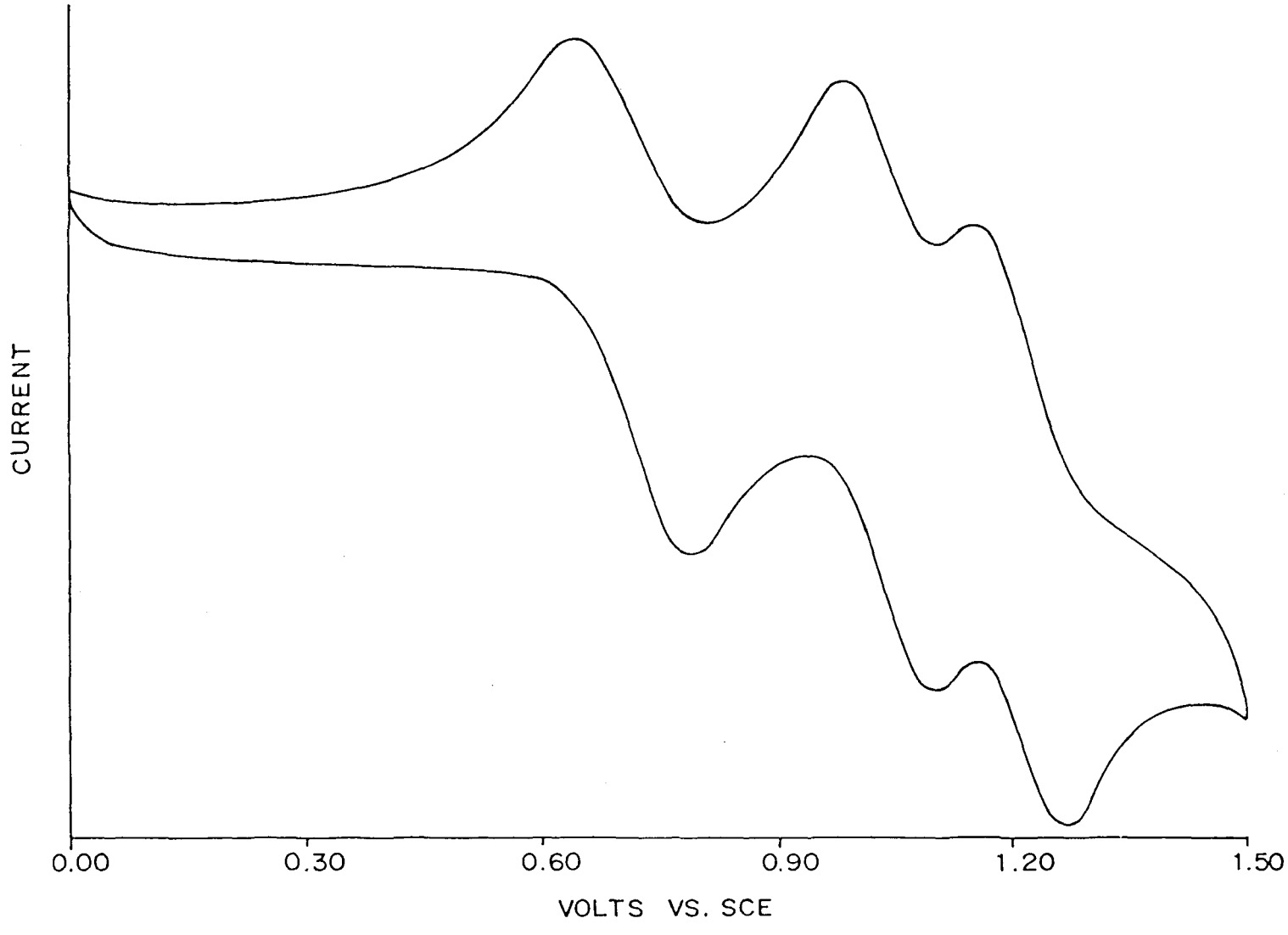

Figure 5.1.3. Cyclic voltammogram of $CoTPP(Br_3)$ in CH_2Cl_2 containing 0.1 M TBAP at room temperature. Scan rate 100 mV/s

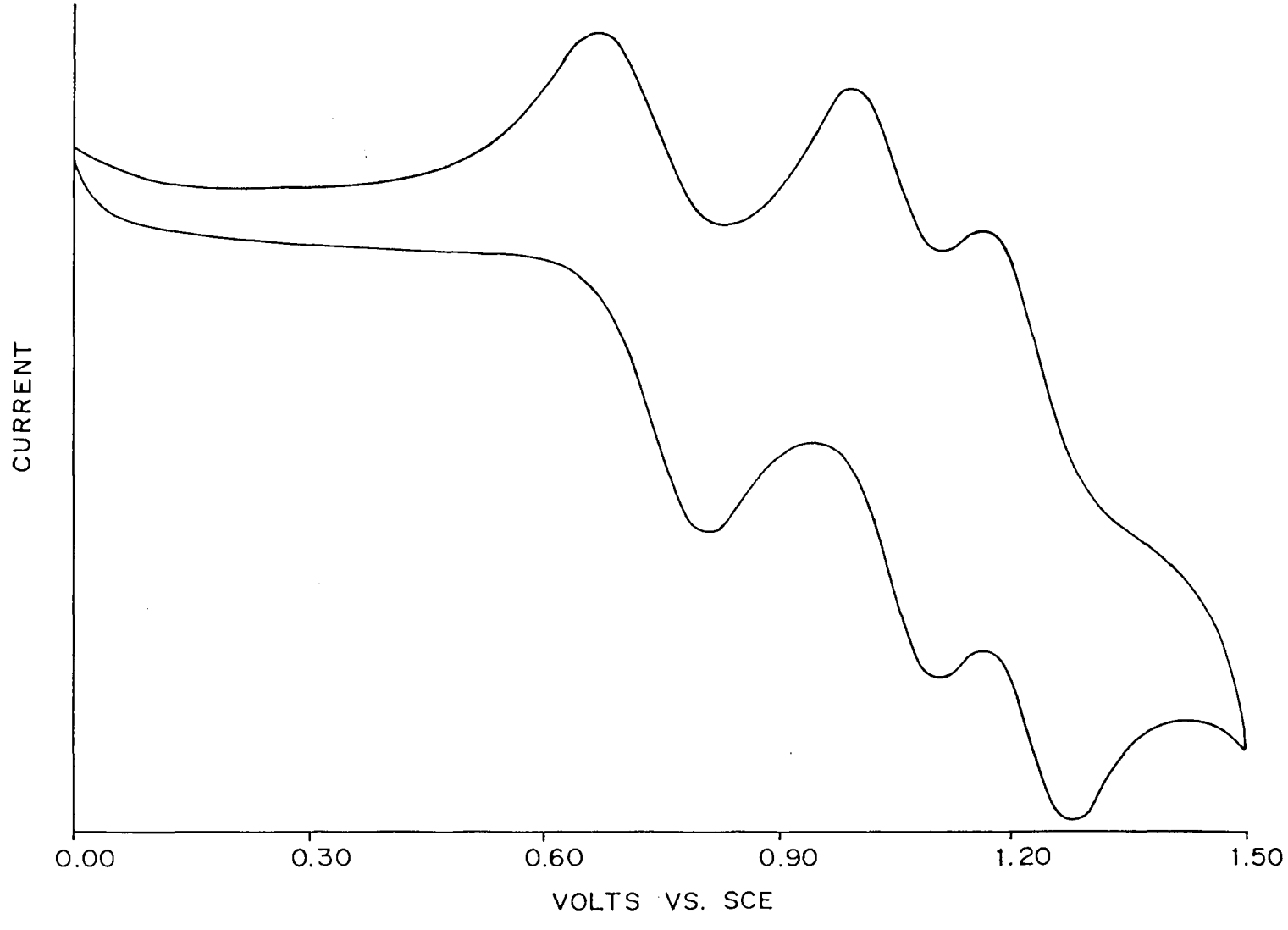

Figure 5.1.4. Cyclic voltammogram of $CoTPP(Br_4)$ in CH_2Cl_2 containing 0.1 M TBAP at room temperature. Scan rate 100 mV/s

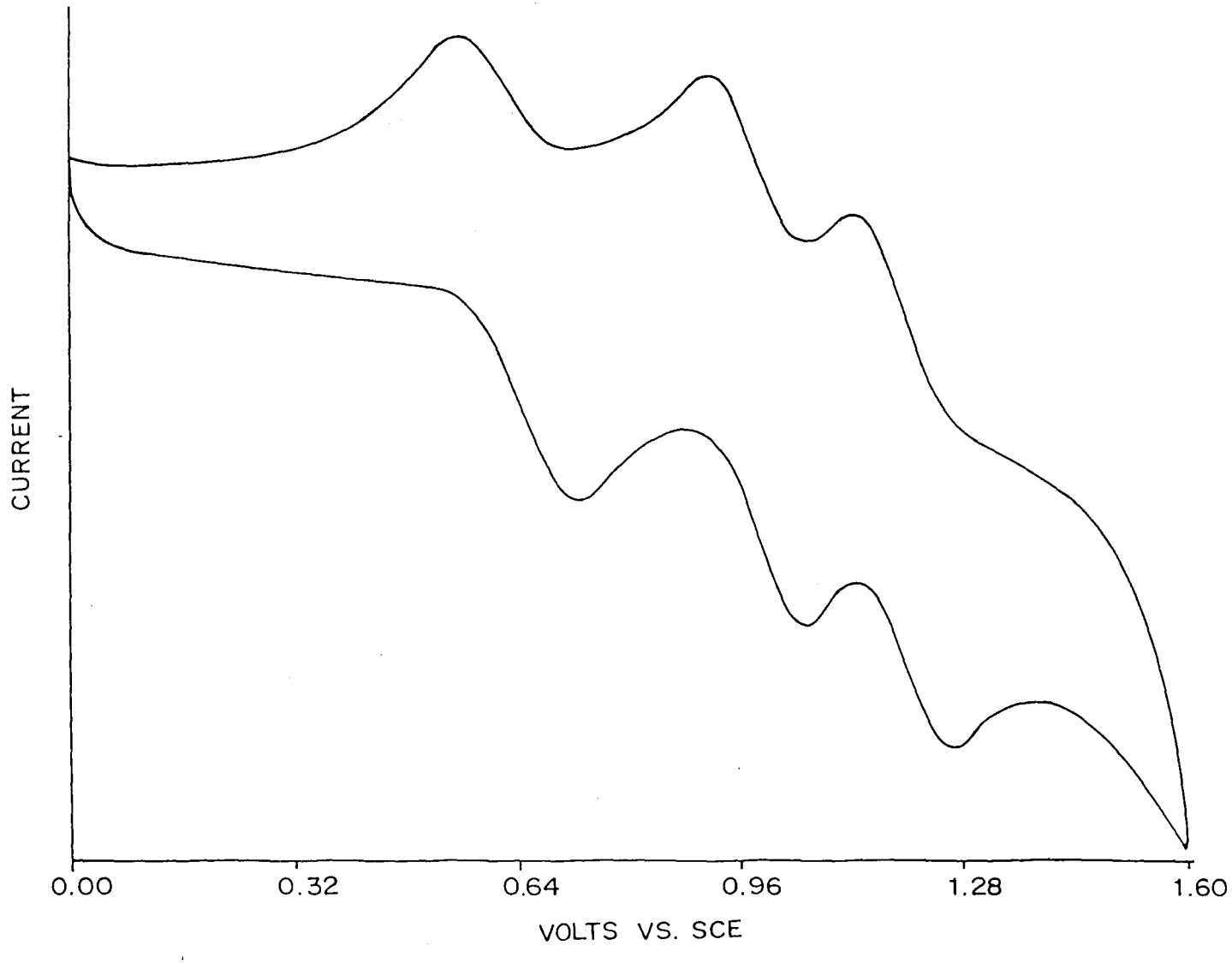

Figure 5.1.5. Cyclic voltammogram of Co(T(*m*-NO_2)PP) in CH_2Cl_2 containing 0.1 M TBAP at room temperature. Scan rate 100 mV/s

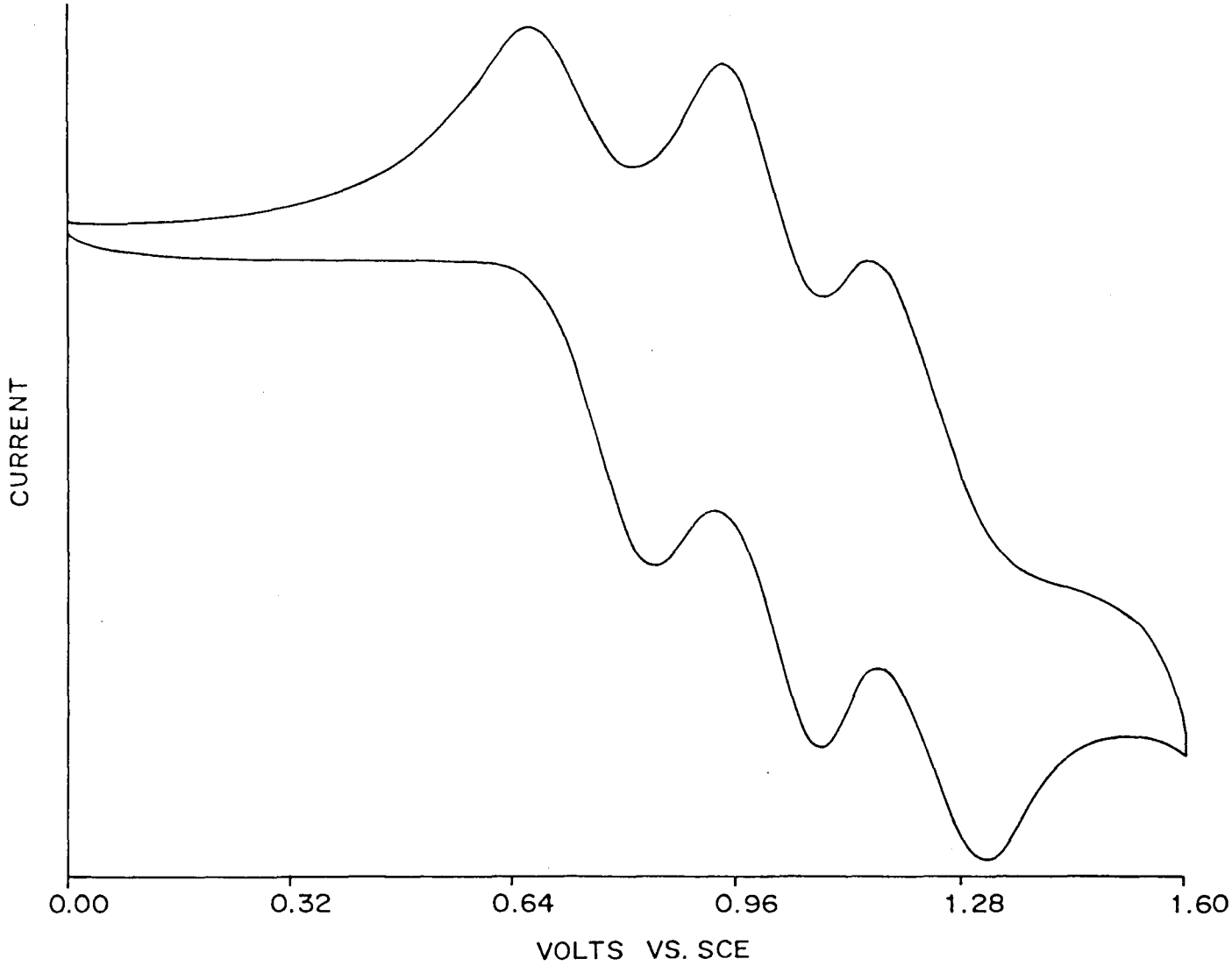

Figure 5.1.6. Cyclic voltammogram of Co(T(*o*-CH_3)PP) in CH_2Cl_2 containing 0.1 M TBAP at room temperature. Scan rate 100 mV/s

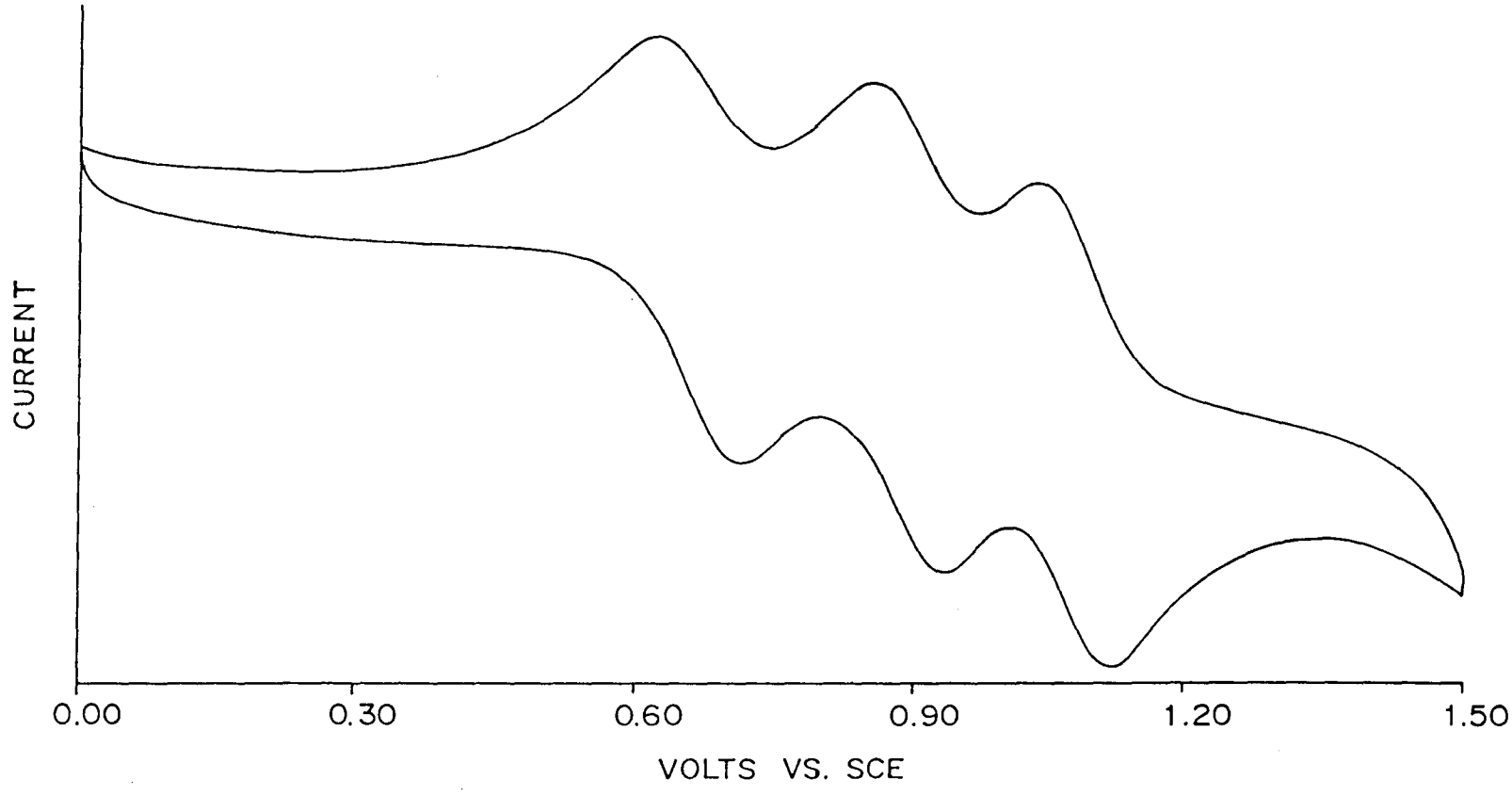

Figure 5.1.7. Cyclic voltammogram of Co(T(*p*-OCH_3)PP) in CH_2Cl_2 containing 0.1 M TBAP at room temperature. Scan rate 100 mV/s

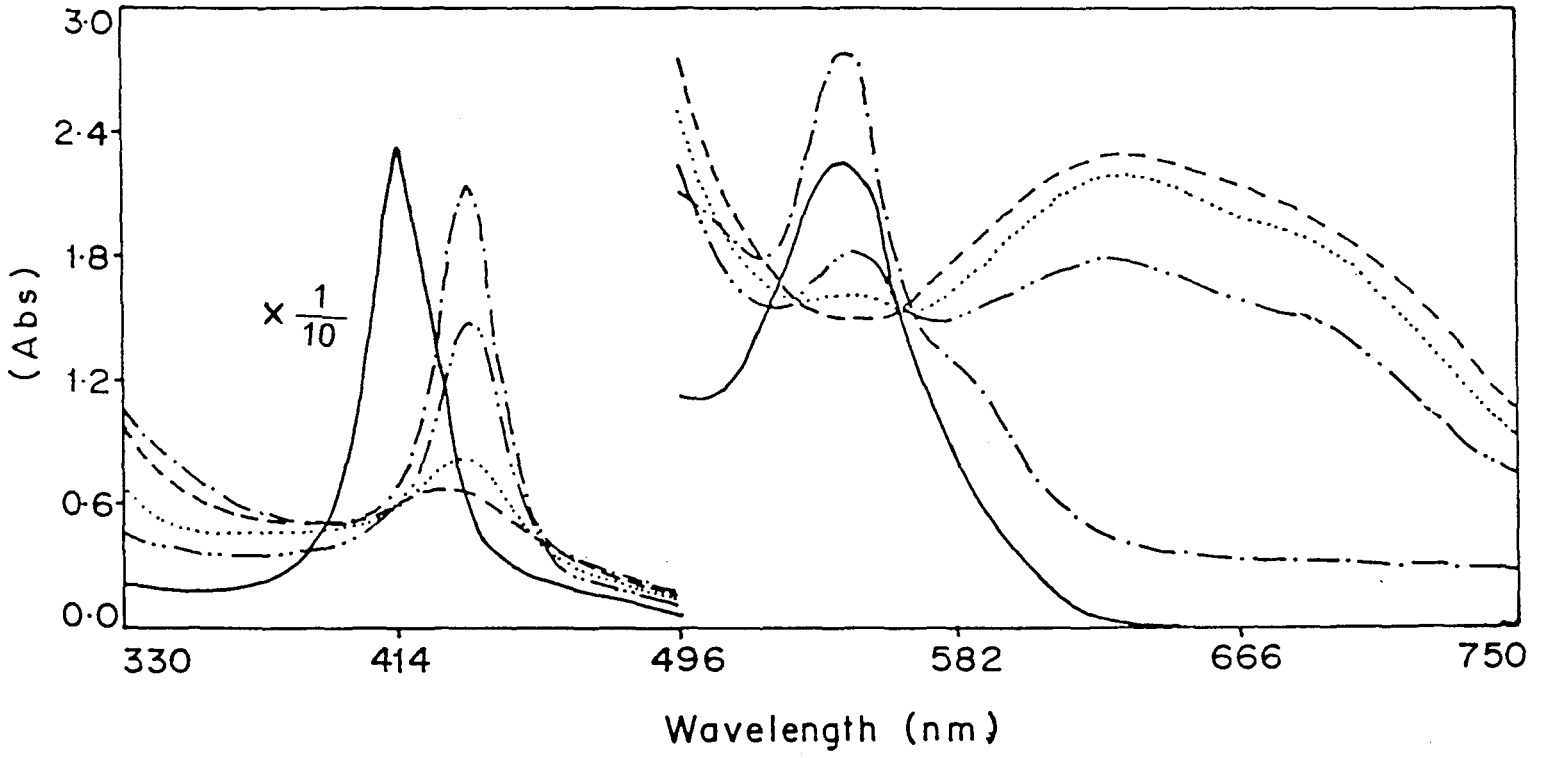

Figure 5.2.1. Visible absorption spectra of $CoTPP(Br_3)$ in CH_2Cl_2 Unoxidised ——, Oxidised (with 0.1 M $SbCl_5$) — ·· — ··, ·····, - - - - - and Reduced (with dimethylamine) — · — ·

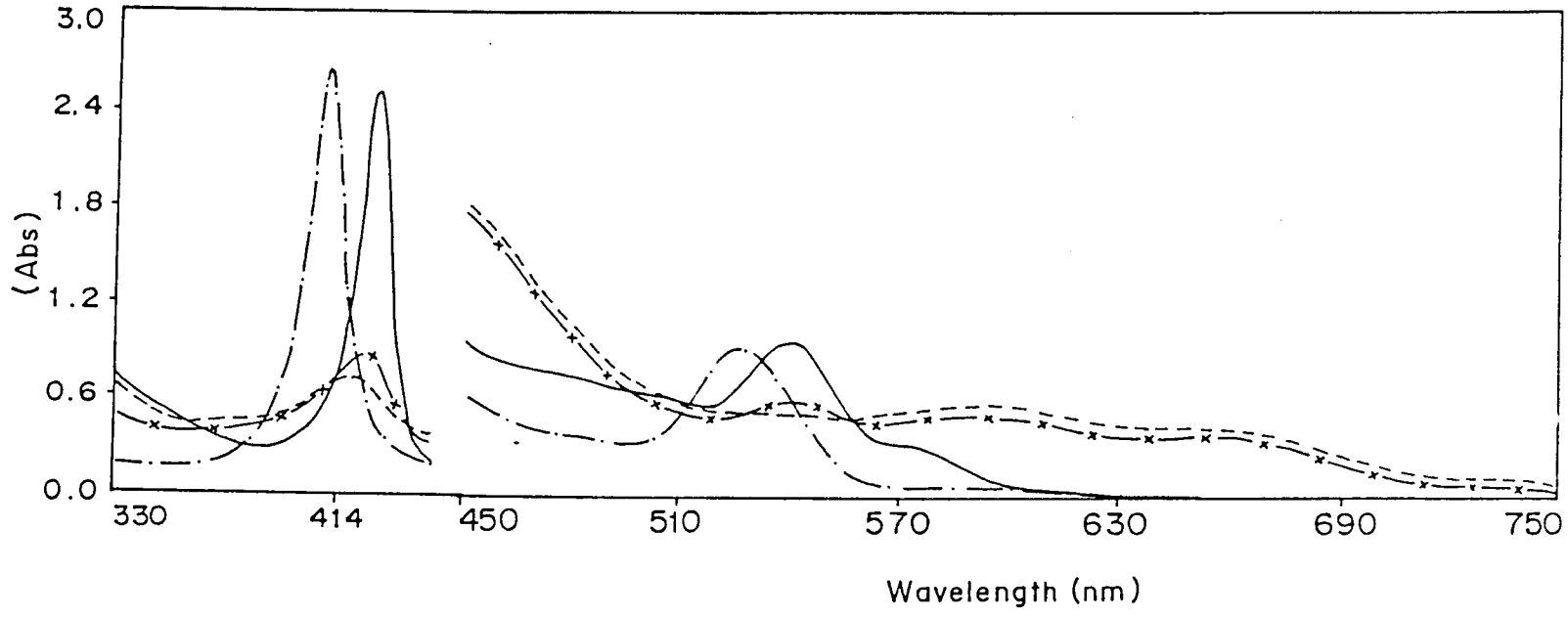

Figure 5.2.2. Visible absorption spectra of Co(T(*m*-NO_2)PP) in CH_2Cl_2 Unoxidised — · — ·, Oxidised (with 0.1 M $SbCl_5$) — · — ·, - - - - -, and Reduced (with dimethylamine) ——

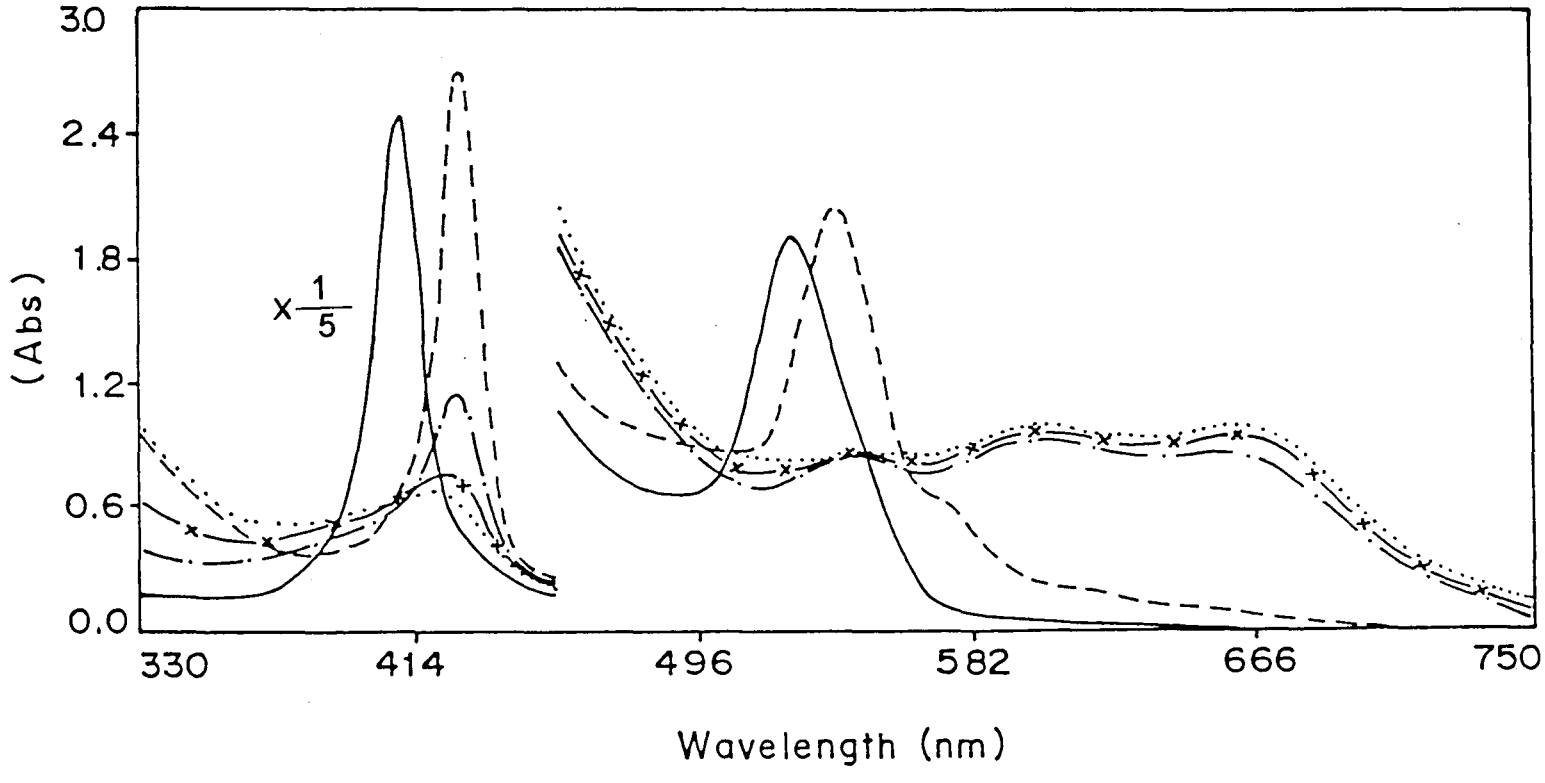

Figure 5.2.3. Visible absorption spectra of Co(T(*o*-CH_3)PP) in CH_2Cl_2 Unoxidised ——, Oxidised (with 0.1 M $SbCl_5$) —·—·, —•—•,·····, and Reduced (with dimethylamine) - - - -

REFERENCES

1. Louis D. Rollmann and R. T. Iwamoto, *J. Am. Chem. Soc.* **90**, 1455 (1968).
2. F. A. Walker, *J. Am. Chem. Soc.* **92**, 4235 (1970).
3. F. A. Walker, *J. Magn. Resonance.* **15**, 201 (1974).
4. K. Ichimori , H. Ohya-Nishiguchi, N. Hirota and K. Yamamoto, *Bull. Chem. Soc. JPN.* **58**, 623 (1985).
5. K. M. Kadish, L.A. Bottomley and D. Beroiz, *Inorg. Chem.* **17**, 1124 (1978).
5. X. Q. Lin, B. Boisselier-, Cocolios and K.M. Kadish, *Inorg. Chem.* **25**, 3242 (1986).
6. K.M. Kadish, X.Q. Lin and B.C. Han, *Inorg. Chem.* **26**, 4161 (1987).
7. K.M. Kadish, X.H. Mu and X.Q. Lin, *Inorg. Chem.* **27**, 1489 (1988).
8. X.H. Mu and K.M. Kadish, *Inorg. Chem.* **28**, 3743 (1989).
9. C. Araullo - McAdam and K.M. Kadish, *Inorg. Chem.* **29**, 2749 (1990).
10. Y. Hu, B. C. Hun, L.Y. Bao, X. H. Mu and K.M. Kadish, *Inorg. Chem.* **30**, 2444 (1991).
11. M.Satosh,Y. Ohba, S. Yamauchi and M. Iwaizumi, *Inorg. Chem.* **31**, 293(1992).
12. F. D'Souza, A. Villard, E. V. Caemelbecke, M. Franzen, T. Boschi, P. Tagliatesta and K.M. Kadish, *Inorg. Chem.* **32**, 4042 (1993).
13. Sh. Fukuzum, K. Miyamoto, T. Suenobu, E. V. Caemelbecke and K.M. Kadish, *J. Am. Chem. Soc.* **120**, 2880 (1998).
15. D. Dolphin, D.J. Halko and E. Johnson, *Inorg. Chem.* **20**, 4348 (1981).
16. X.Q. Lin and K.M. Kadish, Anal. Chem, **57**, 1498 (1995).

17. J. Fajer, D. C. Borg, A. Forman, D. Dolphin and R.H. Felton, J. Am. Chem. Soc. 92, 3451 (1970).

18. Chunnian Shi and Fred C. Anson, Inorg. Chem. 37, 1037 (1998).

19. Brian M. Hoffman, Damon L. Diemente and Fred Basolo, J. Am. Chem. Soc. 92, 61 (1970).

SUMMARY

SUMMARY

This thesis entitled " ELECTROCHEMICAL AND EPR STUDIES OF SOME OXIDISED METALLOPORPHYRINS" embodies the information, results of investigations on the oxidation products of some metalloporphyrins. It consists of five (5) chapters and an appendix. We restrict our investigations mainly to cyclic voltammetry and EPR studies of some transition metals like VO, Co and Ni porphyrins.

In the introduction occurrence of the metalloporphyrins π - cation in nature is briefly mentioned. Besides, the importance of the EPR and cyclic voltammetric studies of metalloporphyrins are also mentioned very briefly.

In chapter 1 a brief review of VO, Co and Ni meso-tetraphenylporphyrins are presented. Emphasis is given to the EPR and cyclic voltammetric studies. This review provides us the background information to pursue our research investigation in the right direction.

Chapter 2 describes the detail experimental procedures such as the synthesis, purification and characterization of samples as well as the purification of reagents and solvents used during the course of investigations. Besides, instrumental parameters and the procedure of measurements are also described.

Chapter 3 discusses the cyclic voltammetry, EPR and UV-vis spectra of substituted meso-tetraphenyl vanadyl porphyrins. In general the voltammograms of

vanadyl porphyrins exhibit two reversible oxidation waves. Thus, the voltammogram of VO(T(*m*-NO_2)PP) consists of two reversible one-electron oxidation – reduction waves. The oxidation potentials are shifted more positively and show higher potentials even compared to that of VOTPP(Xn) where X=Br systems.

The room temperature EPR spectra of the oxidations of VOTPP which are not available in the literature are also presented in this chapter. It also gives a good comparative study for the substituted VOTPP systems. The pre-oxidised species of VOTPP show line width inversion and reduction in the coupling constant.

The triplet state of these vanadyl porphyrins do not vanishes at room temperature but broadens out which are visible at higher modulation. Since all the substituted VOTPP systems show similar type of EPR spectra. We discuss the spectra of VO(T(*m*-NO_2)PP). The EPR of $[VO(T(m\text{-}NO_2)PP)]^+$ at 77K gives a triplet state spectrum which resembles that of the radical cation of VO meso-porphyrin. The data from the low temperature EPR spectrum are presented in the table 3.2.

A value of 3.575 ± 0.05Å is obtained as an inter-electron distance between the two unpaired electrons. Similarly, we obtain inter-electron distance for the rest of the vanadyl porphyrins. Shorter distance between the unpaired electrons indicates that the unpaired spin density is more in a_{1u}. But the room temperature spectra of the triplet state do not vanish. This also points that the unpaired spin density in a_{2u} is not negligible.

Chapter 4 deals with the EPR and cyclic voltammetric studies of Nickel porphyrins. Normally, Ni(II)P do not give any EPR spectrum because Ni(II) is d^8

UV-vis spectra of Nickel porphyrins exhibit hypso type of spectrum although the shifts are not much. Thus, it is likely that metal – ligand back bonding does exist. On oxidation with $SbCl_5$ the Ni(py)P exhibit a split in the soret band. Besides, the intensity of the visible band decreases and a new broad band emerges in the region 600nm – 900nm.

Chapter 5 discusses the cyclic voltammetry and UV-vis spectra of the Cobalt porphyrins. As Co in also an electron active, oxidations will occur in both the metal center as well as the ligand. If there is a strong metal-ligand interaction, then on oxidation there may be some changes in the metal center oxidation potentials. However, we could not observe any accountable changes in the oxidation potential of the cobalt.

UV – vis spectra of Cobalt porphyrins do not show much difference on substitutions at different positions. Only some red shifts are observed for tetra bromo systems.

In the appendix, necessary theories such as voltammetry of metalloporphyrins, spin Hamiltonian for axially symmetric systems and other molecular orbital coefficients calculations are incorporated.

APPENDIX – A[1,2]

CYCLIC VOLTAMMETRY OF METALLOPORPHYRINS

Let us consider one –electron oxidation of a molecule R

$$R \underset{+e}{\overset{-e}{\rightleftharpoons}} R \quad \ldots\ldots\ldots\ldots (1)$$

During the forward triangular sweep (triangular wave) a peak is obtained at a potential E_a corresponding to the process $R \rightarrow R^+$. In the reverse sweep the species R^+ is reduced back to R at a peak potential E_c. Thus, we obtain half – wave potential corresponding to this redox couple.

$$E_{1/2} = \frac{E_a + E_c}{2} \quad \ldots\ldots\ldots\ldots (2)$$

For a reversible process, the peak – to – peak difference is given by

$$E = E_a - E_c = \frac{0.059V}{n} \quad \ldots\ldots\ldots\ldots (3)$$

at 25°C.

If the peak currents are i_{pa} and i_{pc} corresponding to E_a and E_c respectively, then for a one –electron reversible process,

$$\frac{i_{p_a}}{i_{p_c}} = 1 \quad \ldots\ldots\ldots\ldots (4)$$

For a metalloporphyrin having D_{4h} or C_{4h} symmetry, the two highest occupied MO (HOMO) a_{1u} and a_{2u} are nearly degenerate. During oxidations, electrons are

removed from the HOMO levels. Removal of electrons may be either from the metal or from the porphyrin ring or may be from both. In a metalloporphyrin, the central metal ions such as Zn, Cu etc. are quite in – active to the redox process while metal ions such as Fe, Co, Mn, Ni etc. are electro active and redox process may occur in the metal center as well as in the ligand. This can be understood by considering HOMO levels of the metal as well as the ligand. Thus, it can be represented as

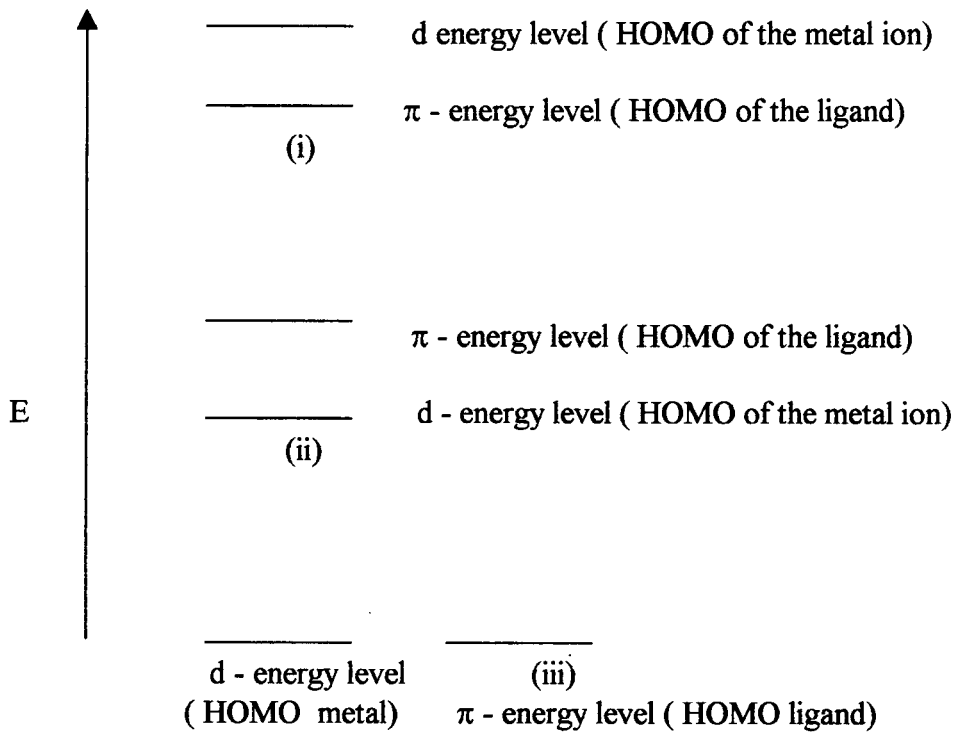

Fig.1. HOMO representative for metallo porphyrin.

System (i) contains electron – active metal center. Therefore, the redox process will occur first in the metal center and then the ligand. System (ii) contains non-electroactive metal center , therefore, redox process will occur in the ligand. System (iii) contains electron active metal center, therefore, redox process will occur in both the metal as well as in the ligand. Thus, this process becomes complicated.

In general one can represent the redox process by the following scheme

System I, considering a bivalent metal.

$$M(II)P \underset{E^{ox}_{1/2}(1)}{\overset{-e}{\rightarrow}} M(III)P^{+} \underset{E^{ox}_{1/2}(2)}{\overset{-e}{\rightarrow}} M(III)^{+\cdot} \underset{E^{ox}_{1/2}(3)}{\overset{-e}{\rightarrow}} M(III)^{++}$$

$$M(II)P \underset{E^{red}_{1/2}(1)}{\overset{+e}{\rightarrow}} M(III)P^{-} \underset{E^{red}_{1/2}(2)}{\overset{+e}{\rightarrow}} M(III)^{-\cdot} \underset{E^{red}_{1/2}(3)}{\overset{+e}{\rightarrow}} M(III)^{--}$$

$$\Delta_{ox} = E^{ox}_{1/2}(2) - E^{ox}_{1/2}(1)$$

$$\Delta_{red} = E^{red}_{1/2}(1) - E^{red}_{1/2}(2)$$

For ring oxidation and reduction a constancy of Δ_{ox} and Δ_{red} are observed. $\Delta_{ox} \approx$ 0.3eV and $\Delta_{red} \approx 0.5$eV.

Also, $\delta = E_{1/2}(1) - E_{1/2}(2)$ is constant for a variety of metallo porphyrins (i.e. 2.20 ± 0.15V), where the redox processes involve the ligand only. It is observed that Δ_{ox} or Δ_{red} of the metal is independent and is explained in terms of HOMO (a_{1u} and a_{2u}) or LUMO (e_g) π-molecular orbitals of the porphyrin ligand and metal central

orbitals. There is negligible mixing between the metal orbitals and the porphyrin π -orbitals. Thus, the metal ion exerts an inductive Coulombic effect on the π -orbitals of the ligand through σ frame work. It effects only the absolute values of π energy levels but not the relative values i.e. the difference in the energies between HOMO and LUMO. Using PPP π electron energies, the value of Δ_{ox} , Δ_{red} and δ have been estimated which agree reasonably well with the corresponding experimental data. However, when metal – centered redox process occur, this correlation fails.

APPENDIX – B[3-6]

B.1. SPIN HAMILTONIAN: The spin Hamiltonian for a metalloporphyrin having an unpaired electron on the central metal atom is presented here.

Liquid/Solution state: In solution/liquid media the spin Hamiltonian is simple and is given by

$$\mathcal{H}_{iso} = g\beta_e H_z S_z + a_M \hat{I}_M.\hat{S} + \hat{S}.\sum_i a_{li}\hat{I}_{li} \quad \text{---------- (1)}$$

where g = isotopic g-value

a_M= Hyperfine Coupling of the metal atom

a_{li} = Hyperfine coupling of the ligand

$\hat{I}_M$= nuclear spin of the metal atom

$\hat{I}_{li}$ = nuclear spin of the ligand atoms

and $\hat{S}$ = unpaired electron spin of the metal atom

Solid state (frozen solutions/glass state/single crystal)

The spin Hamiltonian is given by

$$\mathcal{H} = \beta_e[\, g_{11}H_zS_z + g_\perp(H_xS_x + H_yS_y)] + A_{11}S_zI_z + A_\perp(S_xI_x + S_yI_y) \text{ ---------- (2)}$$

Neglecting the nuclear quadrupole interaction for a nucleus of spin I>1.

It is to be noted that $\hat{S}$ is a fictitious spin operator containing both orbital angular momentum (**L**) and spin angular momentum ($\hat{S}$). For metal atom with unpaired electrons in the d-orbital, the effect of the spin-orbit coupling is included as perturbation term ($\lambda \mathbf{L}\hat{S}$) while the interaction such as **L**.H and **L**.$\hat{I}$ are considered as second-order corrections to the g- and A-values. Consider a d^9 system (having an unpaired electron) in a square - planar ligand field and assuming that each of the four nitrogens of the ligand has available 2s, $2p_x$, $2p_y$ and $2p_z$ orbitals with 3d orbitals of the metal atom. Assigning x and y axes along M-N bonds, then the antibonding molecular orbitals are

$$B_{1g} = |\, x^2 - y^2\rangle = \alpha d_{x^2-y^2} + (\alpha'/2)(-\sigma^a_x + \sigma^b_y - \sigma^c_x - \sigma^d_y) \text{ ---------- (3)}$$

$$B_{2g} = |\, xy\rangle = \beta_1 d_{xy} - (\beta'_1/2)(p^a_y + p^b_x - b^c_y - p^d_x) \text{ ---------- (4)}$$

$$A_{1g} = \alpha_1 |\, 3z^2 - r^2\rangle = \alpha_1 d_{3z^2-r^2} - \alpha'_1/2\,(\sigma^a_x + \sigma^b_y - \sigma^c_x - \sigma^d_x) \text{ ---------- (5)}$$

$$E_g = \left\{ \begin{array}{l} |\, xy\rangle = \beta d_{xy} - \beta'/\sqrt{2}\,(p_z^{(1)} - p_z^{(3)}) \\ |\, yz\rangle = = \beta d_{yy} - \beta'/\sqrt{2}\,(p_z^{(2)} - p_z^{(4)}) \end{array} \right\} \text{ ---------- --- (6)}$$

where $\sigma^{(i)} = np^{(i)} \pm (1-x^2)^{1/2} S^{(i)}$ for $0 \leq n \leq 1$ ---------- (7)

Bonding orbitals are constructed by replacing the unprimed by primed and the primed by minus the unprimed coefficients in the antibonding orbitals.

The A_{1g} level do not contribute even in the second order correction. B_{1g} represents in - plane σ bonding, B_{2g} represent in a plane σ - bonding while E_g represents out – of plane π bonding. The orbitals σ_x ,σ_y etc. are sp^2 hybridised σ lone pairs of the nitrogen atoms, that are bonded to the metal atom. On normalizing equation (3), we get

$$\alpha^2 + \alpha'^2 - 2\alpha\alpha' S = 1 \quad \text{---------- (8)}$$

where S is the overlap integral between the metal and the ligand orbitals. The coefficients α, α' can be evaluated using the EPR data as follows:

$$g_{\parallel} = 2.0023 - 8\rho [\alpha \beta_1 - \alpha'(1- \beta_1^2)^{1/2} T(n)/2] \quad \text{---------- (9)}$$

$$g_{\perp} = 2.0023 - 2\mu [\alpha\beta - \alpha'\beta S - (\alpha'(1-\beta^2)^{1/2} T(n)\sqrt{2}] \quad \text{---------- (10)}$$

$$A_{\parallel} = p[- \alpha^2 (4/7 + k_o) + (g_{\perp} - 2) + 3/7(g_{\parallel} - 2) + \text{terms containing } T(n)] \quad \text{----- (11)}$$

$$A_{\perp} = p[- \alpha^2 (2/7 - k_o) + 11/14 (g_{\perp} - 2) + \text{terms containing } T(n)] \quad \text{---------- (12)}$$

where $\rho = \lambda_o \alpha\beta_1/(E_{xy}-E_{x^2-y^2})$ ---------- (13)

$$\mu = \lambda_o \alpha\beta/(E_{xz}-E_{x^2-y^2}) \quad \text{---------- (14)}$$

$$p = 2.0023 g_N \beta_N \beta_e \langle r^{-3} \rangle$$

$$\approx 2\gamma\beta_o\beta_N \langle d_{x^2-y^2} | r^{-3} | d_{x^2-y^2} \rangle \quad \text{---------- (15)}$$

λ_o is the spin-spin coupling constant for the free metal ion which is given by the integral

$$<3d\,|\lambda(r)|\,3d>$$

and k_o is the Fermi – contact interaction for the free ion.

The term T(n) is given by

$$T(n) = n - (1-x^2)^{1/2} R^8 (Z_p Z_s)^{5/2} (Z_s - S_p)/(Z_s + Z_p)^5 a_o \quad \text{---------- (16)}$$

Where Z_s and Z_p are the effective nuclear charges on the s and p orbitals respectively and a_o is the Bohr radius. The values of effective charges from the literature[7] are

For Nitrogen	For Oxygen	For Copper
$Z_{2s} = 4.50$	$Z_{2s} = 5.25$	$Z_{3d} = 11.86$
$Z_{2p} = 3.54$	$Z_{2p} = 4.06$	

For Vanaium

$Z_{3d} = 7.22$

Using the above values the overlap integrals for nitrogen and oxygen are calculated. Considering ligand – to – metal distance $R = 3.62a_o$ and $n=(2/3)^{1/2}$

The overlap integrals

$S_{nitrogen} = 0.093$

$S_{oxygen} = 0.076$

And T(n) values are

$T(n)_{nitrogen} = 0.333$

And $T(n)_{oxygen} = 0.220$

$\lambda_o = -828cm^{-1}$, $p=0.036cm^{-1}$

Generally the orbital excitation energies (for copper complex)

$\Delta Exy \approx 15{,}000cm^{-1}$

$\Delta Exz \approx 25{,}000cm^{-1}$

and knowing g_π, $g_\perp$, A_π and $A_\perp$ one can calculate α, β_1 and β_1'. An approximate expression for α^2 is written as

$$\alpha^2 = -(A/P) + (g_\pi - 2) + (3/7)(g_\perp - 2) + 0.04$$

If $\alpha^2 = 1$, then the band will be ionic. If the overlap integral is vanishingly small and $\alpha^2 = 0.5$, then band will be completely covalent. Thus, smaller the value of α^2 more is the covalent character.

B.2. Superhyperfine structure: In metalloporphyrin the interaction of the metal unpaired electron with the four N nuclei give rise to superhyperfine structure. The Hamiltonian is expressed as

$$\mathcal{H}_{suphyp} = \hat{S} \sum_{n=1}^{4} A_n \hat{I}_n \qquad \text{----------} \qquad (17)$$

For D_{4h} symmetry

$$\mathcal{H}_{suphyp} = A^N_{\parallel} S_z I_z^N + A^N_{\perp}(S_x I_x^N + S_y I_y^N) \qquad \text{----------} \qquad (18)$$

Where I_x^N, I_y^N and I_z^N are the nuclear spin components of the nitrogen atom along the three co-ordinates. In most cases the superhyperfine tensors are found to be isotropic i.e. $A^N_{\parallel} \approx A^N_{\perp}$. However, $A^N_{\parallel}$ and $A^N_{\perp}$ can be express as

$$A^N_{\parallel} = g_e g_N \beta_o \beta_N \langle (\alpha'/2)^2 [\gamma^2 (8\pi/3) |S(o)|^2 + 4/5(1-\gamma^2) \langle r^{-3} \rangle 2p \quad \text{---------- (19)}$$

$$A^N_{\perp} = g_e g_N \beta_o \beta_N \langle (\alpha'/2)^2 [\gamma^2 (8\pi/3) |S(o)|^2 - 2/5(1-\gamma^2) \langle r^{-3} \rangle 2p \quad \text{---------- (20)}$$

The equations are expressed in terms of 2s and 2p orbitals of nitrogen.

The first term within the square brakets is the isotropic part of the hyperfine coupling arising from the spin density at 2s – orbital of the nitrogen atom. The second term is the dipolar coupling arising out of the spin density in the p_x and p_y orbitals of the ligand atom. The sp^2 hybridised orbitals of the nitrogen is given by

$$|\sigma\rangle = \gamma |2s\rangle + (1-\gamma^2)^{1/2} |p_\sigma\rangle \quad \text{---------- (21)}$$

The value of γ^2 can be obtained from the magnitude of $A^N_{\parallel}$ and $A^N_{\perp}$. Thus, one can obtain α and α' of the equation (3).

The magnitude of d-d transitions can be obtained from the optical spectra.

The coefficient β, β_1 and β_1' are also obtained in the similar way (using the EPR data).

APPENDIX – C

TRIPLET STATE : A metalloporphyrins containing an unpaired electron on the metal atom on oxidation another unpaired electron is generated in the ligand. Thus, a triplet state (S=1) is generated in the molecule. A spin Hamiltonian for such a system can be written as

$$\mathcal{H} = \beta[S_1.g_1.H + S_2.g_2.H] + S.A.I + S_1.D.S_2 + JS_1.S_2 \quad \text{---------- (1)}$$

where the indexes 1 and 2 represents unpaired electron on the metal atom and the unpaired π-electron on the ligand respectively. The hyperfine coupling between the ligand π-electron and the metal atom nucleus is neglected. Also, the value of J is larger then the microwave frequency (X- band). Thus, an approximate Hamiltonian can be written as

$$\mathcal{H} = \beta gSH + SAI + SDS \qquad \text{---------- (2)}$$

Here we consider the contribution to the zero – field splitting (ZFS) in only from the dipolar coupling.

For an axially symmetric system

$$\mathcal{H} = \beta gSH + D_{\perp}(S_x^2 + S_y^2) + D_{\parallel} S_z^2 \qquad \text{---------- (3)}$$

In terms of D and E

$$\mathcal{H} = \beta gSH + D[(S_z^2 - 1/2\ S(S+1) + E(S_x^2 - S_y^2)] \qquad \text{---------- (4)}$$

where $D = 3/2\ D_{\pi}$

D and g terms are expressed in the same principle axis system with the four – fold symmetry axis as the Z- axis. Considering the inter electron axis is in the plane of the porphyrin ring and expressing the ZFS tensor along the interelectron axis (z′) :

$$\left.\begin{array}{l} D_{xx'} = D_{y'y'} = -D_{z'z'}/2 \\ \\ \text{Hence} \quad D_{\pi} = D_{x'x'} = D_{y'y'} = -D_{z'z'}/2 \end{array}\right\} \qquad \text{---------- (5)}$$

$$D_{z'z'}(\text{in MHz}) = 1.298 \times 10^4 g^2/R^3 \quad \text{---------- (6)}$$

where R is expressed in Å and

$$g^2 = g_{\parallel}^2 + 0.5 g_{\perp}^2 \quad \text{---------- (7)}$$

C.1. Basis functions (triplet state)

As there are two unpaired spins, we have the following basis functions

$\alpha(1)\,\alpha(2)$, $\alpha(1)\,\beta(2)$, $\beta(1)\,\alpha(2)$ and $\beta(1)\,\beta(2)$

$$\left.\begin{aligned} |T_{+1}\rangle &= \alpha(1)\,\alpha(2) \\ |T_o\rangle &= 1/\sqrt{2}[\,\alpha(1)\,\beta(2) + \beta(1)\,\alpha(2)] \\ |T_{-1}\rangle &= \beta(1)\,\beta(2) \end{aligned}\right\} \quad \text{---------- (8)}$$

Antisymmetric (singlet state, S = 0)

$$|S\rangle = 1/\sqrt{2}[\,\alpha(1)\,\beta(2) - \beta(1)\,\alpha(2)] \quad \text{---------- (9)}$$

Re – writing the triplet functions along x,y and z axes

$$\left.\begin{aligned} |T_x\rangle &= 1/\sqrt{2}[\,\beta(1)\,\beta(2) - \alpha(1)\,\alpha(2)] = 1/\sqrt{2}\,|T_{-1} - T_{+1}\rangle \\ |T_y\rangle &= 1/\sqrt{2}[\,\beta(1)\,\beta(2) + \alpha(1)\,\alpha(2)] = 1/\sqrt{2}\,|T_{-1} + T_{+1}\rangle \\ |T_z\rangle &= 1/\sqrt{2}[\,\alpha(1)\,\beta(2) - \beta(1)\,\alpha(2)] = 1/\sqrt{2}\,|T_o\rangle \end{aligned}\right\} \quad \text{---------- (10)}$$

The following computer program were obtained from Prof. J. Subramanian, Department of Chemistry, Pondicherry University, Pondicherry, INDIA (i) ZFS and (ii) powder and the spectrum were printed using MSExel

REFERENCES

1. R. H. Felton, in " The porphyrins", Edited by Dolphin (Academic press, New York, 1979), Vol. V. p. 53.
2. D. G. Davis, in "The porphyrins, Edited by Dolphin (Academic press, New York, 1979), Vol. V. p. 127.
3. D. Kivelsion and Neiman, J. Chem. Phys. 35, 149 (1961).
4. A. H. Maki and B.R. McGarvey, , J. Chem. Phys. 29, 31 (1958).
5. D. Kivelsion and Sai – Kwing Lee, J. Chem. Phys. 41, 1896 (1964).
6. E. M. Roberts, W.S. Koshi and W.S. Caughey, , J. Chem. Phys. 34, 591 (1961).
7. D.R. Hatree, The Calculation of Atomic spectra (John Wiley & Sons, New York, 1957).